

**A NOAA AVHRR cloud
climatology over Scandinavia
covering the period 1991-2000**

Cover: Mean cloud frequencies in the afternoon in July (in colour) and the annual course of cloud cover for some selected positions in the Scandinavian area (curve plots) derived from a ten-year NOAA AVHRR data set 1991-2000.

**A NOAA AVHRR cloud
climatology over Scandinavia
covering the period 1991-2000**

Karl-Göran Karlsson

Report Summary / Rapportsammanfattning

Issuing Agency/Utgivare Swedish Meteorological and Hydrological Institute S-601 76 NORRKÖPING Sweden	Report number/Publikation RMK No. 97	
	Report date/Utgivningsdatum June 2001	
Author(s) Författare Karl-Göran Karlsson		
Title (and Subtitle) Titel A NOAA AVHRR cloud climatology over Scandinavia covering the period 1991-2000		
Abstract Sammandrag A ten-year NOAA AVHRR cloud climatology with a horizontal resolution of four km has been compiled over the Scandinavian region based on results from near real-time cloud classifications of the SMHI SCANDIA model. The frequency and geographic distribution of the cloud groups Low-, Medium- and High-level clouds, water and ice clouds and deep convective clouds have been studied in addition to the ten-year monthly means of total fractional cloud cover in the region. Furthermore, attempts to estimate the diurnal cycle of cloudiness and typical cloud patterns in various weather regimes (e.g., North Atlantic Oscillation phases) have been made. The cloud climate in the region was found to be significantly affected by the distribution of land and sea. In particular, the Baltic Sea was shown to suppress summertime cloudiness substantially and this effect was shown to influence cloud conditions in major parts of the Scandinavian region. However, interesting deviations from this cloudiness pattern were found in the Scandinavian mountain range, in the northern part of Scandinavia and over the Norwegian Sea. The quality of the satellite-based cloud information was examined by comparing with corresponding surface-observations given by SYNOP-based cloud climatologies for the same period. Results showed good agreement but specific problems were found in winter. In addition, some effects of the degradation of visible AVHRR channels were noticed. Comparisons have also been made with internationally used global cloud climate data sets, namely the SYNOP-based CRU data set and the cloud climatologies from the ISCCP D2 series.		
Key words sök-, nyckelord Cloud climatology, NOAA AVHRR, multispectral processing, cloud classification, validation of satellite-derived cloudiness		
Supplementary notes Tillägg	Number of pages Antal sidor 95	Language Språk English
ISSN and title ISSN och titel 0347-2116 SMHI Reports Meteorology and Climatology		
Report available from Rapporten kan köpas från: SMHI S-601 76 NORRKÖPING Sweden		

1	INTRODUCTION	1
2	THE SCANDIA CLOUD CLASSIFICATION MODEL	4
2.1	THE ORIGINAL SCANDIA MODEL - VERSION 1.....	4
2.2	THE MODIFIED SCANDIA MODEL – VERSION 2.....	9
3	COMPILATION OF SCANDIA CLOUD CLIMATOLOGIES	14
4	THE SATELLITE DATA SET	20
5	RESULTS FOR THE NORDIC REGION – SCANDIA VERSION 1	23
5.1	TOTAL CLOUD COVER AND CLOUD FREQUENCIES	23
5.1.1	<i>Seasonal and monthly means over the period</i>	23
5.1.2	<i>The annual cycle of cloudiness</i>	28
5.1.3	<i>Inter-annual variability of cloudiness</i>	34
5.1.4	<i>The diurnal cycle of cloudiness</i>	37
5.2	THE SEPARATION INTO VARIOUS CLOUD GROUPS.....	40
5.2.1	<i>Opaque cloud groups</i>	40
5.2.2	<i>Semi-transparent Cirrus clouds</i>	41
5.2.3	<i>Ice and water clouds.....</i>	43
5.2.4	<i>Fog and Stratus</i>	45
5.2.5	<i>Precipitating clouds and deep convective clouds.....</i>	46
5.2.6	<i>Fractional sub-pixel cloudiness</i>	48
6	RESULTS FOR THE NORTHERN EUROPEAN REGION –SCANDIA VERSION 2.....	49
7	VALIDATION RESULTS	52
7.1	COMPARISONS WITH SYNOP OBSERVATIONS	52
7.1.1	<i>Validation of cloud climatologies from SCANDIA Version 1.....</i>	52
7.1.2	<i>Validation of cloud climatologies from SCANDIA Version 2.....</i>	62
7.2	COMPARISONS WITH SOLAR RADIATION MEASUREMENTS.....	63
7.3	COMPARISONS WITH ISCCP, CRU AND CLIMATE SIMULATION DATASETS.....	67
8	THE IMPORTANCE OF INHERENT CALIBRATION ERRORS IN THE NOAA AVHRR DATASET.....	69
8.1	BACKGROUND AND STATUS OF THE AVHRR CALIBRATION PROBLEM FOR VISIBLE CHANNELS	69
8.2	IMPACT ON THE SCANDIA CLOUD CLIMATOLOGY	70
9	DISCUSSION	74
9.1	SUMMARY OF ACHIEVEMENTS REGARDING SCANDIA CLOUD CLIMATOLOGIES.....	74
9.2	THE QUALITY OF SCANDIA CLOUD CLIMATOLOGIES.....	75
9.3	FUTURE PLANS: THE SUCCESSOR TO SCANDIA AND ENGAGEMENTS IN INTERNATIONAL CLIMATE MONITORING PROGRAMMES	77
9.3.1	<i>Future use of SCANDIA cloud climatologies</i>	77
9.3.2	<i>The successor to SCANDIA</i>	78
9.3.3	<i>SMHI engagements in future international cloud climate monitoring activities</i>	80
10	ACKNOWLEDGEMENTS	80
11	REFERENCES	81
APPENDIX 1.	ACRONYM LIST.....	84
APPENDIX 2.	MONTHLY CLOUD CLIMATOLOGIES 1991-2001.....	85

1 INTRODUCTION

Measurements from high resolution imaging sensors onboard both geostationary and polar orbiting satellites have up to the current date been available to the meteorological community for more than three decades. These sensors were particularly designed to enable monitoring of cloudiness and cloud systems and for monitoring of surface conditions over cloud-free areas. However, despite the produced wealth of information during this long period, only a limited number of studies on cloud conditions presenting results from long-term quantitative applications (i.e., climatologies) have been presented. This could be compared to the relatively large number of studies concerning surface conditions (e.g., studies on surface parameters like NDVI – Normalised Difference Vegetation Index – and others, for example as reported by Gutman, 1989 and Glasser and Lulla, 2000). This is explained by the fact that the rather short life cycle of clouds and cloud systems require utilisation of images with high temporal and spatial resolution as a contrast to for example studies of surface parameters. Consequently, the required data amount from high-resolution imagers to enable such studies is enormous.

Quantitative efforts have so far been limited to the compilation of coarse resolution data sets on the global scale to be used e.g. in global climate studies. The most well known example here of such a satellite-based cloud climate data set is produced by ISCCP – the International Satellite Cloud Climatology Project (Rossow and Garder, 1993, and Rossow and Schiffer, 1999). This data set consists of a complete and consistent set of global cloud and radiance parameters derived from sensors on both geostationary and polar orbiting satellites. However, the focus on the global scale has forced the use of a quite limiting sub-sampling technique. Consequently, only a small fraction of the available global satellite data set has been utilised, both in terms of the used spatial resolution and the number of used spectral bands of the sensors. The applied sampling strategy basically means that it is assumed that the dynamical evolution of cloud systems is randomly distributed within a larger segment. Consequently, it should be sufficient to select data from only a few high resolution pixels (for ISCCP with a spacing of about 30 km) within the segment and from this sub-set of data construct statistics from very long time-series of measurements to describe mean conditions valid for the entire segment. This methodology is justified for areas with a weak dependence on local scale features (e.g., over oceanic areas) but for other areas (e.g., near coastlines or steep orography) the method is likely to give unrealistic results.

Even if the interest on global climate studies is continuously high, an increasing attention on the effects of climate change on the regional and local scale has been noticed lately. Many national meteorological services (NMS) and other agencies have launched scientific programmes to try to downscale and interpret the effects of a globally predicted climate change (e.g., see Rummukainen et al., 2000 and Rummukainen et al., 2001). As a consequence of this development, the need of high-resolution data sets for validation of regional climate model simulations of the present and the future climate has increased as well. Here, satellite observations have become increasingly important since this is the only data source that can give a sufficiently good regional coverage of some of the studied meteorological parameters. This concerns in particular cloudiness parameters since the information from the surface observation network is very limited. In addition, reductions in the surface observation network in recent years have cut the amount of available information

and further reductions here are foreseen in the near future. Since there is a direct link between cloud and radiation conditions, it is of utmost importance that cloud conditions are known and modelled correctly in climate models. The treatment of cloudiness is still one of the major uncertainties in climate simulations of today (as discussed by Arking, 1991) and progress must be made here on the global as well as on the regional scale in order to increase the confidence in climate simulations.

Fortunately, progress in computer and archiving facilities have in recent years reached a level that is compatible with the required processing demands for climatological satellite data studies on the local and regional scale. Efforts to compile various kinds of cloud climatologies have consequently been undertaken at some NMS's and at other institutes. The basis for these studies is most often the systematic use of cloud classification models operated on individual satellite scenes. One example of such a data set with relatively high spatial resolution is the METEOSAT CDS data set (EUMETSAT, 1998) which has been produced from operational METEOSAT images for several years now. Other examples are given by Karlsson (1997) and by Kästner and Kriebel (2001).

This report describes results and validation of a ten-year cloud climatology produced by systematic processing of high-resolution multispectral imagery from the AVHRR (Advanced Very High Resolution Radiometer – Lauritson et al., 1979) instrument on the polar orbiting NOAA satellites. The basic tool has been the use of the SCANDIA model – The SMHI Cloud ANalysis model using DIgital AVHRR data (Karlsson, 1996). This model utilises information from all five spectral channels of the NOAA AVHRR instrument - two visible (VIS) channels and three infrared (IR) channels - as a contrast to many previous cloud climatology data sets using only a sub-set of the available AVHRR channels. Of particular interest here is the fact that the data set has been produced using a fixed or frozen cloud classification scheme for the entire period from 1991 to 2000. In this way, the quality of the data set has not been influenced by any updates or changes of the algorithm which means that the quality characteristics is the same for the entire data set as concerns pure model characteristics. This fact is of great importance, e.g., in applications where results are compared to climate simulations. Furthermore, there is no dependence on forecast data from numerical weather prediction (NWP) models in the cloud climatology which further strengthens the use of the data as an independent validation data source for climate models. Although there are more advanced cloud processing schemes available today at SMHI (see Dybbroe et al., 2000) and at other NMS's, the achieved cloud climatology results from the SCANDIA model are believed to be useful and of acceptable quality for many applications. Furthermore, the fact that most cloud classification schemes are very seldom tested and validated during such a long period justifies in itself this study. Validation results for the entire ten-year period is here presented based on a corresponding SYNOP-based climatology over the studied area.

A description of the SCANDIA model is given initially in section 2 followed by a presentation of the method for compilation of cloud climatologies in section 3. The used satellite data set is presented in section 4 and resulting cloud climatologies are then shown in sections 5 and 6. Notice here that a separate study of the effect on the achieved results when introducing a dependency on forecasted surface temperatures from NWP models is also included (section 6). The reason for adding this comparison is that most of the presently world-wide used cloud classifications schemes utilises information from NWP models as an ancillary data source in the cloud screening process. A comparison of results from two different versions of SCANDIA should therefore be able to give some indications of the possible gains and losses in quality after introduction of NWP data use in cloud classifications

in comparison to the original SCANDIA scheme using only static temperature threshold parameters.

Section 7 contains results from an extensive validation effort utilising cloud observations (SYNOP) over Sweden from the same ten-year period. Also comparisons with a few other data sets are shown (including ISCCP).

Section 8 discusses two of the more serious error sources in the described data set (e.g. as emphasised by Cracknell, 2001), namely errors due to degrading satellite sensors and the effects caused by the use of a multi-satellite data set. Processing and archiving constraints at SMHI have not permitted a fully acceptable compensation for these effects. SCANDIA was initially designed for exclusive use in operational weather forecasting applications and the requirements for using the results also in quantitative cloud climate applications (e.g., the use of a high quality calibration of visible radiances) were therefore given little attention initially. Section 8 discusses the possible impact of these defects on the quality of the compiled cloud climatologies. Attempts to estimate the introduced errors are described and some results are presented.

Finally, section 9 presents the major conclusions from this study and outlines the future prospects for the continuation of cloud climate studies based on high-resolution multispectral satellite imagery.

2 THE SCANDIA CLOUD CLASSIFICATION MODEL

The SCANDIA cloud classification model has been described in detail in several previous reports (e.g., Karlsson and Liljas, 1991 and Karlsson, 1996a) and only a brief summary of the most important features is given here. However, details having a major influence on the produced cloud climatologies are highlighted and discussed.

Two versions of the SCANDIA model have been used here:

1. SCANDIA Version 1: Original model used for cloud analysis over the Nordic region for the entire period 1991-2000.
2. SCANDIA Version 2: Modified version using forecasted surface temperatures from a Numerical Weather Prediction (NWP) model and with an improved compensation for varying sun elevations over an extended area.

The reason for involving also the second version of SCANDIA here is to enable a limited study of the importance of the introduction of NWP model data in the cloud classification process and, in addition, the use of an improved compensation for varying illumination conditions. SCANDIA version 2 is also applied on a much larger geographical area covering a large part of northern Europe which means that examples of cloud climatologies on the northern European scale can be shown in addition to the original analyses on the Nordic area. However, due to the necessary increase in the data volume for SCANDIA Version 2, the comparison here is restricted to a period starting in July 1994 and ending in January 1997.

2.1 The original SCANDIA model - Version 1

The SCANDIA model makes use of calibrated and geometrically transformed imagery from all five AVHRR channels at maximum horizontal resolution (at nadir 1.1 km). AVHRR scenes are classified by using seven image features for two different areas (denoted SSWE and NSWE - see Figure 2.1) covering Sweden and large parts of surrounding countries. The pixels in each scene are labelled and separated into a maximum of 23 cloud and surface types (Table 2.1). The main use of each classification image feature is summarised in Table 2.2.

SCANDIA differs significantly from many other internationally reported and operationally used AVHRR-based cloud classification schemes (e.g., APOLLO – described by Saunders and Kriebel, 1988– and LUX – described by Derrien et al., 1993). The difference is related to the fundamental cloud detection methodology. The latter schemes generally apply a sequence of cloud detection tests which are independent and based on data from individual image channels. Thus, if the test in one channel is positive, a cloud is detected regardless if tests in all or several other channels are negative. This methodology is here considered to be quite risky since the cloud separability in some AVHRR channels may be very weak depending on the actual situation. Thus, erroneous cloud detection in such a channel is generally not compensated for by use of more reliable information in other channels. Only an indication that the result has a lower confidence level can be obtained (i.e., this cloud test may be the only test which is positive). As a contrast, SCANDIA uses a systematic coupling between

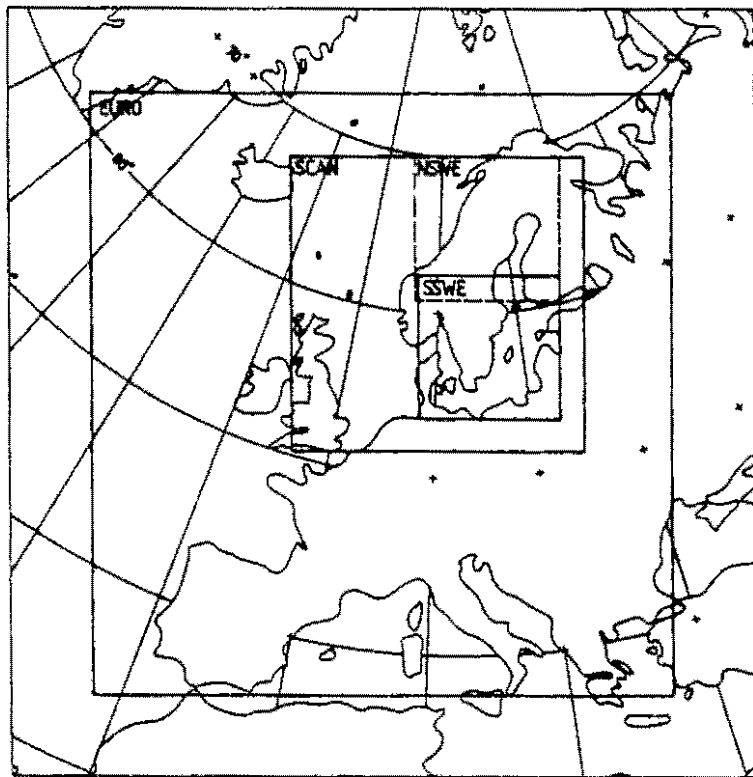


Figure 2.1 Used processing areas for operationally produced AVHRR satellite scenes at SMHI. Cloud climatologies are produced exclusively for the SSWE, NSWE and SCAN areas.

Table 2.1 Cloud and surface classes separated by SCANDIA.

Class number and class description	
1 Open sea without ice	13 Cumulus congestus over sea
2 New ice without snow	14 Small Cumulonimbus
3 Snowcover (also on ice)	15 Extensive Cumulonimbus
4 Winter forest	16 Altocumulus and Altostratus
5 Land (free from snow)	17 Nimbostratus
6 Haze or sub-pixel clouds over land	18 Thin Cirrus over land
7 Haze or sub-pixel clouds over sea	19 Thin Cirrus over sea
8 Fog and Stratus	20 Cirrus over low level clouds
9 Stratocumulus	21 Cirrus over middle level clouds
10 Small Cumulus over land	22 Thick Cirrostratus
11 Small Cumulus over sea	23 Sunglint
12 Cumulus congestus over land	

Table 2.2 Classification image features used by SCANDIA. Calibrated AVHRR channels are denoted CH1, CH2, CH3, CH4 and CH5. TEX4 means a local (in a 5x5 pixel window) highpass filtering of CH4 followed by a lowpass filtering (in a 11x11 pixel window) to measure the small scale variation of brightness temperatures.

Feature Number	Composition	Quantity	Main use for classifier
1	CH1	Bi-directional reflectance	Daytime separation of clouds and snow from land surfaces. Used coupled with feature 4.
2	CH1-CH2	Reflectance difference	Daytime separation of land surfaces with vegetation from sea surfaces. Used also for snow detection.
3	Land mask	Land or sea indication	Geographic map used for land/sea-separation at night and for low sun elevations.
4	CH3-CH4	Brightness temperature difference	Separates all clouds from land and sea surfaces during daytime. Important at night for fog, Stratus and Cirrus detection. Coupled with feature 1 during daytime.
5	CH4	Brightness temperature	Separates main cloud groups Low, Medium and High clouds by comparing with mean temperatures at 500 hPa and 700 hPa.
6	CH5-CH4	Brightness temperature difference	Separates thin clouds (especially Cirrus clouds) from thick clouds both night and day.
7	TEX4	Temperature variance	Separates clouds with high small scale texture (e.g. Cumulus) from more homogeneous clouds (e.g. Stratus).

image data from several individual AVHRR channels in order to optimise the cloud separability. This method is sometimes referred to as “grouped thresholding”.

Thus, the SCANDIA strategy has been to use several AVHRR channels simultaneously for the basic cloud detection task. During daytime, these channels are channels 1, 3 and 4 in the form defined by features 1, 4 and 5 in Table 2.2 and during night, the channels are channels 3, 4 and 5 (features 4, 5 and 6 in Table 2.2). At twilight, also AVHRR channel 1 (feature 1) is used together with the three infrared channels. Remaining AVHRR channels are used later in the further sub-division into different cloud and surface classes. For example, features 1, 4 and 5 are used together for cloud detection during daytime while features 6 and 7 provide complementary information for the cloud type separation.

Feature 4 is obviously central for the SCANDIA classifier since it plays a major role in cloud discrimination, both day and night. The variation of the cloud threshold for this feature is described in Figure 2.2 as a function of sun elevation. As indicated here, the SCANDIA thresholds are defined in discrete sun elevation intervals and there is also a limited seasonal dependence (see Karlsson, 1996a, for further details). Of importance here is that only one set of thresholds (valid for only one sun elevation interval as determined by the conditions in the

central portion in each of the processing areas in Figure 2.1) is used for each individual cloud classification.

Figure 2.2 shows that all clouds are separated from cloud-free surfaces by use of the same feature 4 threshold during day (i.e., the feature is used as a lower cloud threshold at medium to high sun elevations). To be remembered, however, is that the threshold is conditionally used together with the threshold in feature 1. This circumstance enables an effective separation between clouds and snow covered surfaces utilising that snow surfaces do not reflect in AVHRR channel three in contrast to clouds. Notice also how thresholds for the two categories *water clouds* and *ice clouds* diverge from each other at night and in twilight. For ice clouds, the threshold is here used as a lower cloud threshold while for water clouds it is used as an upper threshold. However, it must be emphasised that the term ice clouds is here restricted to mean exclusively semi-transparent Cirrus clouds. Thick ice clouds (e.g. including Nimbostratus and Cumulonimbus cloud types) are not identified by use of these thresholds. The latter clouds are identified by use of feature 5 at night/twilight as described in Figure 2.3. Notice here that feature 5 is only used for discrimination of thick medium- or high-level clouds and not for low-level clouds.

The daytime coupling between features 1 and 4 is also crucial for the separation of sunglint and water clouds. It is here utilised that the relative effect of sunglint in feature 4 (in terms of the achieved brightness temperature difference) is larger than for water clouds which have resulted in the sunglint thresholds described in Figure 2.4.

For the final separation into different cloud types, several threshold tests follow based on all features except feature 3. Water and ice clouds (here including Nimbostratus and Cumulonimbus cloud types) during daytime are separated by use of features 4 and 6. The separation into low-, medium- and high-level cloud types is accomplished by use of feature 5 where the used thresholds are defined by the average temperature in the 700 and 500 hPa

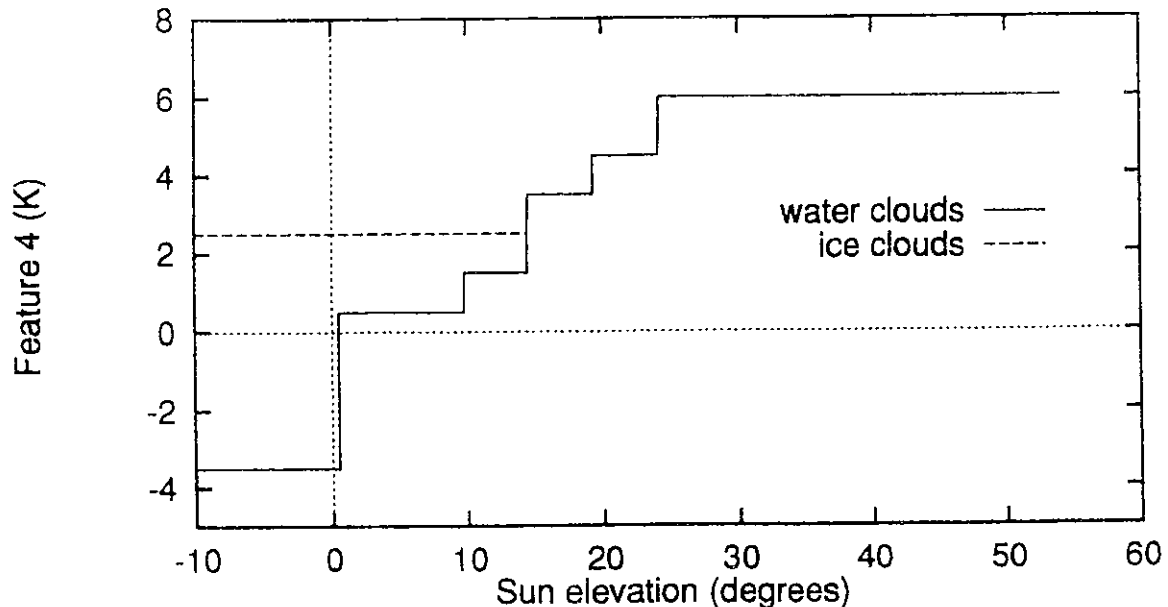


Figure 2.2 Feature 4 thresholds (temperature differences) as a function of sun elevation.

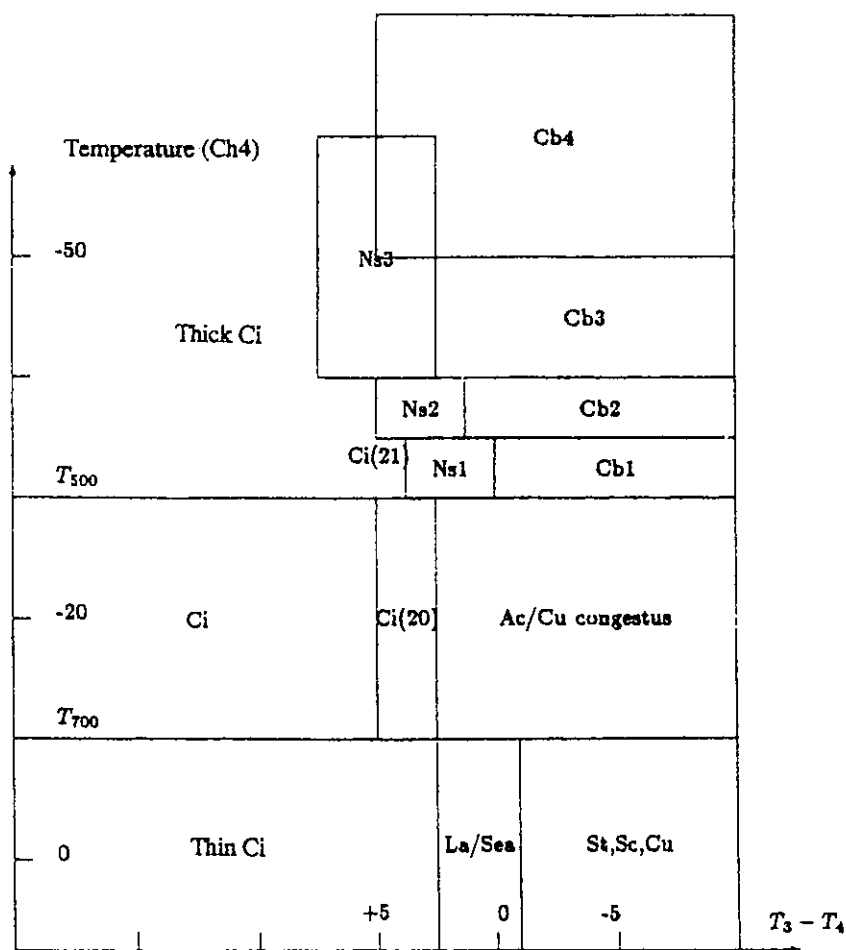


Figure 2.3 SCANDIA cloud classification during night using features 4 (here denoted $T_3 - T_4$) and 5 (here denoted Temperature Ch4).

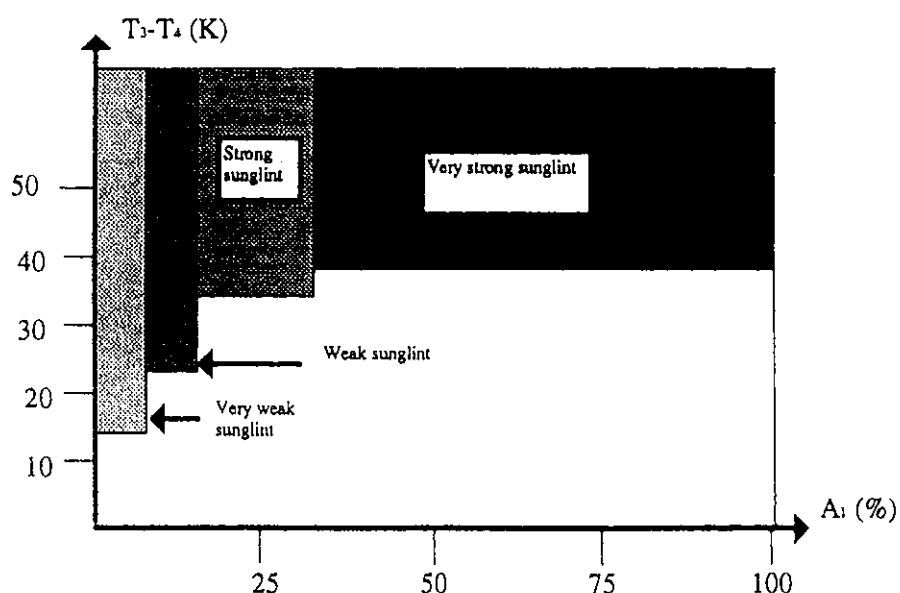


Figure 2.4 SCANDIA sunglint discrimination using features 1 (here denoted A_1) and 4.

levels, respectively, computed from operational NWP analyses (the HIRLAM model – see Källén, 1996). As a last step completing the number of classes in Table 2.1, the different low-level cloud groups are separated by use of the texture feature (feature 7). Some more details on the separation into the different cloud types are given later in section 3.

It should also be mentioned that, in addition to the basic classes described in Table 2.1, attempts to make even a further separation and identification of classes have been performed. This concerns the identification of sub-pixel or fractional clouds in a separate category as well as a further sub-division of the precipitating cloud types (Nimbostratus and Cumulonimbus) into qualitative precipitation intensity classes. The fractional cloud category aims at identifying very thin cirrus clouds and very small cumulus cloud elements. It is composed by those pixels having feature values very close (on the cloud-free side) to the used cloud detection thresholds. The precipitation categories (mainly describing the three categories Weak, Moderate and Heavy precipitation) were defined based on simple assumptions on relationships between reflectances in AVHRR channel 1, brightness temperatures in channel 4 and the reflectance characteristics in channel 3 (as defined by feature 4). More details on this separation are given in Karlsson (1996a).

An example of a sequence of SCANDIA cloud classifications from the original model version is shown in Figure 2.5 . However, notice here that the two processing areas SSWE and NSWE have now been merged and the image resolution has been reduced to 4 km (for reasons becoming more obvious later in section 3).

Finally, it must be made clear that SCANDIA is a supervised cloud classification scheme where thresholds were determined from examination of a large number of AVHRR scenes in the period 1986-1991 (from satellites NOAA-9, NOAA-10, NOAA-11 and NOAA-12). These studies relied basically on data in the central portions of AVHRR scenes viewed with relatively low satellite zenith angles. Thus, SCANDIA results in parts of AVHRR scenes with high satellite zenith angles (near swath edges) are not considered as being fully reliable. The reason is the absence of appropriate corrections for both the anisotropic behaviour of reflection and the increased effect of atmospheric absorption in infrared channels at high viewing angles.

2.2 The modified SCANDIA model – Version 2

A modified version of SCANDIA was introduced at SMHI in July 1994 to be operated on a much larger area covering a substantial part of northern Europe (area SCAN in Figure 2.1). However, in order to avoid a large increase in data volume, resulting if deciding to continue using imagery at maximum horizontal resolution and also including the data added when introducing new ancillary information, it was decided to process the modified SCANDIA version on a coarser resolution at 4 km. The reduction of the image resolution made the use of the texture feature (feature 7 in Table 2.2) questionable and it was therefore omitted. However, the decision to utilise forecast information from the HIRLAM NWP model introduced three additional image features (see Table 2.3). These additional features consist of HIRLAM temperature forecasts interpolated from the 55-km grid resolution to the nominal AVHRR image resolution of 4 km. It must here be clarified that the additional HIRLAM image features are used mainly for defining geographically varying thresholds applied to feature 5. For example, we are here using the interpolated value of the 700 and 500 hPa temperatures, respectively, taken from the closest HIRLAM gridpoints for each pixel instead of the average over the entire area as in the original version of SCANDIA.

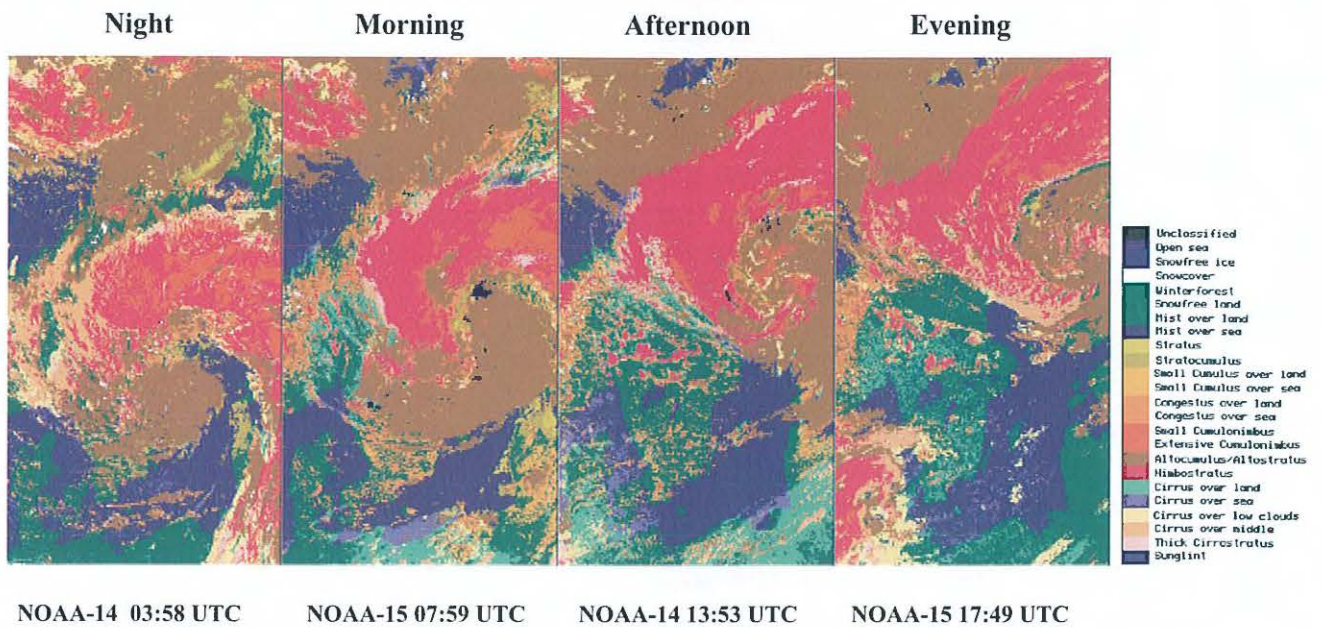


Figure 2.5 Sequence of four SCANDIA cloud classifications with the original model version from May 26 2000. The pictures show merged results on both areas SSWE and NSWE with a reduced pixel resolution (4 km).

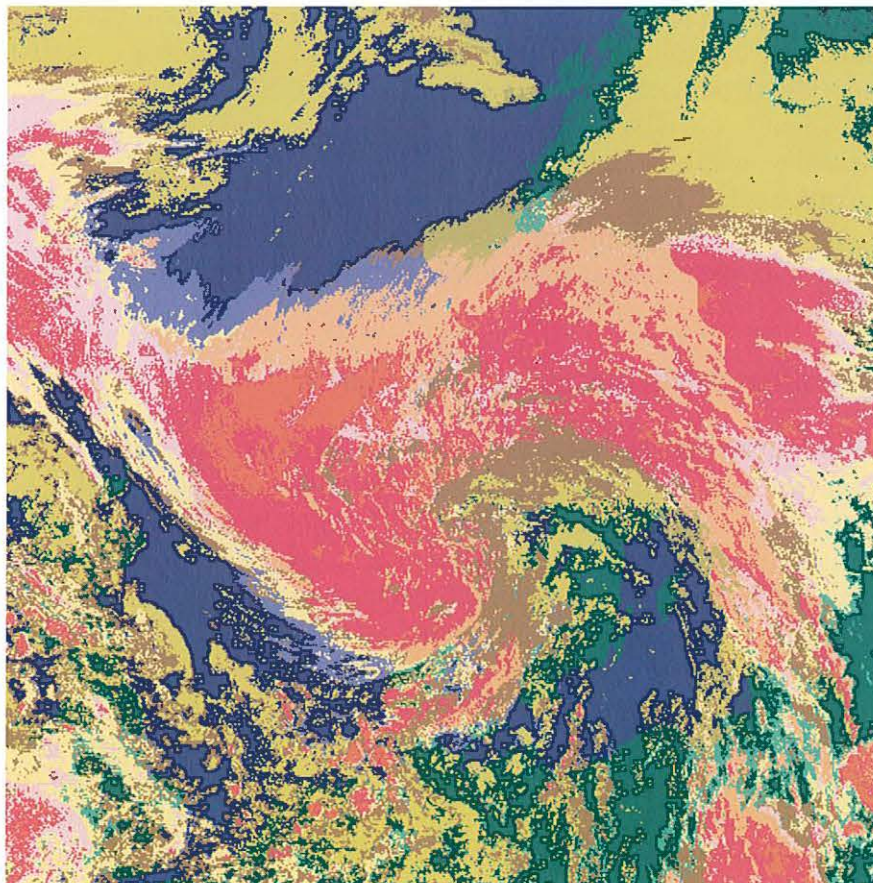


Figure 2.6 SCANDIA NOAA-11 cloud classifications for area SCAN with the modified model version from 9 September 1994 at 15:07 UTC. Same colour legend as in Figure 2.5.

Table 2.3 *Image features used by the modified SCANDIA model. Same notation as in Table 2.2.*

Feature number	Composition (name)
1	CH1
2	CH1-CH2
3	Land mask
4	CH3-CH4
5	CH4
6	CH5-CH4
7	HIRLAM forecast of 700 hPa temperature (T700)
8	HIRLAM forecast of 500 hPa temperature (T500)
9	HIRLAM forecast of surface temperature (TSUR)

In addition, the use of very short range forecasts (9-12 hours forecast lead time) instead of analyses should be able to give a better description of tropospheric temperature changes in cases of rapid weather developments. NWP analyses are normally only accessible after several hours (2-4 hours) and therefore the used values in the original SCANDIA version was often found invalid, especially in connection with rapid weather developments.

Beside the use of spatially varying thresholds for the infrared channel in feature 5, it must also be mentioned that SCANDIA version 2 also uses a correct assignment to the used sun elevation categories for each pixel. This differs from SCANDIA version 1 where pixels near the corners of the processing area could be processed with thresholds valid for an incorrect sun elevation category.

However, the most drastic change compared to SCANDIA version 1 was the introduction of forecasted surface temperatures (the TSUR feature in Table 2.3) for the interpretation of feature 5 values. Previously, the use of feature 5 was very limited for the fundamental cloud detection process (restricted to nighttime identification of mid- and high-level clouds – see Figure 2.3). The reason for this was that, although it is clear that apparent brightness temperatures of clouds most often are much colder than the corresponding temperatures for the cloud free surface, it was very problematic to assign a proper value of the used threshold due to the very large variation of true surface temperatures. Especially during night conditions and during the winter season in northern latitudes, the apparent brightness temperature difference between the surface and low-level (in winter even mid-level) clouds is often low. However, progress of NWP modelling had in 1994 enabled access to useful forecasted surface

Table 2.4 *Important parameters defining dynamic thresholds for the new version of the SCANDIA model.*

Parameter	Meaning	Typical value
TEMPADD	Requested minimum temperature difference (feature 5 - feature 9) between surface and clouds for cloud discrimination.	8 K
TSURBIAS	Compensation for bias in HIRLAM surface temperature forecasts (too warm in extremely cold situations).	10 K
COLDLAND	Cloud tests using TEMPADD excluded for surfaces colder than COLDLAND (in cold winter situations) in feature 9.	270 K
NOISETEMP	Noise filtering by a 5x5 pixel wide low-pass filter. Performed in feature 4 for areas colder than NOISETEMP in feature 9.	277 K

temperatures which then could be used as a good first guess of true surface temperatures. This fact changed also the sequential order of threshold test in the modified version of SCANDIA. Instead of relying heavily on feature 4, SCANDIA version 2 started its basic cloud screening with a single test using feature 5. Additional clouds could thereafter be assigned by use of feature 4 and other features in the same way as in SCANDIA version 1 followed by a further sub-division of cloud and surface types.

A few additional model parameters were introduced as described in Table 2.4. The most important here is TEMPADD, describing the required temperature difference between the forecasted surface temperature and the apparent brightness temperature in feature 5 for the assignment of a pixel as being cloudy. This parameter must be optimally chosen since if it is too small the risk is high for mis-classifications due to uncertainties in the NWP forecast and if it is too large there is a risk that near surface clouds remain undetected. The TSURBIAS parameter is used in an attempt to compensate for the NWP model problem to correctly forecast very low minimum temperatures (partly also due to the difference in spatial resolution). The COLDLAND parameter is used to stop discrimination of low-level clouds by the TEMPADD thresholding test in cold weather situations at night and in twilight due to the high risk of presence of near-surface temperature inversions. In addition, at surface temperatures higher than COLDLAND, the TEMPADD test is also omitted if the forecasted surface temperature is lower than the forecasted 700 hPa temperature (indicating the existence of strong near-surface temperature inversions). In the latter case, pixels are left unclassified if there are no additional signs of cloud presence in other features (especially in feature 4). However, this category has in this study been treated as being cloud-free since experience from operational use has shown that the situations with very strong temperature inversions are predominantly cloud-free and very seldom cloudy. The risk for mis-classifications here were therefore assumed to be low (although now depending on reliable NWP model forecasts) despite the obvious non-separability of cold cloud-free surfaces and mid- and high-level ice

clouds as shown in Figure 2.3. The validity of this assumption will be discussed later in sections 6 and 7.1.

More details about the treatment of conditions with near-surface temperature inversions in SCANDIA were given by Karlsson (1996a) and Godøy (1998) and Hultgren et al. (1999) have later presented additional aspects.

Finally, the parameter NOISETEMP is used to introduce a filtering of values in feature 4 for cold situations in order to reduce effects caused by noise in AVHRR channel 3.

An example of a SCANDIA cloud classification with the modified model version is shown in Figure 2.6. Notice, however, that all low-level cloud classes are here treated as one single category (yellow colour) as a contrast to SCANDIA version 1 in Figure 2.5.

Finally, it must be mentioned that results from the modified version of SCANDIA have been quantitatively used in the mesoscale objective analysis scheme MESAN at SMHI since 1996 (Häggmark et al., 1997, Häggmark et al., 2000 and Michelson et al., 2000).

3 COMPILATION OF SCANDIA CLOUD CLIMATOLOGIES

A method for compilation of SCANDIA cloud climatologies has earlier been described by Karlsson (1994), Karlsson (1995) and Karlsson(1997). Here, a slightly modified version of this method has been used.

The idea has been to exclusively use AVHRR scenes with good viewing conditions (i.e. low satellite zenith angles) over the area. This should minimise possible SCANDIA errors due to the present lack of an appropriate correction for effects caused by large viewing angles. Consequently, only the satellite passage with the highest satellite elevation among several consecutive passages at descending and ascending passage nodes has been chosen. This means that with two operational NOAA satellites four useful AVHRR scenes per day were chosen over the area at the reception site in Norrköping. In practice, this meant that only satellite scenes with a maximum satellite elevation exceeding approximately 45° were selected.

Table 3.1 shows an overview of the selected satellite scenes and their associated passage times. Notice here that passage times are given in Central European Time (CET= UTC + 1 hour) in order to correspond as closely as possible to the true solar time over the area. At least one passage with sufficiently low satellite zenith angles is normally guaranteed within the indicated time-windows in Table 3.1 each day. However, the NOAA satellite orbits are not perfectly stable which means that considerable deviations from these time windows occurred for some years in the period (for more details here, see next section).

Table 3.1 Approximate time-windows (CET) valid for the used satellite scenes during the period 1991-2001 (see also text for further discussion).

Time of day	Time-window (CET)	Satellites
Night	02:30 – 04:30	NOAA-11 + NOAA-14
Morning	07:30 – 09:30	NOAA-10 + NOAA-12 + NOAA-15
Afternoon	14:00 – 16:00	NOAA-11 + NOAA-14
Evening	17:30 - 19:30	NOAA-10 + NOAA-12 + NOAA-15

The chosen satellite passages describe roughly cloud conditions at night, in the morning, in the afternoon and in the evening as visualised by the previous cloud classification example in Figure 2.5. Thus, the compiled cloud climate data set has a potential to describe mean cloud conditions during these four time-periods. It is hoped that the four daily observations can be used to roughly describe mean daily cloud conditions and the diurnal cycle of cloudiness. Cloud climatologies from surface stations (SYNOP) have been compiled in a similar way for many years now (based on observations at 00 UTC, 06 UTC, 12 UTC and 18 UTC). The method described here brings a possibility to extend this method to be applied over large areas with a homogeneous and constant spatial resolution as offered by satellite

measurements. Furthermore, a comparison of the satellite data set with a corresponding data set from SYNOP is presented later in section 7.

Regarding the analyses of total cloud amounts, the cloud climatologies from SCANDIA were compiled as described by the following seven steps:

- I. Cloud classification result images were resampled by use of a nearest neighbour resampling technique in order to reduce the nominal horizontal resolution from one km to four km.
- II. Classification results for the two areas (SSWE and NSWE in Figure 2.1) were merged into one result image (as shown in Figure 2.5).
- III. Each pixel in the classification image was labelled cloudy or cloud-free depending on the resulting cloud and surface types.
- IV. Pixels classified as sub-pixel clouds (cloud contaminated) were identified and given half the weight as compared to pixels labelled as cloudy.
- V. Daily cloud frequencies were estimated by averaging results from the four observation times.
- VI. Cloud frequencies for entire months were estimated by calculating the fraction of the total number of selected scenes within a month where the pixel was labelled as cloudy.
- VII. Conversion of cloud frequencies to fractional cloud cover was finally accomplished by averaging over nine by nine pixels (representing a quadratic area of approximately 36 by 36 km in size).

The reason for reducing the nominal spatial image resolution in Step I was mainly to keep the data volume tractable. This measure may seem inappropriate at present time when storage media and storage methods easily allow treatment of high-resolution data sets (e.g., SCANDIA 1 km results have in fact been stored since 1997). However, the wish to create a climatology over an as long as possible time period forced the use of the coarser resolution to keep the data set homogeneous and consistent. Furthermore, standard methods for image navigation based on both the TBUS and TLE orbital modelling approaches (described by Rosbourough et al., 1994) have been used at SMHI. This means that the absolute accuracy of navigation is not compatible with the maximum nominal image resolution of 1 km. An accuracy of approximately 4 km is more realistic here which supports the use of a reduced resolution. The task to compile climatologies at maximum nominal resolution requires specific efforts for ensuring a corresponding accuracy in navigation (e.g., as described by Bordes et al., 1992). Finally, an obvious disadvantage of the use of the nearest neighbour resampling technique here is that only a small fraction (one pixel out of a total of 16 pixels in the original high resolution classification image) has finally been utilised when compiling the cloud climatologies. In this sense, the presented SCANDIA cloud climatology is also formed by use of a sub-sampling technique (as for e.g. ISCCP as mentioned in Section 1) but here with a much denser spacing (4 km sampling in comparison to approximately 30 km for ISCCP).

The method of treating pixels labelled as cloud contaminated in Step IV was chosen as the most appropriate way of handling this problem. SCANDIA does not interpret any fractional cloud cover within a single pixel, it only indicates pixels that most likely contain sub-pixel sized cloud elements. It is in practice impossible to apply one single reliable method for estimation of sub-pixel fractional cloud cover since the method need be different depending on the actual cloud type which generally is not known. Consequently, a compromise method giving these pixels a 50 % weight in calculations of fractional cloud is used. This should be able to minimise errors in the calculations (see Kidder and Vonder Haar, 1995).

The conversion of cloud frequencies to fractional cloud cover in Step VII is evidently required if wanting to compare results with corresponding SYNOP observations. Furthermore, this quantity is probably one of the more valuable quantities to be used in comparison with results from NWP and climate simulation models. The choice of an averaging area size of 36 by 36 km was based on previous experiences made when comparing satellite observations with ground observations (Karlsson, 1995, Karlsson, 1996a and Wollenweber, 2000). However, for many of the specifically studied cloud categories (see description below) results were kept in the form of 4-km resolution cloud frequencies in order to study possible small-scale geographical variations. It should also be noted that in theory, the cloud frequencies should in the statistical sense converge towards the true value of the mean cloud cover if using data from very long time series. If also assuming that cloud fields (here including fields of cumulus cloudiness) are often much larger in their horizontal dimensions than the used AVHRR pixel resolution this becomes even more evident.

Some problems with NOAA HRPT receptions occurred during the studied period (see also section 4). In serious cases entire satellite scenes were lost but more common was that individual or often several adjacent scan lines in scenes were lost during reception. This generated erroneous results in SCANDIA classifications, mainly because of the effects introduced by use of the spatial filtering feature (feature 7 in Table 2.2). Since this error couldn't be automatically removed and since also other corrupt classification scenes could be generated due to technical processing problems, all used classification images were also visually inspected. Images with the above mentioned defects were either manually edited (areas with missed scan lines were masked) or removed (if a large part of the image was affected). However, no results other than those affected by the mentioned technical processing and reception problems were removed from the satellite data set.

From Table 2.1 it is clear that, besides the estimation of the total fractional cloud cover, it should also be possible to estimate the contribution to the fractional cloud cover or the 4 km cloud frequency from individual cloud types. However, from the experience of using results from SCANDIA in operational weather forecasting, it was clear that a realistic separation of all of the listed cloud classes in Table 2.1 was only possible in cases of good observation and separability conditions (i.e., at high sun elevations and in the summer season). Consequently, a further grouping of the cloud types have been used here to investigate the contribution from different cloud types. The cloud groups and their composition are listed in Table 3.2 together with a brief summary of the main discrimination method for each group.

For a correct understanding of the various cloud groups listed in Table 3.2 it is important to consider that the satellite perspective generally does not allow a correct estimation of cloudiness below the topmost cloud layer. Some attempts are made here for semi-transparent cirrus clouds but the task to identify sub-layer clouds is impossible in case of opaque high- and medium-level clouds.

It is also evident that a few more cloud groups could be composed from the cloud groups in Table 3.2. The following two categories are of importance here:

- **Water clouds = Opaque low-level clouds + Opaque medium level clouds**
- **Iceclouds = Semi-transparent Cirrus clouds + Opaque Cirrus clouds**

It should be repeated here that the separation of these two groups is based on the following typical spectral differences for the two groups:

- Nighttime separation of water clouds and semi-transparent ice clouds by use of feature 4 (see Figure 2.2)
- Daytime separation of water clouds and semi-transparent ice clouds by a combined use of features 4 and 6
- Daytime identification of Cumulonimbus and Nimbostratus clouds (assumed to be ice clouds here) by use of features 1, 4 and 5
- Nighttime identification of Cumulonimbus and Nimbostratus clouds (assumed to be ice clouds here) by use of feature 5.

The appearance in feature 4 is judged as the most important spectral signature for the discrimination of these two groups. This is explained by the fact that ice clouds are more absorbing than water clouds in this spectral region which is visualised by simulated single scattering albedos for typical ice and water clouds in Figure 3.1. However, the use of fixed

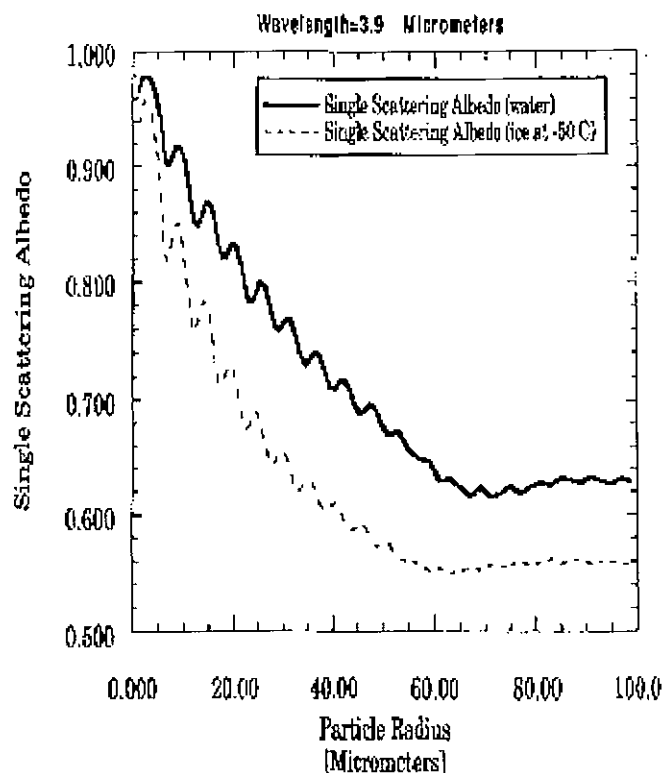


Figure 3.1 Single scattering albedos at $3.9 \mu\text{m}$ for typical ice and water clouds as a function of particle radius. (from NOAA/NESDIS and CIRA, 2001)

Table 3.2 Studied cloud groups in the SCANDIA cloud climatology. Cloud group composition is shown and the corresponding main discrimination method is briefly described (see also previous section 2 and Table 2.2).

Cloud group	Cloud types	Principal discrimination method
Total fractional cloud cover (cloud mask)	All cloud types including fractional clouds (see below)	SCANDIA Version 1: Daytime: Pixels with values exceeding feature 1, 4 and 5 thresholds. Nighttime: Pixels exceeding feature 4 ice cloud thresholds (semi-transparent clouds), or falling below feature 4 water cloud thresholds or exceeding feature 5 thresholds (opaque mid- and high-level clouds). SCANDIA version 2: Same as above but, in addition as a first step screening, pixels falling below the forecasted surface temperature minus an offset value in feature 5.
Semi-transparent Cirrus clouds	Thin Cirrus, Thin Cirrus over low-level clouds, Thin Cirrus over mid-level clouds	Cloud pixels exceeding feature 6 threshold (1.5 °C).
Opaque Cirrus clouds (Opaque high-level clouds)	Thick Cirrostratus, Cumulonimbus, Nimbostratus	Cloud pixels with feature 6 values below a threshold and feature 5 values lower than 500 hPa temperatures.
Opaque medium-level clouds	Altocumulus/-Altostratus, Cumulus congestus	Opaque clouds pixels with feature 6 values below a threshold and with feature 5 values between temperatures of the 700 hPa and 500 hPa levels.
Opaque low-level clouds	Fog/Stratus, Stratocumulus Small Cumulus	Opaque cloud pixels with feature 6 values below a threshold and feature 5 values higher than 700 hPa temperatures.
Fog and Stratus	Fog/Stratus	Same as above but with feature 7 values below a threshold.
Fractional clouds	Very thin Cirrus, Very small Cumulus, Haze/Sub-pixel clouds	Pixels very close (on the cloud free side) to the thresholds in features 1 and 4.
Precipitating clouds	Cumulonimbus, Nimbostratus	Cloud pixels with values exceeding thresholds in features 1, 4 and 5.
Deep convective clouds	Sub-division of Cumulonimbus and Nimbostratus	Same as above but using thresholds modified by an offset value (to delineate very cold and very bright clouds).

thresholds (at every sun elevation category) in SCANDIA will not be able to completely cover the true variation of the ice and water cloud appearance due to the complex dependency on cloud microphysics. For example, it is clear that a water cloud with relatively large cloud droplets at cloud top level could potentially produce a spectral appearance in AVHRR channel 3 which is almost identical to an optically thick ice cloud with small ice crystals (compare with Figure 3.1). Thus, the SCANDIA separation of ice and water clouds should in reality better be characterised as a separation of clouds with small and large effective cloud droplet radii.

Finally, there is also one class in Table 3.2 consisting of the single cloud type **Fog/Stratus** which has been specifically studied. The idea here was to see if it was possible to get indications on preferred geographical locations for the formation and persistence of fog and Stratus clouds.

4 THE SATELLITE DATA SET

Satellite data from a complete ten-year period has been used in this study. The data set starts in February 1991 and ends in January 2001. This particular choice of period is explained by historical reasons and shows that the main motivation for starting archiving the SCANDIA cloud classifications was not primarily for the creation of cloud climatologies. This possibility slowly emerged after some years of completed archiving. The archiving facility only permitted the storage of cloud classification results and some limited additional original visible and infrared scenes. Consequently, no reprocessing of cloud classifications was possible from raw AVHRR scenes which has limiting implications for the quality of the data set. This topic is further discussed in section 8. A fully successful archiving of the required NOAA AVHRR scenes (according to Table 3.1) would theoretically result in a total number of 14 336 cloud classifications during the period. Unfortunately, due to HRPT reception problems, technical processing problems and unforeseen failures of operational NOAA satellites (NOAA-11 in September 1994 and NOAA-15 in July 2000), only 87 % (12 470) of the theoretically available satellite scenes have been used. The use of night and afternoon passages stayed at 86 % of the theoretically available scenes while the level of used scenes in the morning and in the evening was slightly higher; 89 % and 88 %, respectively. The loss of the night and afternoon satellite (NOAA-11) between September 1994 and March 1995 explains the major part of this difference.

Figure 4.1 gives an overview of the entire satellite data set during the period and a year-by-year summary of the degree of utilisation compared to the number of theoretically available scenes is shown in Table 4.1. Notice that the passage times in Figure 4.1 are given in Central European Time (used in Sweden) in order to give an indication of the true solar time during the satellite passages. To be noticed in Figure 4.1 are the following details:

- NOAA-10 was used in the morning and in the evening until September 1991 (Sep 4) when it was replaced by NOAA-12.
- NOAA-11 was used at night and in the afternoon until September 1994 (Sep 14) when it was abruptly lost. It wasn't replaced by NOAA-14 until in February 1995 (February 28).
- NOAA-12 was used in the morning and in the evening between September 1991 (September 5) until September 1998 (September 13) and between July 2000 (July 23) and January 2001 (due to the loss of NOAA-15). In addition, data from the morning passage was also used in March-April 1999 during experiments with NOAA-15 (transmission of AVHRR channel 3A data at 1.6 microns).
- Archiving problems (tape failure) lead to the loss of all data from June 1998.
- NOAA-15 was used in the morning and in the evening between September 1998 (September 14) and July 2000 (July 22) when it was abruptly lost. The reappearance of useful data from NOAA-15 occurred unfortunately after the end of the studied period (in February 2001).

The instability of satellite orbits caused considerable variation of passage times during the period, for some periods even outside the targeted time windows described earlier in Table 3.1. This concerns especially conditions at the end of the period when passage times for NOAA-12 and NOAA-14 converged and partially overlapped. The instability of orbits is further illustrated in Figure 4.2 which also shows the typical detailed pattern of useful NOAA-14 scenes day by day during one particular month (July).

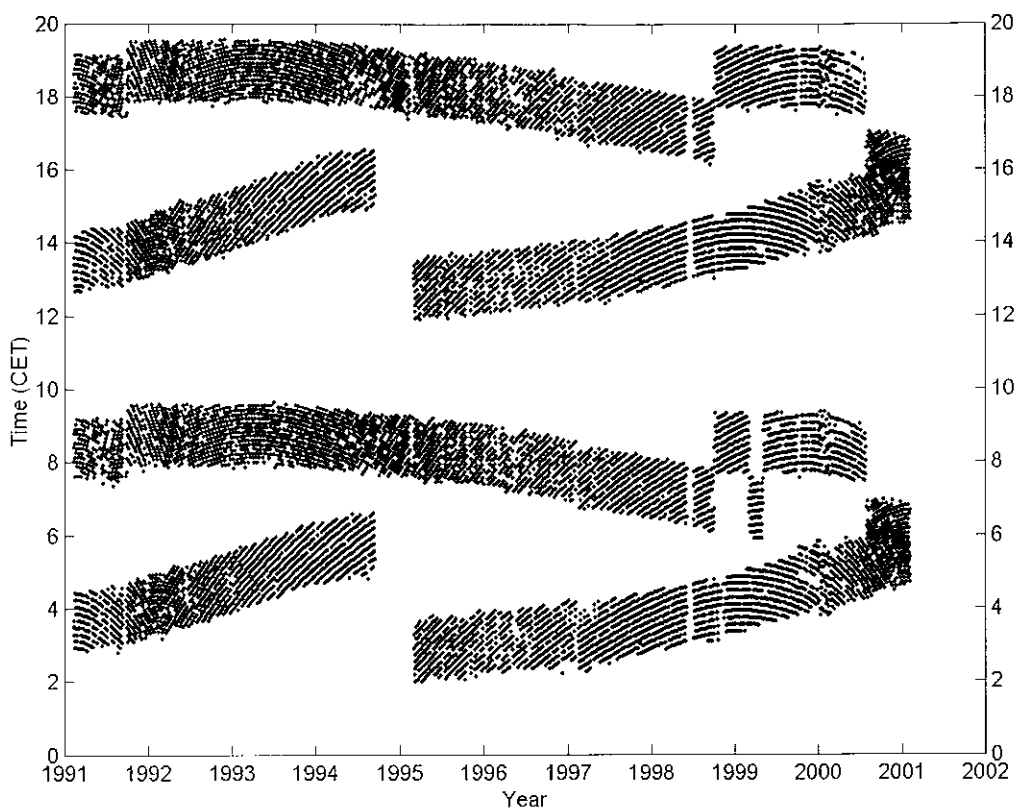


Figure 4.1 Display of all the used satellite scenes (each dot denotes an individual satellite passage) and their corresponding passage times in Norrköping in the period February 1991 until January 2001.

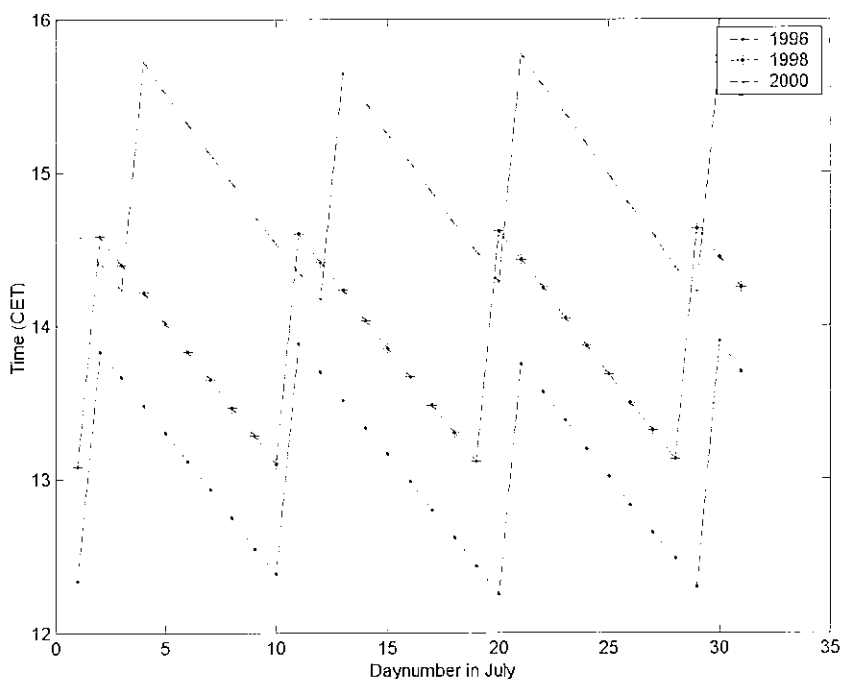


Figure 4.2 Detailed display of useful NOAA-14 afternoon scenes during the three July months of 1996, 1998 and 2000.

Table 4.1 Summary of utilised compared to theoretically available satellite scenes (%) year by year in the period February 1991 until January 2001.

Year	<i>Total utilisation</i>	<i>Night</i>	<i>Morning</i>	<i>Afternoon</i>	<i>Evening</i>
	(%)	(%)	(%)	(%)	(%)
1991	78	79	75	81	79
1992	92	93	92	91	92
1993	92	95	90	94	91
1994	78	67	93	65	88
1995	80	75	88	73	84
1996	78	80	78	78	77
1997	90	90	89	90	90
1998	86	83	89	86	87
1999	92	93	91	95	90
2000	84	89	83	88	78
2001	90	84	97	84	97

5 RESULTS FOR THE NORDIC REGION – SCANDIA VERSION 1

Results for all the cloud groups given by Table 3.2 have been compiled. Here, results concerning the overall group *total fractional cloud cover* are given most of the attention (section 5.1). One reason is that this is the parameter that most conveniently can be compared to surface observations (see also section 7.1). Furthermore, the quality of this parameter determines basically the potential of the cloud screening method for being used in many other applications (e.g., for pre-processing in SST and NDVI derivations). It can also be said that this parameter is a primary cloudiness parameter to be used when checking the quality of simulated cloudiness in NWP and climate models. Because of the primary importance of this cloud parameter, a complete collection of results from all individual months in the period is shown in Appendix 2.

For the other cloud parameters (described in section 5.2), which complements and brings further details on cloud types, we must remember that they have to be evaluated in the light of the performance of the basic cloud masking method.

5.1 Total cloud cover and cloud frequencies

5.1.1 *Seasonal and monthly means over the period*

The mean total fractional cloud cover for the four seasons Winter (December-February), Spring (March-May), Summer (June-August) and Autumn (September-November) is shown in Figure 5.1. Notice here that all months except January are taken from the period 1991-2000. For January, the period 1992-2001 has been used. This means that to get ten complete winter seasons, the tenth and last one has been composed by December 2000, January 2001 and February 1991. To illustrate also the resulting small scale features, cloud frequencies with the maximum 4 km pixel resolution are also shown in Figure 5.2 for the selected months of January, April, July and October. Notice here that the lateral discontinuity in cloud frequencies indicated in the central portion of the area (most clearly seen for October) is caused by differences when processing images in the two areas SSWE and NSWE as described earlier in section 2.1. During the dark seasons, it was very common that night conditions prevailed in area NSWE (only IR data used) while area SSWE had twilight conditions (both IR and VIS data used). This caused inevitably a discontinuity in result images.

A typical feature of the cloud climate in the region is the overall high cloud amounts in the winter and autumn seasons, ranging from 70 to 85 % with only a small geographical variation. A weak minima in cloudiness is found in an area around the Swedish coast of the Bothnian Sea. The appearance of this minima is likely to be a result of the frequent occurrence of mild winter months with strong westerly winds over the area during the 1990's (e.g. in 1993 and 2000 - see Appendix 2). Weak maxima are found over the inner part of southern Sweden, over the Scandinavian mountain range and over the outer parts of the Norwegian Sea. Cloud amounts appear also to be quite high over large areas in Finland and in the Baltic States, especially in winter. However, the high inland values in Finland and in northern Sweden are generally found to be too high and caused by the non-separability of

cloud-free very cold ground surfaces and mid- and high-level ice clouds (as indicated in Figure 2.3). This problem is further discussed later in section 7.1).

As a contrast to winter and autumn conditions, much less cloudiness and much larger geographical variations are found during the spring and summer seasons. The influence of seawaters and major lakes is pronounced causing drastic reductions in cloudiness, especially in summer. However, one remarkable exception from this pattern is found over the visible offshore parts of the Norwegian Sea. Here, cloud amounts continue to be high and even increases slightly compared to the darker and colder seasons. Since at the same time cloud amounts in the Scandinavian mountain range increase during spring and summer, a remarkable minimum in cloudiness appears in the inner part of the Norwegian Sea close to the coast. This minimum is most clearly seen during spring (most remarkable in Figure 5.2). The reason for the formation of this minimum is believed to be a combination of several dynamical and surface-forcing mechanisms. Convection creates during the summer half of the year high cloud amounts in the Scandinavian mountain range (caused by the well-known slope-and-valley circulation –see Atkinson, 1981). The induced secondary circulation as well as the more ordinary sea-breeze circulation in the area may lead to that an area of enhanced subsidence can form near the coast. Since at the same time the seawaters here are relatively cold (mainly due to the large and cold freshwater contributions from melting snow, particularly in spring), cloud formation may be even further suppressed. A weak minimum of sea surface temperatures normally forms near the Norwegian coast in spring (see Karlsson, 1995) supporting this theory. It is not likely that the cloudiness minimum is caused by large-scale circulation patterns (i.e., easterly winds causing leeward subsidence) since even during spring the main wind direction is from the southwest in the area. Conditions in the outer part of the Norwegian Sea are discussed further in sections 5.2.1 and 5.2.4.

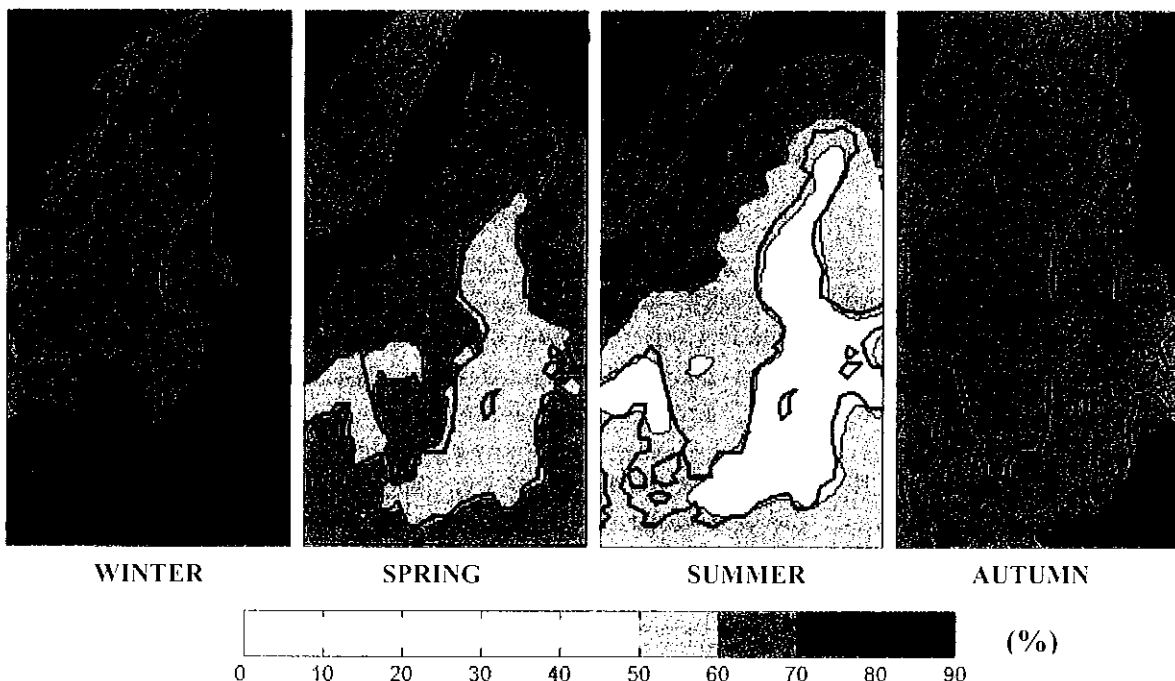


Figure 5.1 Mean total fractional cloud cover for (from left to right) the four seasons Winter, Spring, Summer and Autumn. Results are calculated within 36 by 36 km bins with data from the entire ten year period (explained in section 3).

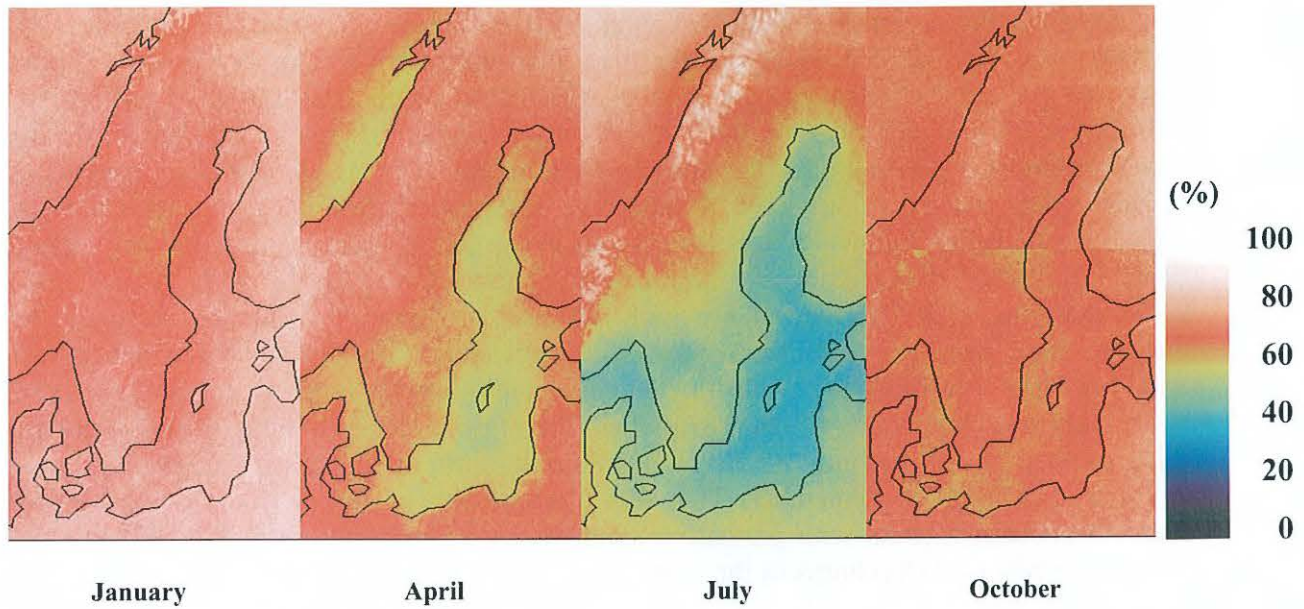


Figure 5.2 Period mean of cloud frequency (%) with 4 km horizontal resolution in the months of January, April, July and October.

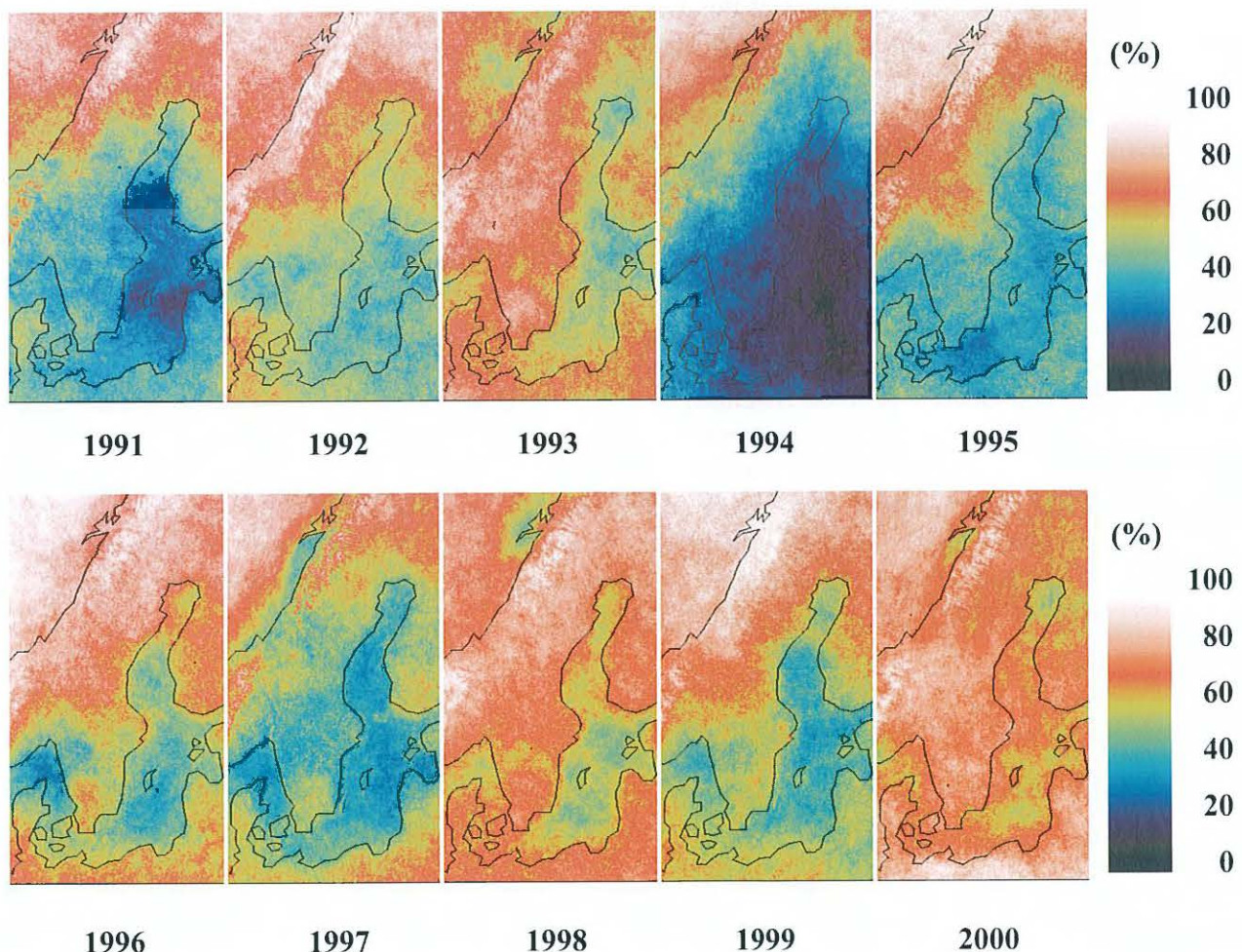


Figure 5.3 Cloud frequencies for the month of July in the period 1991-2000.

More details of the yearly evolution of cloudiness over the area can be found in Figure 5.4 showing results for all individual months (see also next section). As above, data for all months are from 1991-2000 except for January which is based on data from years 1992-2001. From Figure 5.4 it is clear that, on the average, July has been the least cloudy month during the period for most places except the Scandinavian mountain range and the outer regions of the Norwegian Sea where we have summertime maxima of cloudiness. A cloud amount minimum with values below 40 % is here found in the Baltic Proper to the east of Gotland and with individual cloud frequency minima at pixel resolution as low as 35 %. Notice again cloud conditions in the Norwegian Sea with the most pronounced differences between the inner and outer parts in April and in May. The most cloudy month in the area during the period has been November except for the Scandinavian mountain range where June were the most cloudy and over the Norwegian Sea where the highest cloud amounts were found both during summer and winter months. An interesting minimum in cloudiness is also found over the Norwegian coast in September. This was most probably caused by the occurrence of several September months with prevailing southerly or south-easterly winds causing a lee-effect with decreased cloudiness in the mentioned area (e.g., in 1994, 1995, 1998 and 2000 – see Appendix 2).

Studies of corresponding results of high-resolution (4-km) cloud frequencies (as in Figure 5.2) reveal interesting small-scale patterns and features. Some of them are also partly visible in the picture on the front cover of this report and in other figures of this section. Despite this fact, no attempts to interpret features of the very finest scales close to the maximum spatial resolution has been made here. The reason is that, due to the inherent navigation errors mentioned in section 3, their existence cannot be guaranteed in reality. For example, large navigation errors (~5-10 km) would easily result in false clouds due to inappropriate sunglint treatment. The sunglint treatment is only in effect where ocean and lakes are assumed to be located according to the used land mask (feature 3 in Table 2.2). If there is a mismatch between the land mask and the navigated image, false clouds may appear at sunglint viewing angles in lake and sea regions erroneously assumed to be land pixels. This will create patterns that correlate with coastlines and it is evident that such patterns are visible in some of the figures. For example, errors of this kind can be noticed and suspected for the island of Öland (in the south-eastern part of Sweden) and for the lake Vättern (inland lake of southern Sweden) in Figure 5.2. The appearance of systematic departures from the targeted satellite viewing geometry has recently been reported by Brunel and Marsouin (2000) and may to a large extent explains these very small scale features. Thus, the achieved results in this study for scales below approximately 10 km must be used with great care considering the possible navigation errors. Future studies with more accurate navigation methods are suggested for successful retrieval of the very fine-scale patterns.

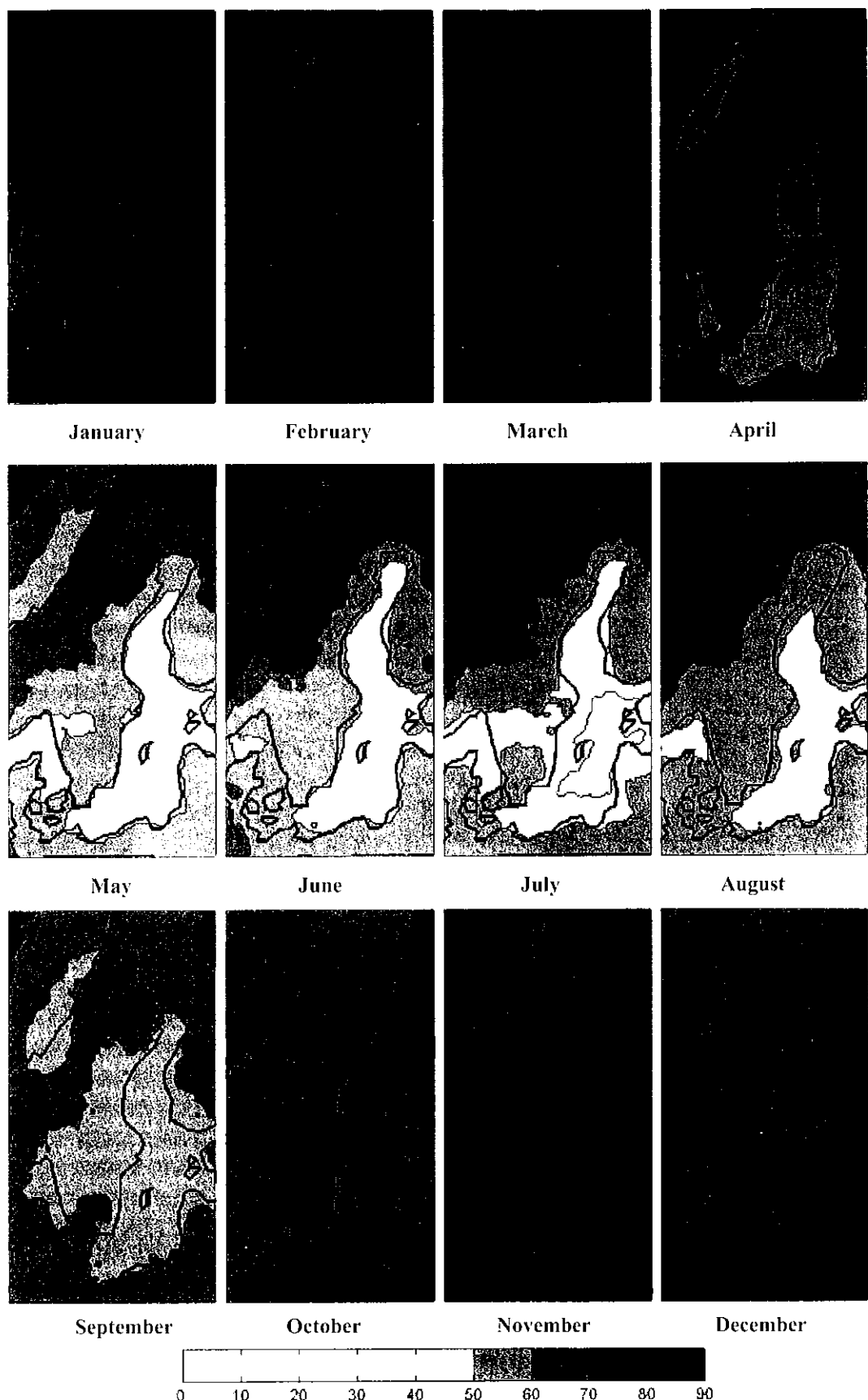


Figure 5.4 Mean monthly total fractional cloud cover (%) over the entire year in 36 km resolution.

5.1.2 The annual cycle of cloudiness

The annual cycle of cloudiness over the area was earlier indicated by the monthly means shown in Figure 5.4. In this section, a more detailed description is shown for some selected places in the area. Figure 5.5 gives an overview of the positions of these places. The criterion for their selection has been to choose positions from where no or only very limited cloud observations have been reported before (e.g., over the Baltic and Norwegian Seas and in the Scandinavian mountain range). In addition, also cloud observations from some selected islands, coastal and inland positions, major lakes and some major cities in the area will be shown. For each position, the mean cloud cover has been calculated from cloud frequencies defined in 36-by-36 km bins (i.e., based on 9-by-9 pixel regions). Figures 5.6-5.7 show the annual course of cloud cover computed as daily means (thin line) and five-day means



Figure 5.5 Selected places for visualisation of the detailed annual course of cloudiness in the following Figures 5.6-5.7.

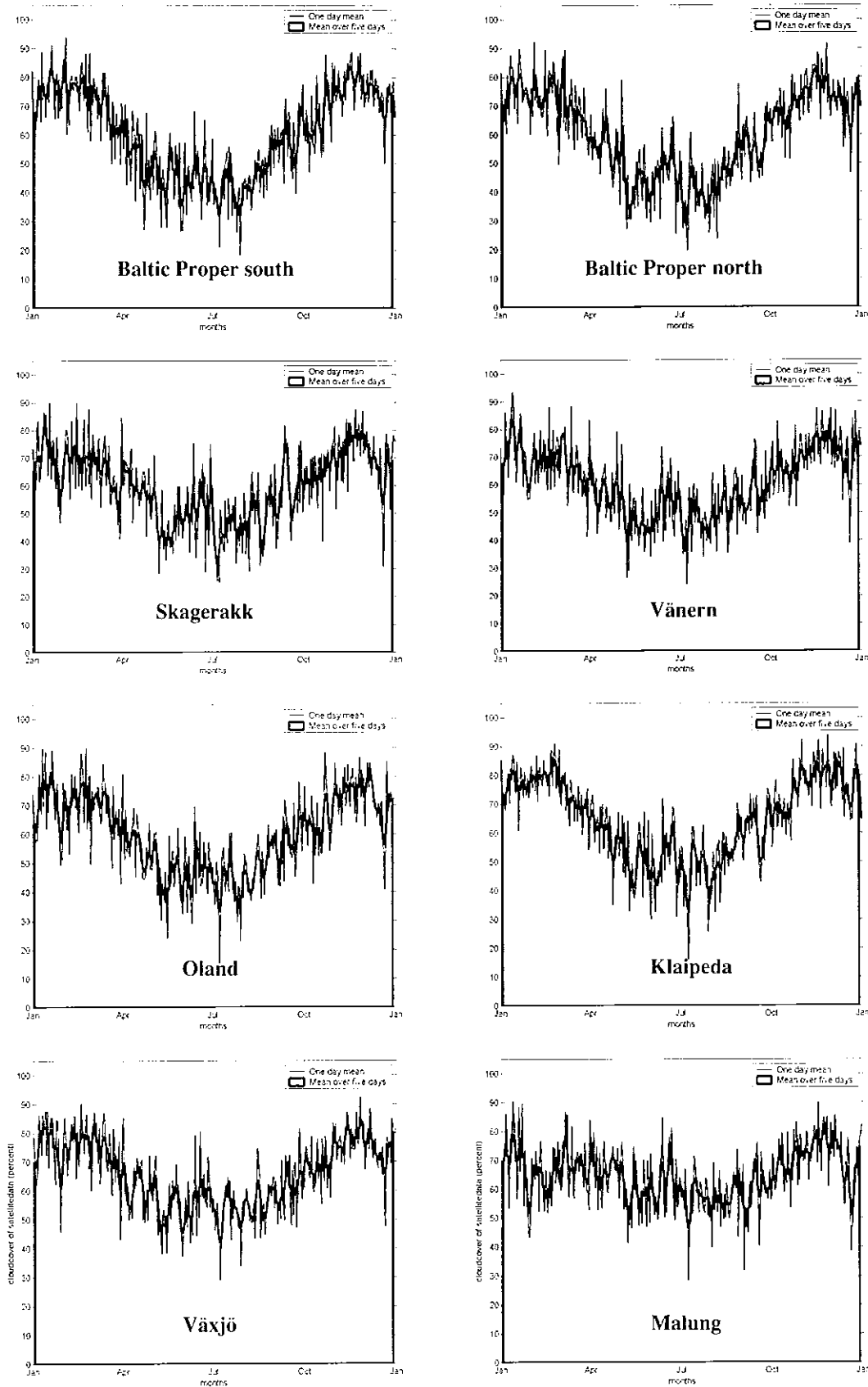


Figure 5.6 The annual course of cloud cover (%) for selected positions shown in Figure 5.5.

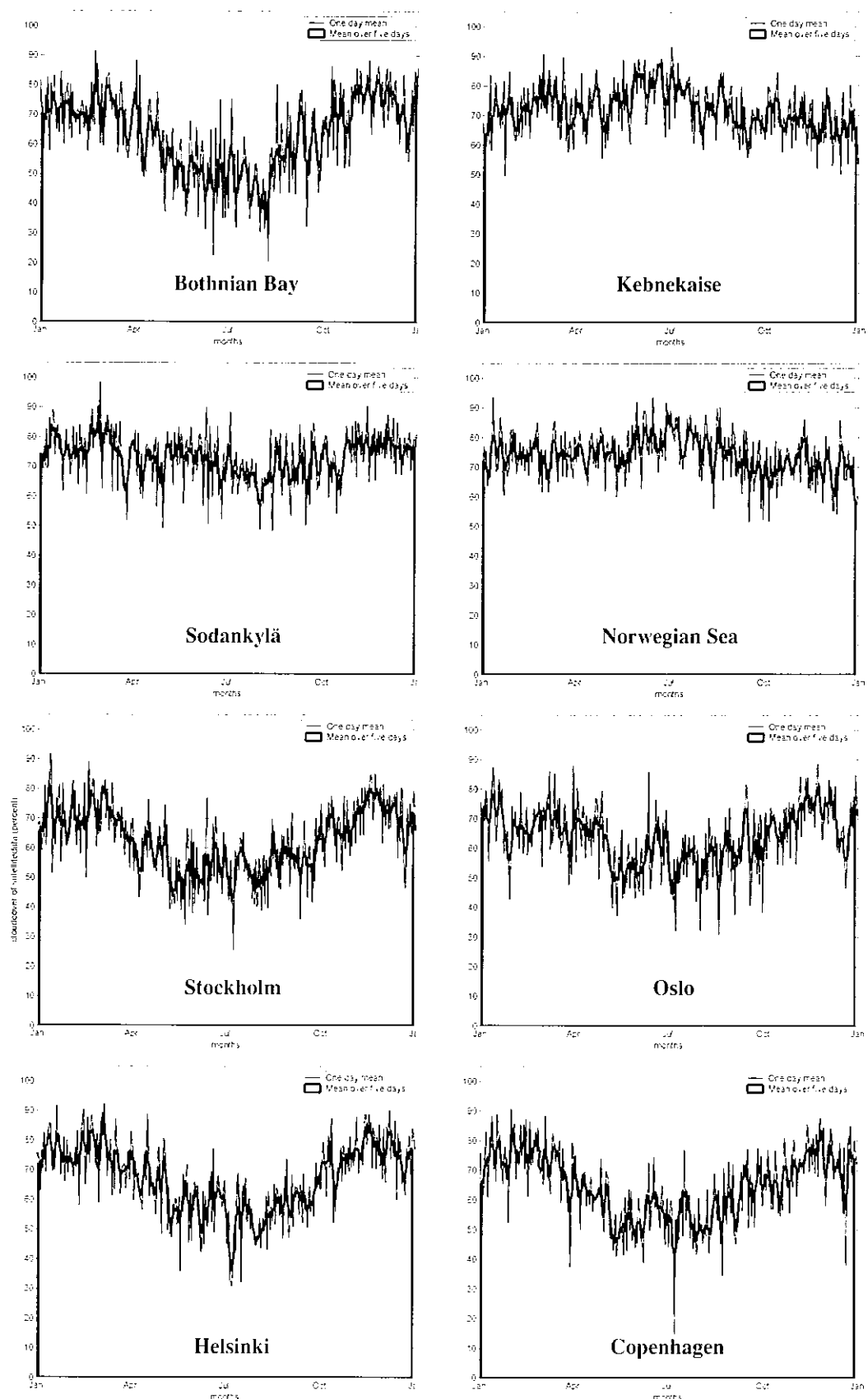


Figure 5.7 . The annual course of cloud cover (%) for selected positions shown in Figure 5.5.

(thick line with shading beneath) over the entire ten-year period for the selected positions. Figure 5.6 shows results for positions in southern Scandinavia and Figure 5.7 results from northern Scandinavia and some capital cities in the area.

In Figure 5.6 we notice the pronounced annual cycle of cloudiness over sea areas with a summertime minimum and wintertime maximum. Also for lake Vänern, a similar annual cycle can be seen but with a slightly smaller amplitude. The largest amplitude is seen for the two positions in the Baltic Proper which have winter cloud amounts close to 80 % and summer cloud amounts close to 35 %. For most positions (except some in northern Scandinavia), an absolute cloudiness maximum is seen in November while the corresponding time in summer for the annual minimum varies slightly between the positions. The variation in cloud conditions on the short time scale (~weekly) is considerable and it is obvious that there are also large individual differences between the studied positions. Only two features on the short time scale appear to be common for all positions and these are:

- Existence of a cloudiness minimum in December (values drop from 75-80 % in November to 60-65 % in December)
- Higher cloud amounts in June than in May and July

Some of the positions (Skagerakk, Vänern and possibly also Bothnian Sea) appear to have a distinct cloudiness minimum in May which is not seen for other positions here. Otherwise, the variation appears largely to be random and not connected to cloudiness features on a larger scale.

The results for the Baltic Sea coastal or island positions (Öland and Klaipeda) are very similar to the results found for positions in the Baltic Proper. A small but discernible difference is that the minimum cloud amounts in summer are generally not as low as for the positions offshore. However, it is remarkable how similar results are for the position Öland and for Baltic Proper south. At Öland, it seems as the sea-breeze circulation forced by the mainland in the north-western direction effectively prevents the formation of convective cloud elements over the adjacent land portion of Öland.

The same short time-scale features as could be seen for the Baltic Proper positions in Figure 5.6 is generally also seen for the coastal/island positions at Öland and Klaipeda. However, these are not always easy to isolate from a more or less random variation of cloudiness with time on the short time-scale. A noteworthy feature is the rather high cloud amounts in November and February/March for Klaipeda compared to previously studied positions. At Klaipeda, also secondary minima in cloudiness in August and in the end of September can be seen. Similar features were also found for positions at Gdansk and Bornholm (not shown here) although not as pronounced.

Cloud conditions at the two inland positions Växjö and Malung in Figure 5.6 differ to some extent from the previously discussed positions. An annual cycle in cloudiness is clearly seen for Växjö but the amplitude is now remarkably decreased. However, for Malung the amplitude has decreased even further and it is hardly visible. Here, cloud amounts in February are almost compatible with summertime cloud amounts. The short-term variation is very large for both positions and seemingly with no significant correlation. Nevertheless, it is interesting to notice the cloudiness minimum in December, a feature that has been common for all previously studied positions.

For the inland position in the most northern part of the area (Sodankylä) in Figure 5.7 there is almost no sign of an annual cycle of cloudiness. Cloud amounts are close to 65 % throughout the year, although with considerable variation on the short time-scale. Thus, from this result and the results from positions Växjö and Malung in Figure 5.7, we may conclude that with increasing distance from the central portions of the Baltic Sea (the Baltic Proper), the amplitude in the annual cycle of cloudiness decreases for inland stations in Scandinavia.

The results for the position in the Scandinavian mountain range in Figure 5.7 (Kebnekaise) are very similar to results at Sodankylä but differ in one important aspect: A summertime maximum in cloudiness is visible. Results at Kebnekaise show maximum cloud amounts in June and July. This maximum is likely to be caused by the summertime thermal heating differences between mountain sides and surrounding valleys or low-land areas. These heating differences are the driving mechanism for the slope-and-valley wind circulation systems resulting in cloud formation at mountain ridges (described by Atkinson, 1981 and illustrated later in Figure 9.1).

The found summertime maximum in cloudiness over the mountain peaks of the Scandinavian mountain range (clearly visible in Figure 5.2 for July) is considered to be a reliable feature and not caused by separability problems (e.g. between snow cover and clouds). Wet snow surfaces and clouds may be confused but only in cases when using scenes with large viewing angles being close to sunglint conditions but these scenes have been avoided in the SCANDIA cloud climatology. Furthermore, the areas with snow cover are very small in the mountains during the summer season and not as extensive as the indicated areas with high cloud amounts. It seems also unrealistic that the cloud separation should have particular problems during the summer season when the amount of useful information in multispectral imagery is at maximum (high sun elevations, no risk of strong surface temperature inversions, etc.).

For the position over the Norwegian Sea in Figure 5.7, we can also see a summertime maximum in cloudiness very similar to the results for the Scandinavian mountain range. However, this maximum is not pronounced for positions closer to the Norwegian coast where instead a minimum in cloudiness can be seen earlier in spring. A pronounced cloudiness minimum is here seen for inner positions in Norwegian Sea where cloud amounts are decreasing from approximately 70 % in early spring down to 55 % in April and May to become higher again in June and July. These interesting results are discussed further in section 5.2.1.

The results for the capital cities in Figure 5.7 does not show remarkable features deviating significantly from what has been seen for the previous positions. They are therefore left uncommented here being shown more for curiosity.

Another possibility for showing the annual course of cloudiness in the area is to use the presentation form of the so-called Hovmöller diagram, i.e., a time and space plot describing the annual evolution of cloudiness over a specific geographical region or cross-section. Figure 5.8 show results for two such cross-sections, one ranging from northern Germany over the south-western part of Scandinavia to the northern part of the Norwegian Sea and another ranging from the Polish coast over the entire south-to-north extension of the Baltic Sea reaching the northern part of Finland. Cloud amounts have here been calculated in 36-by-36 km squares and averaged over five days using data from the entire ten-year period.

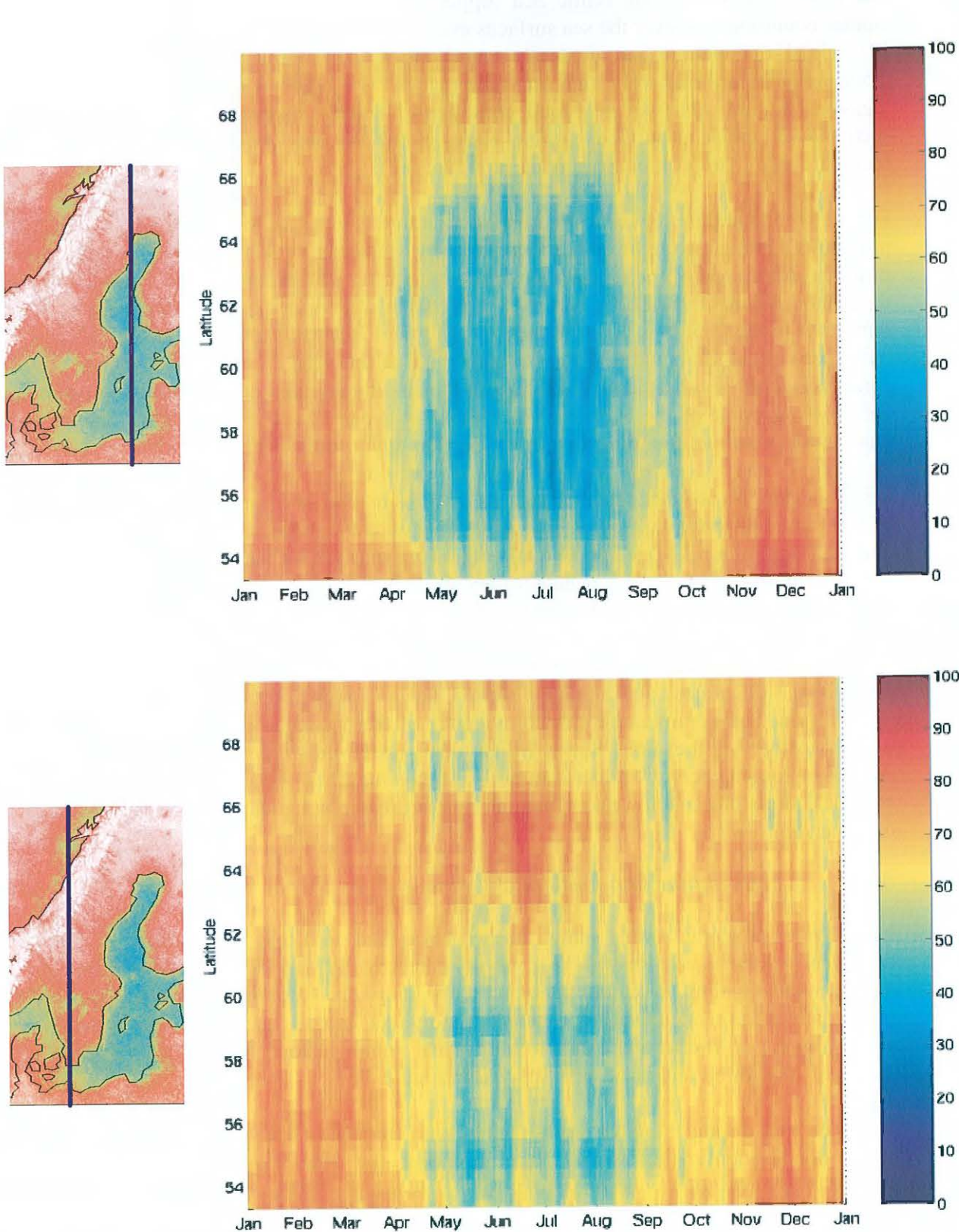


Figure 5.8 Two Hovmöller diagrams showing the average annual course of cloudiness (in % - see text) for two cross-sections displayed to the left of the top and bottom panels (reference image to the left shows afternoon cloud frequencies in June).

The cross section over the Baltic Sea (upper panel in Figure 5.8) shows how remarkably similar conditions are over the sea surfaces even if the geographical extension is considerable. Low cloud amounts are here generally found during the months May through August while cloud amounts are relatively high (at some places even higher than over neighbouring land areas) in autumn and winter. Cloud conditions change, however, rapidly in the northern section over the land surface portion. Here, cloud amounts are high throughout the year (compare also with position Sodankylä in Figure 5.7).

For the second and more westward cross-section in the area (the lower panel in Figure 5.8), a pronounced annual cycle of cloudiness is clearly visible in its southern part. Notice here the bi-modal separation of the cloudiness minima in spring and in summer for Lake Vänern and the southern part of the Baltic Sea, respectively. In the northern part of the cross section, a minimum in cloudiness is again found in spring and in early summer near the Lofoten area but otherwise conditions during the summer half of the year are very cloudy as opposed to conditions in the southern part. Notice again the cloudiness maximum in summer appearing at the crossing point of the Scandinavian mountain range. Another interesting feature is the cloudiness maximum found in November (seen in both panels of Figure 5.8).

It is interesting to see that some cloudiness features extend over the entire geographical range of the cross-sections (e.g., cloud maximum in February, April and October/November and cloud minimum in mid-December) while others are much more local and short-lived. The full meaning of these features, i.e., whether they are true climatological features or (perhaps more likely) caused by the natural climate variability, is not possible to evaluate completely here. Data from much longer time series is probably necessary for making firm conclusions. However, what could be said is that the data available here does not support the existence of some of the cloudiness and climate features that are often referred to by local tradition in Scandinavia. For example, there is no evidence of the existence of a period with sunny and warm weather in the first weeks of October, in Swedish denoted “Brittsommar” (the American equivalence is “Indian summer”). If existing, this phenomenon has a very “weak” statistical signature, much weaker than many other features that can be seen on the time scale of a decade.

5.1.3 *Inter-annual variability of cloudiness*

It is obvious from the results shown in the previous section that the variation in cloudiness from year to year is considerable (e.g., as indicated by the wide scatter seen in Figs 5.6-5.8). A closer examination of cloud frequencies for individual months (shown in Appendix 2) reveals also a tremendous variation between individual months as well as between individual years. To give an illustrating example, individual monthly cloud frequencies for the selected month of July for all ten years are displayed in Figure 5.3.

It is seen that during these ten years mean cloud frequencies have varied remarkably as an effect of the dominating weather regimes over the area. For a month dominated by anticyclonic circulation conditions (e.g. 1991, 1994 and 1997), cloud frequencies as low as between 10-30 % are found in many places in the southern part, generally with the lowest values over the Baltic Proper. As a contrast, months dominated by cyclonic circulation patterns (e.g., 1993, 1998 and 2000) gave cloud frequencies exceeding 50 % in almost the entire area with values as high as 80-90 % in some parts (particularly in the Scandinavian mountain range, over the Norwegian Sea and in Northern Finland). There are also several

years with very different conditions in the southern and northern part of the area (e.g., 1992, 1995 and 1999).

Results indicate that the inter-annual variability is strongest in the summer half of the year while in winter the variation is rather small. However, due to specific problems for cloud classification methods during the winter season (to be discussed later in more detail in section 7.1), the shown variability for this season is generally underestimated by the SCANDIA version 1 model. The main reason is that during anticyclonic winter conditions cloudiness is generally overestimated. Thus, we should expect to have a significant inter-annual variability in cloudiness also for winter months, although probably not with the same amplitude as for summer months.

The quality of SCANDIA cloud classifications during winter could be expected to vary according to the dominating flow regimes with the most problematic conditions associated with flow patterns generating very cold winter situations. A way to reduce or isolate these defects could be to separate results for relatively warm and windy winter months from the corresponding results of cold and calm winter months. Thus, it is here suggested that cloud climatologies for the different weather regimes associated with high North Atlantic Oscillation (NAO) index values could be assembled with reasonable quality while the more dubious results for months of low NAO indices could be isolated. Table 5.1 shows how the winter in the ten-year period can be grouped according to four NAO index categories. The mean cloud cover corresponding to each of the groups is shown in Figure 5.9. The used NAO index values have been supplied by the Climate Research Unit (CRU) of the University of East Anglia (Jones et al., 1997) and are based on the monthly mean pressure differences between Stykkisholmur (Iceland) and Gibraltar. Notice that the winter season has here been extended to include also March (following the convention used by CRU).

Table 5.1 *Categorisation of winter months in the period February 1991 to January 2001 according to monthly NAO indices from CRU.*

NAO-index category	Winter months (Dec, Jan, Feb, Mar)	
	1992: Feb 1993: Jan 1994: Mar	1995: Feb 1997: Feb 2000: Feb
Very High NAO index (NAO > +3)		
	1991: Dec 1992: Mar 1993: Dec, Mar 1994: Jan, Dec	1995: Jan, Mar 1997: Mar 1998: Feb, Mar, Dec 1999: Feb, Dec
High NAO index (+1 < NAO < +3)		
	1991: Feb 1992: Jan, Dec 1993: Feb 1994: Feb 1996: Feb	1997: Dec 1998: Jan 1999: Jan, Mar 2000: Jan, Mar 2001: Jan
Low NAO index (-1 < NAO < +1)		
	1991: Mar 1995: Dec 1996: Jan, Dec, Mar	1997: Jan 2000: Dec
Very Low NAO index (NAO < -1)		

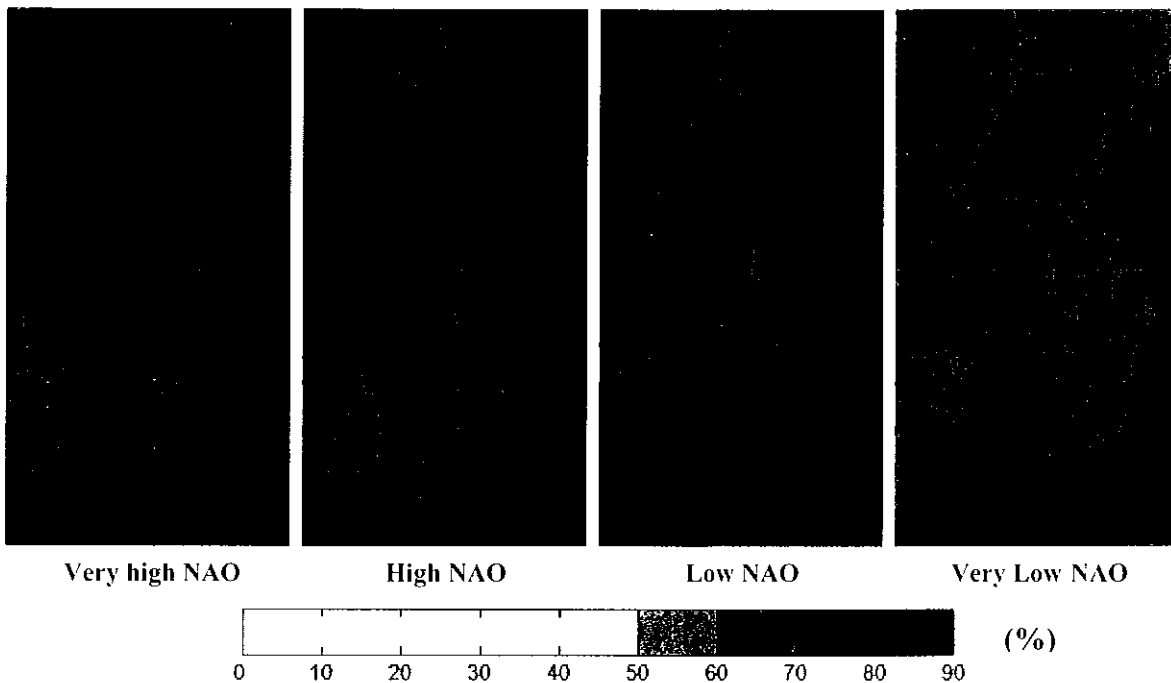


Figure 5.9 Mean monthly cloud cover for the four NAO index categories given in Table 5.1.

The actual choice of the four NAO index categories was based on the wish to get a more or less symmetrical distribution of winter months during the period. However, it must be remembered that the NAO index during the 1990's has been relatively high compared to previous periods. For example, the mean winter NAO index value between December-March has been above zero for all years except for 1996. Consequently, a bias towards high NAO index values is seen in this material.

It is seen in Figure 5.9 that the four NAO index categories give rise to quite different cloudiness patterns in the SCANDIA climatologies. For the Very High NAO index category a very clear depression in the cloudiness field is formed over southern and central Scandinavia. Thus, a minimum in cloudiness is found in the lee of the Scandinavian mountain range and especially its southern part, which could be anticipated due to lee and föhn wind effects. Further to the north, high cloud amounts are seen in most places. For the High NAO index category the cloudiness minimum has decreased in depth and cloud amounts are generally higher in most places. For the Low NAO category cloud amounts start to decrease in the central and northern part of Scandinavia and for the Very Low NAO index category a distinct minimum is even more evident and wider spread. In the latter case, cloud amounts have also generally decreased in most places.

It is reasonable that we should find lower cloud amounts in case of low NAO index values over Scandinavia since this indicates a higher likelihood of periods with wintertime anticyclones. However, it is likely that the indicated decrease in cloudiness is insufficient when knowing about the experienced problems for SCANDIA in very cold winter situations. An attempt to quantify these possible errors and the quality difference between the various NAO groups in Table 5.1 is made later in section 7.1.

5.1.4 *The diurnal cycle of cloudiness*

From Table 3.1, it is seen that the cloud climatology may be sub-divided into four groups with separate observation times. Consequently, it should be possible to get a rough description of the diurnal cycle of cloudiness consisting of mean conditions at night, in the morning, in the afternoon and in the evening. However, notice that some deviations from the time-windows described in Table 3.1 have occurred in the period due to drifting satellite orbital times (see Figure 4.1). In particular the night and afternoon passages have been unstable in this respect.

Figure 5.10 shows the mean diurnal cycle of cloud cover for the four seasons. As expected, a pronounced diurnal cycle can be seen for the spring and summer seasons over land areas. Notice the high correlation of the shape of the cloudiness field and the coastlines in the afternoon. Further details on a very small scale can be seen in Figure 5.11 showing mean cloud frequencies in July. A closer view of the afternoon conditions in July can also be seen in the picture on the front cover of this report. One can easily identify major lakes and islands directly from the cloudiness field in the afternoon. It is also interesting to notice that near coastlines oriented from south-to-north on the eastern side of seawaters (e.g., along the Finnish coast) clouds appear to have penetrated rather far inland. As a contrast, near coastlines on the western side rather high cloud frequencies are found near the coastline and even a bit offshore. A probable explanation is that convective cloud elements have been affected by advection by a mean westerly wind in the area. Consequently, a sea-breeze front and its associated cloudiness appear to have been more easily advected out over the sea surfaces on a western coast than on an eastern coast.

Although the corresponding amplitude in cloudiness variations is comparably small, also results during winter and autumn seasons in Figure 5.10 indicate the existence of a diurnal cycle. Here, the variation has a reversed sign with a maximum of cloudiness during morning and afternoon. However, this feature is found to be quite unrealistic. It was found to be caused by an inadequate treatment in SCANDIA of anisotropic reflection (i.e., mainly enhanced forward-scattering) from both snow-free and snow-covered land surfaces during conditions when the sun is close to the horizon at the satellite observation time. This is also supported by the fact that highest cloud amounts are found in the south-eastern part for the morning passages and in the southern or south-western part in the afternoon passages (following the movement and direction of the sun).

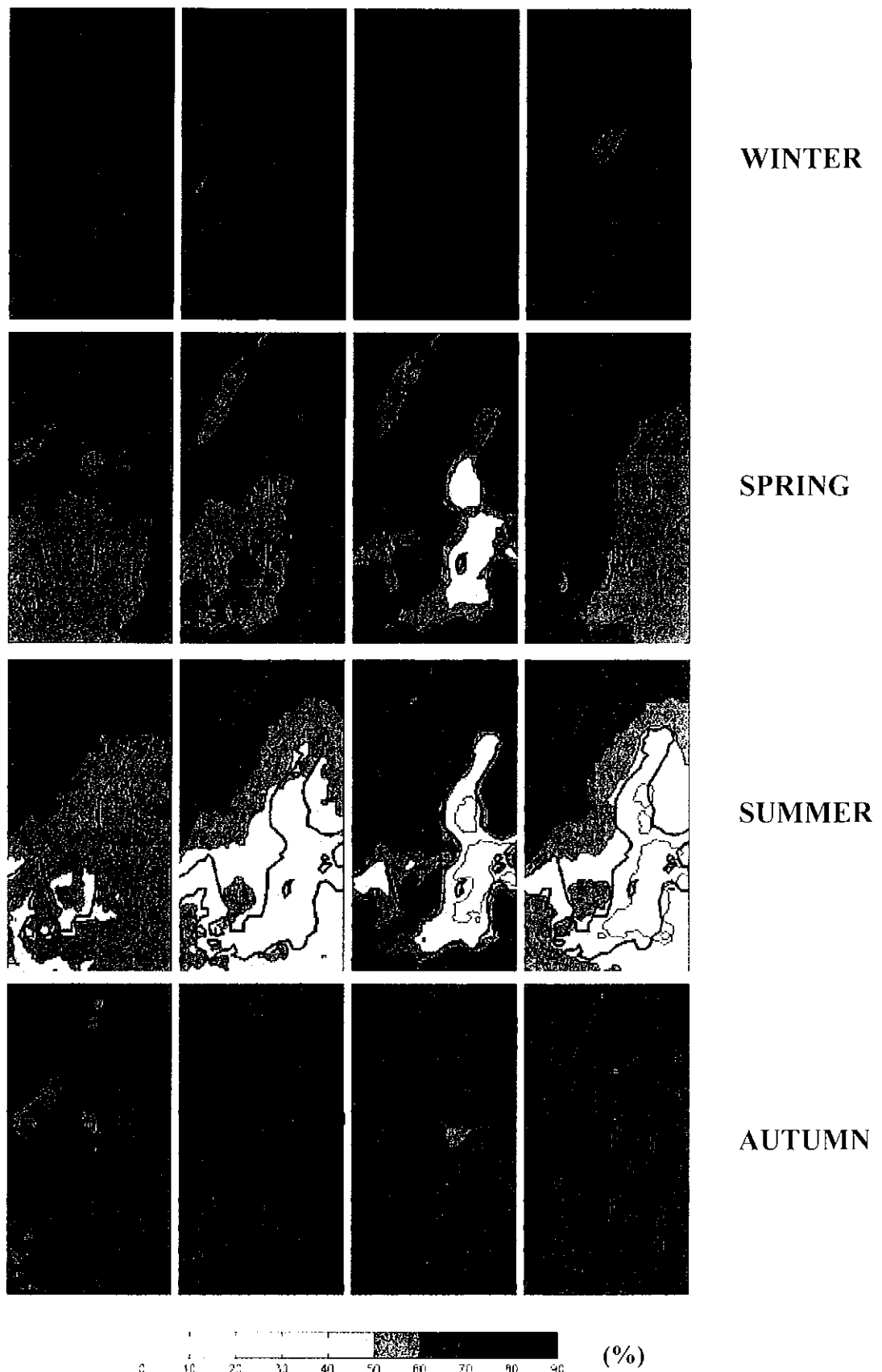


Figure 5.10 The diurnal cycle of cloud cover (night, morning, afternoon, evening) for all four seasons estimated in 36 km horizontal resolution over the entire ten-year period.

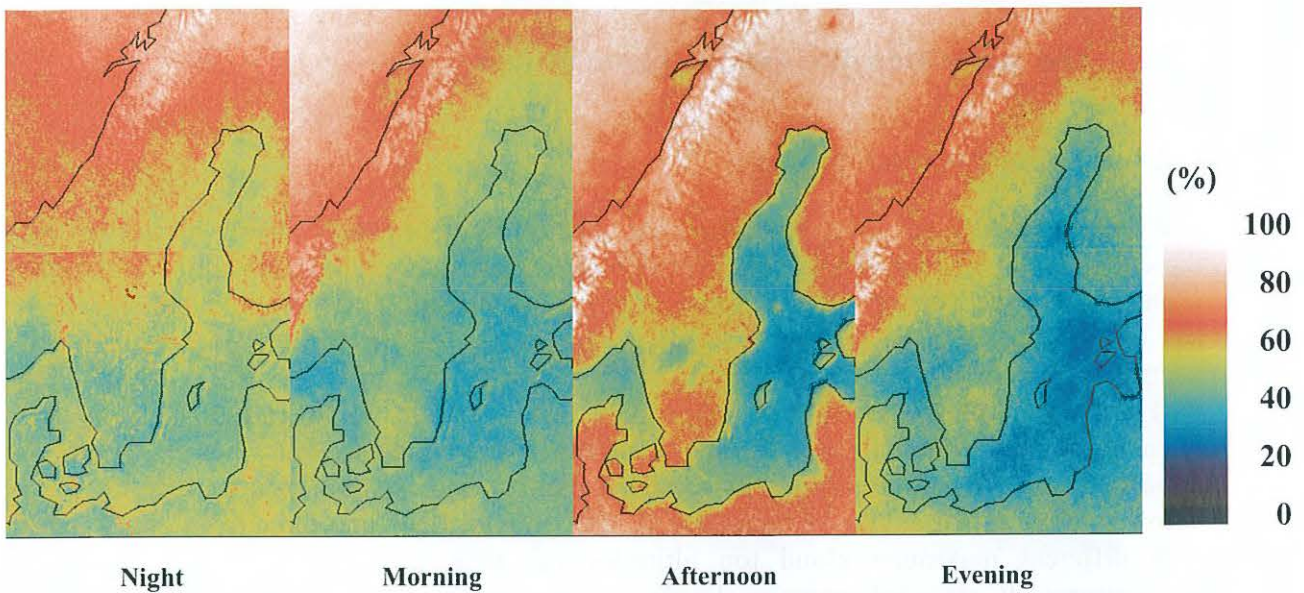


Figure 5.11 The diurnal cycle of 4-km resolution cloud frequencies (night, morning, afternoon, evening) for the month of July estimated over the entire ten-year period.

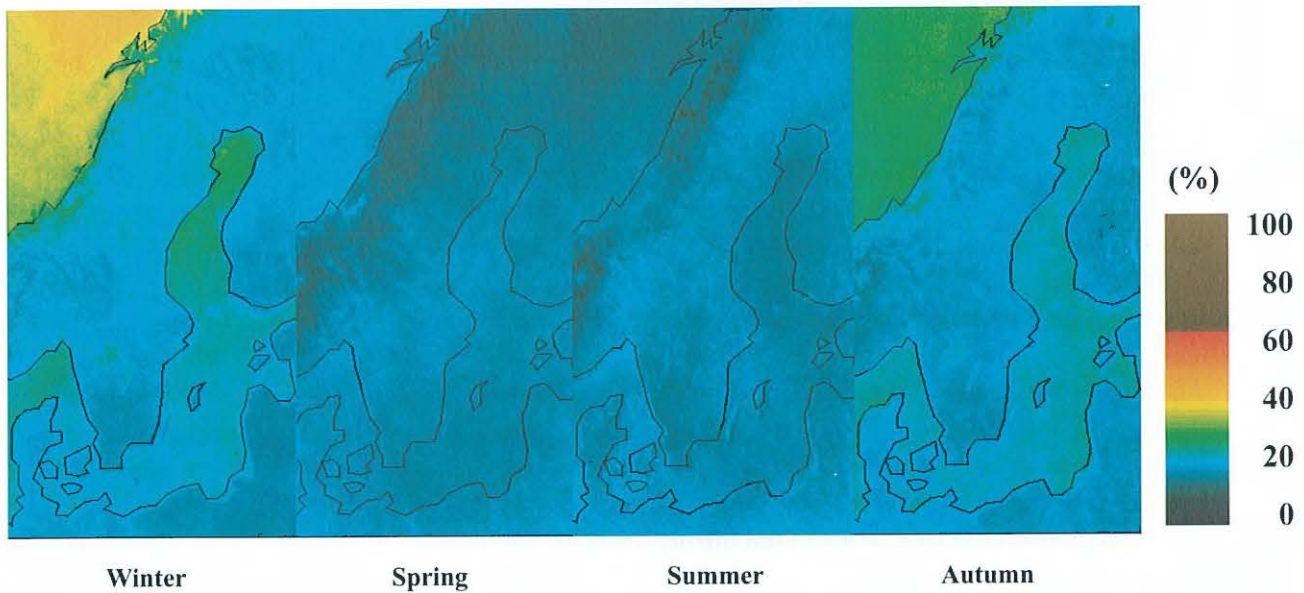


Figure 5.12 Seasonal mean of the contribution to the 4-km resolution total cloud frequency from semi-transparent Cirrus clouds.

5.2 The separation into various cloud groups

5.2.1 *Opaque cloud groups*

The opaque cloud groups are separated from semi-transparent clouds mainly by the fact that these clouds do not exhibit a significant brightness temperature difference between AVHRR channels 4 and 5. This should mean that, if assuming that the basic cloud detection scheme has been successful, the measured signal originates entirely from the cloud itself and no contribution from the underlying clouds or ground surface is included. Consequently, it is then assumed that the cloud top temperature will be close to the measured brightness temperature in AVHRR channel 4. This assumption is most often valid since the additional radiance contribution from atmospheric water vapour is generally small at high latitudes and at low satellite zenith angles. A separation of the opaque clouds into three main cloud groups with different maximum cloud top altitudes can then be made by comparison with temperatures at standard pressure levels as described in Table 3.2. The temperature information is here taken from objective analyses of the HIRLAM forecasting system. These analyses were available at six-hourly intervals in a horizontal resolution of approximately 55 km. However, for the SCANDIA Version 1 model, area averages for the two processing areas SSWE and NSWE were calculated and used.

Figure 5.13 shows the seasonal contribution to the total fractional cloud cover (discussed in the previous section 5.1) from the three opaque cloud groups. For a proper interpretation of these results one must bear in mind that the satellite viewing perspective generally does not allow the detection of cloud layers beneath the topmost layer in case of multi-layered clouds. This means that the results for the medium and low levels in Figure 5.13 only refer to the cases when no upper level clouds were present. Thus, only results for the high-level cloud group can here be interpreted as being an estimate of a true climatology while results for the other two cloud groups will definitely underestimate cloud amounts of a true climatology.

The opaque high-level cloudiness show a seasonal variation over the area with high values during the autumn and winter seasons (especially over the Scandinavian mountain range) and lower values in spring and in summer. However, a substantial contribution (here above 20 %) is generally found also during the latter seasons over the Scandinavian mountain range. The increased values over the entire area during autumn and especially during winter are expected due to the higher frequency and intensity of extratropical cyclones over the area during those seasons. However, the very high values over land areas in the northern part of Scandinavia are found to be quite unrealistic. Here, frequent mis-classification of very cold cloud-free land areas occurred and resulted in erroneous clouds of the Nimbostratus and Cumulonimbus cloud types.

For the medium- and low-level opaque clouds, quite different results are found. In spring and summer seasons, both cloud groups correlate in respect of both amount and location although the low-level cloud group shows slightly higher amounts over the land areas, especially during summer (due to cumulus cloud activity). The reason for the high correlation of the two cloud groups is most probably that the separation into the two groups is highly artificial and not based on a real difference in reality. For example, convective clouds will initially form as low-level clouds (small cumulus) and later evolve into medium-level clouds (cumulus congestus). Furthermore, the Stratocumulus and Altocumulus cloud types are often formed by

the same mechanisms and the separation into two different altitude groups is therefore a bit mis-leading.

Notice in particular the high contributions over the Scandinavian mountain range and over the Norwegian Sea in spring and in summer. We can thus conclude that the maximum in cloud amounts previously found in summer over the Norwegian Sea (compare with Figure 5.2) consists almost entirely of clouds at low and medium levels. Unfortunately, also here we can identify some artefacts in the climatologies, namely the very high contributions over land areas in the most northern part in spring. This is another example of the SCANDIA cloud classification problems occurring when the sun is close to the horizon (discussed previously in section 5.1.4). More problems are also indicated for the winter and spring seasons. For example, a striking lack of low-level clouds is seen over the northern part of Scandinavia. The explanation here is that fog and stratus clouds were frequently mis-classified as medium-level clouds (altocumulus) during the cold seasons. These clouds often form in or below a strong near-surface temperature inversion which means that the cloud top temperature may be relatively low and often lower than the 700 hPa temperature, thus giving rise to the misclassification (compare with Figure 2.3). Unfortunately, another important explanation is that stratus clouds often remained undetected in the particular area during very cold winter conditions. This problem is discussed further in section 7.1.

5.2.2 *Semi-transparent Cirrus clouds*

Referring to the definition of the opaque clouds discussed in the previous section, the semi-transparent Cirrus clouds are identified as those cloud pixels having a significant brightness temperature difference between AVHRR channels 4 and 5 (i.e., at least 1.5 - 2.5 degrees colder in AVHRR channel 5). This difference occurs when radiances from two radiation sources, here the cloud layer and the underlying ground surface or ground surface, are mixed which results in a sum of two contributing effects of the same sign:

1. “Artificial” difference due to non-linear differences of the spectral response in the two spectral channels (e.g., as discussed by Matson et al., 1987 and Coakley and Bretherton, 1982).
2. Cirrus cloud-specific difference due to different cloud transmittances for ice clouds in the two AVHRR channels (discussed by Inoue, 1987 and Hunt, 1973).

Also a third contribution to the brightness temperature difference exists, namely the contribution from the atmospheric water vapour. The second term above generally dominates over the first term and the atmospheric water vapour term for thin Cirrus clouds. Thus, semi-transparent Cirrus clouds are most likely here for cases of the above mentioned temperature differences while fractional or semi-transparent water clouds (discussed in section 5.2.6) normally show small temperature differences.

Results for semi-transparent Cirrus clouds for all four seasons are shown in Figure 5.12. As for the opaque high-level clouds, we have significantly higher contributions from semi-transparent cirrus in autumn and in winter compared to in spring and in summer. A remarkable feature is the very high contribution over sea areas in autumn and in winter, especially over the Norwegian Sea. This difference between land and sea areas is believed to be to a great deal artificial. The described method to identify semi-transparent Cirrus clouds requires in its definition a rather large temperature difference between the cloud layer and the

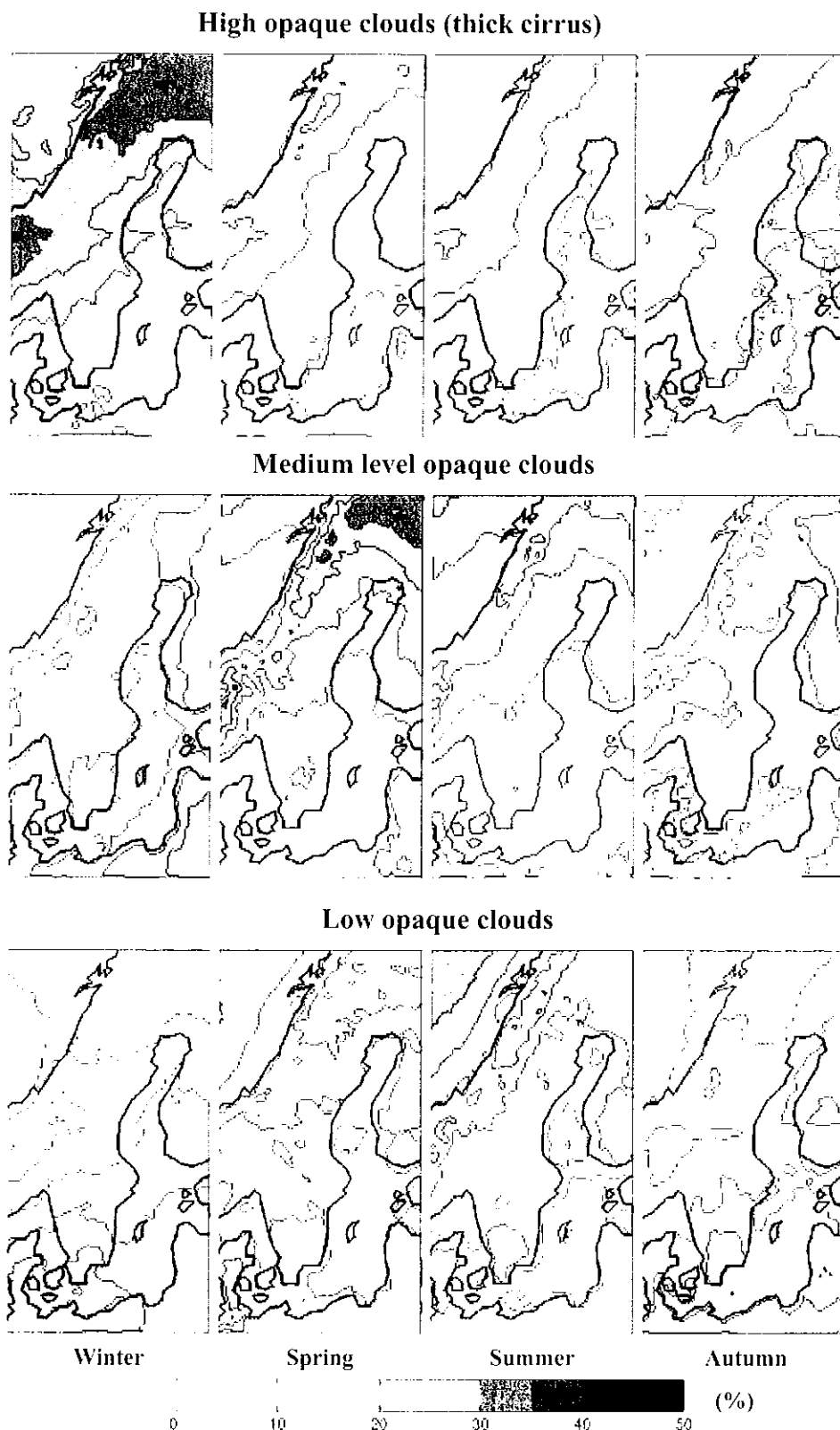


Figure 5.13 Seasonal mean of the contribution to the total fractional cloud cover from opaque High-level clouds (top panel), Medium-level clouds (middle panel) and Low-level clouds (bottom panel).

underlying surface. Consequently, the probability for detection of semi-transparent cirrus clouds is higher over relatively warm, cloud-free and ice-free sea surfaces than over cold land surfaces during the colder and darker seasons. This means that the amount of thin Cirrus clouds is probably underestimated in the area over land surfaces. The same effect probably causes the apparent minimum in the contribution over the Scandinavian mountain range in spring and in summer. Nevertheless, it is interesting to find rather high contributions eastward of the mountain range which could indicate a rather frequent occurrence of lee-wave cirrus over the area (an extreme case is illustrated below in Figure 5.14).

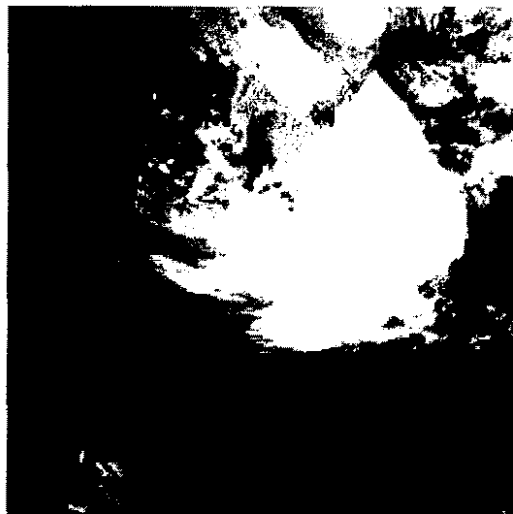


Figure 5.14 Lee-wave cirrus formed eastward of the Scandinavian mountain range in a north-westerly atmospheric flow pattern. Picture from the infrared channel 4 of NOAA AVHRR from May 10 2001 at 05:11 UTC over area SCAN (see Figure 2.1).

5.2.3 Ice and water clouds

The two groups ice and water clouds were formed by merging the opaque high-level and semi-transparent Cirrus cloud groups into the ice cloud group and by merging the two low- and medium-level cloud groups into the water cloud group. Resulting high-resolution cloud frequencies are shown in Figure 5.15. We recognise again some of the features described for the opaque clouds and for the semi-transparent cirrus clouds. Observe that the apparent differences on the very small scale for ice clouds in autumn and in winter (e.g., identifying Lake Vänern, Lake Vättern and the island of Öland in southern Sweden) are basically artificial as discussed earlier in section 5.2.2. An interesting ice cloud feature is the maximum eastward (leeward) of the Scandinavian mountain range in summer indicating the frequent occurrence of lee-wave cirrus clouds (mentioned earlier).

Notice for the water cloud results that we can now identify a clear land-sea difference in the spring and summer seasons reflecting the more frequent formation of convective cumulus clouds over land. Similarly, a high cumulus convection activity is also indicated over the peaks of the Scandinavian mountain range. Here, water clouds appear to persist during more than 50 % of the time. In addition, Figure 5.15 once again emphasises the large contribution from water clouds over the Norwegian Sea (almost 60 %) in summer.

The winter results for water clouds appear unrealistic with a frequent occurrence in the southern part but almost no occurrence in the northern part. This can at least partly be explained by the fact that water clouds are assumed by SCANDIA to show a negative of

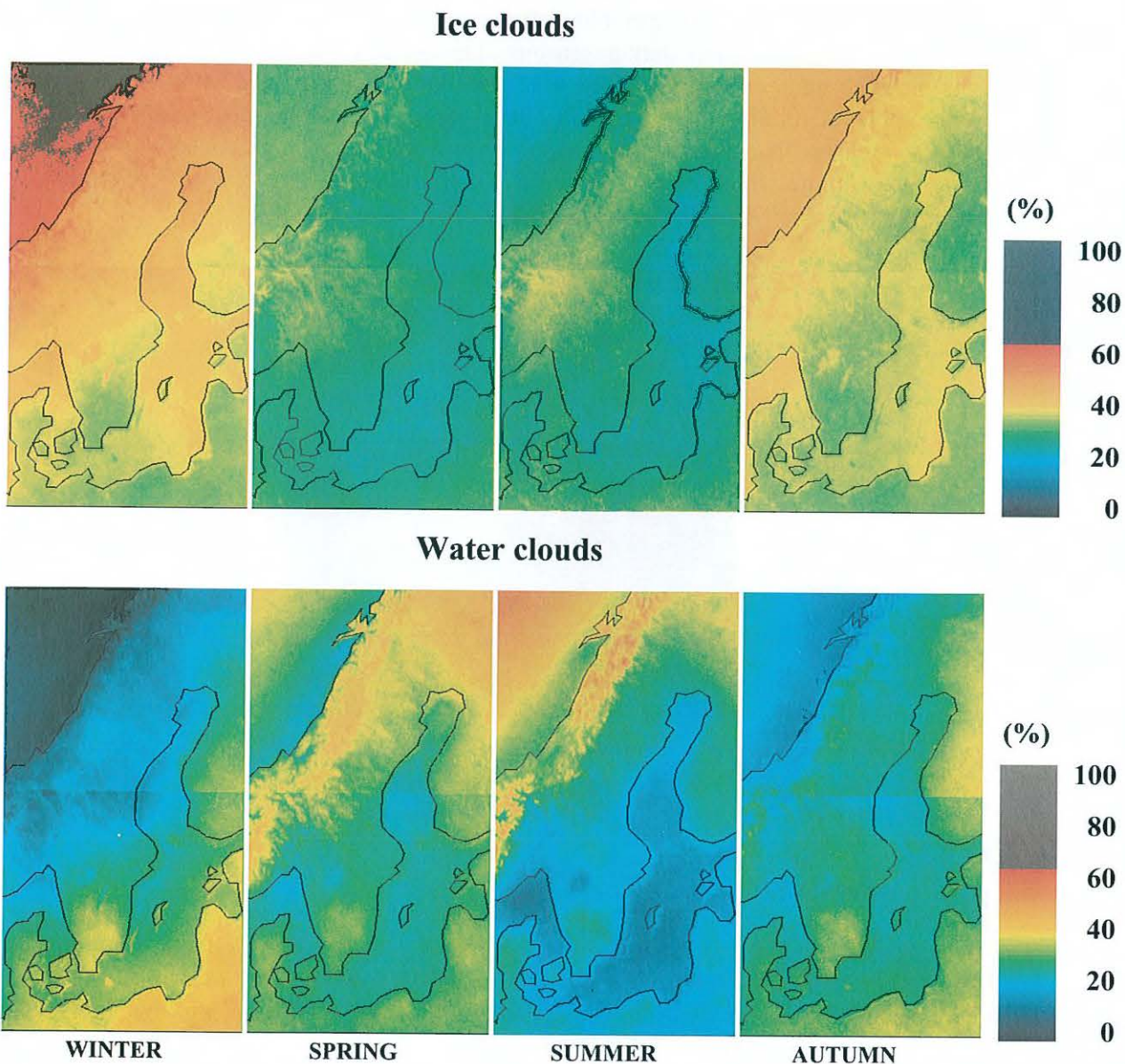


Figure 5.15 Seasonal frequencies of ice clouds (top) and water clouds (bottom) in 4-km horizontal resolution.

brightness temperature difference between AVHRR channels 3 and 4 during dark conditions (see Figure 2.3 and Eyre et al., 1984). However, in very cold winter situations stratus and fog may contain a mixture between ice crystals and water droplets and this might lead to that those clouds could remain undetected. This could be one explanation for the remarkably low frequencies of water clouds in the northern part of the area. On the other hand, snow covered ground should have a suppressing effect regarding the formation of near-surface fog due to the different thermodynamical properties of ice and water (higher water vapour saturation pressure over water surfaces than over ice surfaces). It is unfortunately not possible to estimate the relative importance of these two factors based solely on the contents of the SCANDIA cloud climatology.

5.2.4 Fog and Stratus

An important contribution to the water cloud group and the opaque low-level cloud group comes from the Fog/Stratus cloud category. This category is basically separated from other low-level cloud types by having very small values in the texture feature indicating a very homogeneous cloud top temperature on a small horizontal scale. Figure 5.16 shows the resulting mean seasonal frequencies of stratus/fog over the area.

We notice that the Fog and Stratus category show many features which are similar to the previously discussed water and opaque low-level cloud groups. For example, a pronounced summertime maximum is seen over the Norwegian Sea indicating that a large fraction of the clouds here comes from stratiform low-level clouds. The deficit with suspected too low frequencies in the northern part of the area as seen for water clouds is seen also here. However, notice that a pronounced land-sea difference is seen in winter with higher frequencies over land. Even individual lakes appear to affect results in a similar way (e.g., Lake Vättern in southern Sweden). In spring, frequencies over land decrease while frequencies over sea surfaces (e.g., over the Baltic Proper) remain relatively high. A probable cause could be an increased frequency of advection fog over the cold seawaters in spring while the frequency of radiation fog over land decreases. Unfortunately, occasionally some mis-classified sunglint may contaminate results for the morning passages which makes the high values over the Baltic Sea in spring slightly uncertain. In summer, stratus and fog frequencies are low over land areas even if some regions (e.g., the south-western part of Sweden and over Danish Jutland) show slightly higher values. Interesting is here that the highest frequencies over land areas are found at night which is also true in spring. This agrees well with observational experience from e.g. synoptical stations. In autumn, frequencies over land surfaces increase while the summertime maximum over the Norwegian Sea disappears. The highest frequencies over land occur for most places in autumn (except in the most south-western part where winter frequencies are higher).

It should be mentioned that the results in or near the Scandinavian mountain range (generally showing very low frequencies) are not realistic. The problem is that it is not possible to use a texture feature here to isolate stratus/fog clouds from other cloud types due to the effects caused by the steep and highly varying topography.

Once again, one must remember that the results in Figure 5.16 deal only with the cases when there are no upper level clouds above the stratus or fog layer. Thus, results here cannot be referred to as true fog or stratus climatologies. However, since the formation of radiation fog normally requires cloud-free conditions, one could hope that a major part of the cases of radiation fog is captured. Since the measured frequencies are generally very low (especially in summer), the ten-year period is probably too short for establishing a firm knowledge of the true stratus/fog occurrence and its relation to small-scale geographical features which could be of importance for e.g., an airport location. Longer time series are probably needed here as well as an improved image navigation accuracy. In addition, it is well-known that even stratus and fog cloud decks may have quite a substantial variation of cloud top temperatures which means that a very accurate separation of the stratus and fog cloud category from other low-level cloud categories by the proposed method is probably not possible. Thus, a large number of stratus and fog cases have most probably been assigned to the Stratocumulus cloud category (or even the altocumulus cloud category during winter as discussed in section 5.2.1).

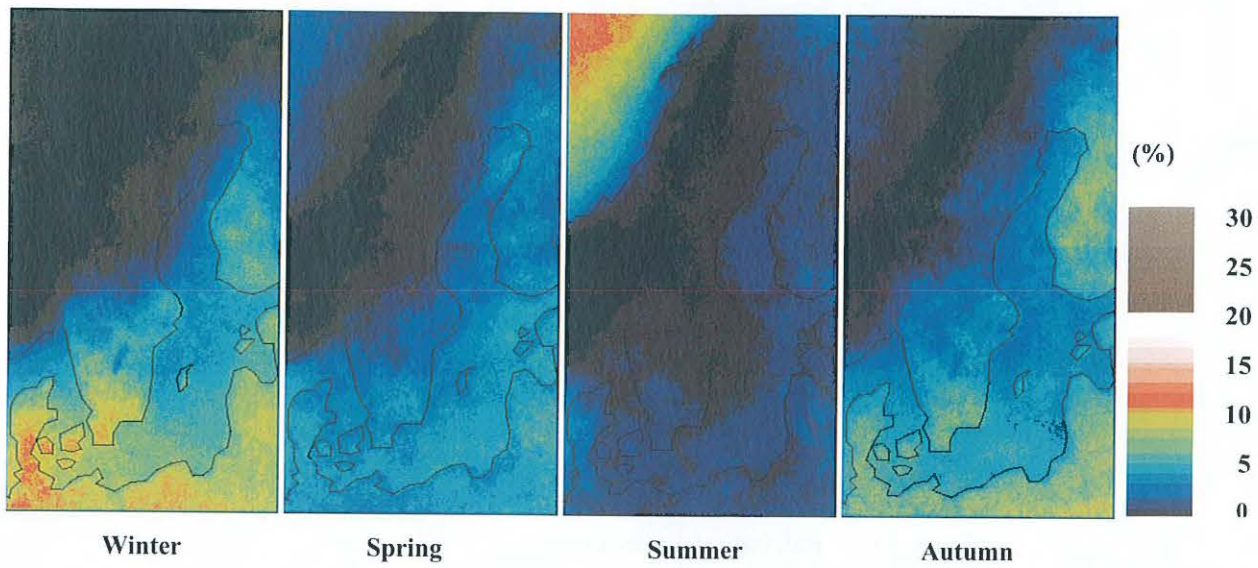


Figure 5.16 Seasonal frequencies of stratus/fog in 4-km horizontal resolution.

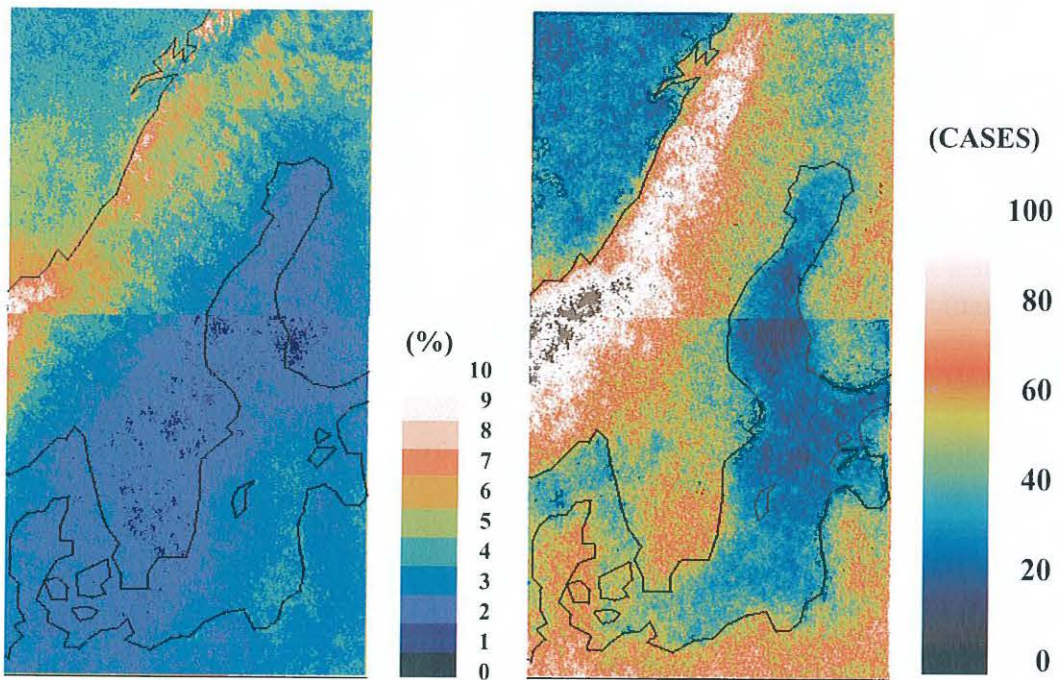


Figure 5.17 Frequency of occurrence of moderately-to-heavy precipitating clouds for the winter season (left) and the absolute number (occurred cases) of moderately-to-heavy precipitating clouds in the afternoon during the summer half of the year (right) in the period February 1991 to January 2001.

5.2.5 Precipitating clouds and deep convective clouds

The SCANDIA attempt to identify precipitating cloud types gave results very similar to the previously shown results for the opaque high-level cloud group in section 5.2.1. As expected from the experience of many previous VIS/IR precipitation estimation studies (e.g., as reported by Allam et al., 1993), very limited skill was shown when comparing to precipitation

climatologies from the available ground measurements of accumulated precipitation over the area. For example, the pronounced inland precipitation maximum near the south-western coast of Sweden is hardly visible in the satellite estimations. This is explained by the low time resolution in satellite observations and the fundamental problem of identifying precipitation from only the cloud top appearance.

Nevertheless, it is believed that some useful information could be extracted from the information as regards the occurrence of deep convective cloudiness over the area. Information on the occurrence of deep convection has earlier been reported based on data from geostationary satellites (e.g., Morel et al., 1997 and Morel and Sénési, 1998) taking advantage of the high temporal image resolution. It is here suggested that similar results could be achieved by use of very long time-series of data (compensating for the low temporal resolution) from the polar satellites. Interesting aspects here are the spatial distribution of Cumulonimbus clouds (Are there preferred regions?) and the frequency of convective clouds over the Baltic Sea (How frequent is the summertime convective precipitation over the Baltic Sea compared to over land areas?). The ten-year cloud climatology could possibly give some indications on conditions here prior to eventually receiving final answers by a future advanced use of weather radar information.

Figure 5.17 shows the frequency of moderately-to-heavy precipitating clouds in the winter season and, in addition, specifically the afternoon conditions in the summer half of the year. This analysis is based on SCANDIA classified pixels being labelled as Nimbostratus or Cumulonimbus clouds and, in addition, having feature 1 and 5 values exceeding additional and increased thresholds. This would yield an additional labelling as being precipitating moderately-to-heavy. Even if this admittedly is a subjective and qualitative labelling, it could give valuable insights into the question of the occurrence of deep convection over the area. Similar studies have earlier been published for low and medium latitude regions based on geostationary imagery with a high temporal resolution but no attempts have so far been made over high latitudes by using imagery with low temporal resolution from polar. For this to become realistic and justified, a very long time series of data is required and it is here suggested that the SCANDIA cloud climatology could be worth trying for this purpose.

Beginning with the afternoon results for the summer half of the year (April-September) in Figure 5.17 (to the right - being judged as the most reliable of the two), it is seen that there is a pronounced difference between land and sea regions in the area with much higher frequencies of deep convective clouds over land areas. Larger lakes (e.g., Lake Vänern) are seen to be able to suppress frequencies while smaller lakes (e.g., Lake Vättern) are not found to affect results at all. High frequencies are found over the Scandinavian mountain range, in the inner and eastern part of southern Sweden, over all land areas south of the Baltic Sea and over central Finland. The very high frequencies found in the Scandinavian mountain range could to a large extent be due to orographic enhancement effects affecting Nimbostratus clouds rather than causing deep convective clouds of the Cumulonimbus type. However, a considerable fraction can also come from true convective precipitation in connection to the clouds formed by slope-and-valley wind circulation systems.

The effect of a differentially advected sea breeze front (discussed previously in section 5.1.4) is clearly seen also here. Land areas with low frequencies of deep convective clouds are found near the south-western coast of Sweden close to Lake Vänern, the eastern part of central and northern Sweden and the most northern and southern parts of Finland. As regards conditions over the Baltic Sea, it is seen that the frequency is reduced by almost a factor of four over the

Bothnian Sea and the Baltic Proper compared to over nearby land areas. However, for the most southern part of the Baltic Sea frequencies are significantly higher. This is probably caused by the fact that Cumulonimbus clouds associated with summertime cold fronts or squall lines are most often oriented in a south-northerly direction when passing eastward over the area. Thus, the convective activity can be quite high when entering the western part of the area but it could later be strongly suppressed when passing out over the regions of the Baltic Proper and the Bothnian Sea.

For the winter season results in Figure 5.17, the information is not easily interpreted due to apparent separability problems, especially in the northern part of the region. Here, erroneously classified Cumulonimbus and Nimbostratus clouds over cloud-free and very cold ground surfaces have contaminated results considerably. However, if omitting results over land areas we can instead have more confidence in the results over the sea surfaces. The most interesting feature here is the relatively high frequencies found in the eastern part of the Baltic Proper (eastward of Gotland). This reflects probably a quite high frequency of occasions with cold air advected with northerly winds over the Baltic Sea giving rise to intensive snow showers reaching the coasts of the Baltic states and Poland. This feature was found to be even more pronounced if studying results exclusively for the months of January and February.

5.2.6 *Fractional sub-pixel cloudiness*

This cloud category consists of a rather small fraction of pixels being very close on the cloud-free side of the applied cloud detection thresholds. In particular, pixels having a small but measurable brightness temperature difference in feature four and six in Table 2.2 belong to this category. This means for example that very small cumulus elements and very thin cirrus clouds have been classified into this cloud category. Since the two features are based mainly on the assumption of a temperature difference between the cloud element and the surface we expect the contributions here to be low over land areas in winter.

In general, the contribution to the mean cloud frequencies has been less than 3 % over the area. Though, one must here remember that these pixels are only given 50 % weight compared to fully cloudy pixels as described earlier in section 3. However, in spring contributions as high as 5 % could be seen over land areas in the most southern part of the area. The annual cycle appears slightly unrealistic with the highest contributions from fractional clouds over land in winter and in spring while values over sea surfaces is at maximum during early summer. Consequently, SCANDIA does not appear to be optimally tuned for the treatment of fractional or sub-pixel cloudiness.

6 RESULTS FOR THE NORTHERN EUROPEAN REGION – SCANDIA VERSION 2

The goal of the second version of SCANDIA (being described earlier in section 2.2) was mainly to improve the treatment of varying illumination conditions over the area and the treatment of cold winter situations. The first problem was handled by introducing realistically thresholds varying with true sun elevation categories instead of using a fixed set of thresholds over a rather large area. The other problem was handled by introducing NWP model forecasted surface temperatures to define the basic IR threshold in feature 5 (see Table 2.2).

In general, similar results as for the SCANDIA version 1 model were achieved during the summer half of the year as is illustrated in Figure 6.1 (compare with corresponding results for SCANDIA version 1 in Appendix 2). This was suspected since the largest modifications of the scheme concerned the treatment of dark conditions and conditions in twilight. The more consistent treatment of the variation of sun elevations over the area had only a marginal effect on the results since for the higher sun elevation categories threshold value variations are generally small. One noticeable change of results was anyhow seen over the Baltic Sea during the spring season. Here, cloud amounts were decreased by approximately 5-10 % indicating that some remaining sunglint problems (which were obvious from visual inspection) were reduced in SCANDIA version 2 by the use of forecasted surface temperatures instead of using climatologically fixed values as in SCANDIA version 1. However, no change was seen in the autumn season (having also frequent occurrence of sun glints) and this was probably because the much warmer sea surface temperatures made the use of climatological and fixed threshold temperatures less dangerous.

For the winter half of the year, significant differences between the two model versions appeared. Here, cloud amounts decreased considerably over land areas for SCANDIA version 2, especially for months being colder than normal. A good example is shown in Figure 6.2 showing results for the comparably cold winter season of 1996 (see also Table 5.1) which can be compared to corresponding results of SCANDIA version 1 in Appendix 2. Cloud amounts have here been reduced by 20-25 % in many places in the northern and central portions of Scandinavia. This has now created a well-defined minimum in cloudiness which should be expected for areas with frequent occurrence of persistent wintertime cold anticyclones (quite typical for the Scandinavian area at the very low NAO index category in Table 5.1). This feature was only faintly visible in the corresponding cloud amount results for SCANDIA version 1 (see Figure 5.9). Thus, the use of ancillary surface temperature information from NWP models seems to have solved or at least partly reduced the wintertime cloud detection problem over the area. Notice also in Figure 6.2 how the cloudiness minimum extends a short distance off-shore the Norwegian coast. This could be conceptually interpreted as an effect of the cold and dry ageostrophic outflow in the lowest tropospheric layers from the wintertime anticyclone. Clouds quickly forms further offshore the coast when convection was initiated over the warmer ocean surfaces. This results almost in a cloudiness feature resembling an inverted sea-breeze front (inverted in the meaning that clouds form over the ocean areas instead of over land – compare also with front cover picture).

More results from the comparisons between the two SCANDIA model versions are shown later in section 7.1.2.

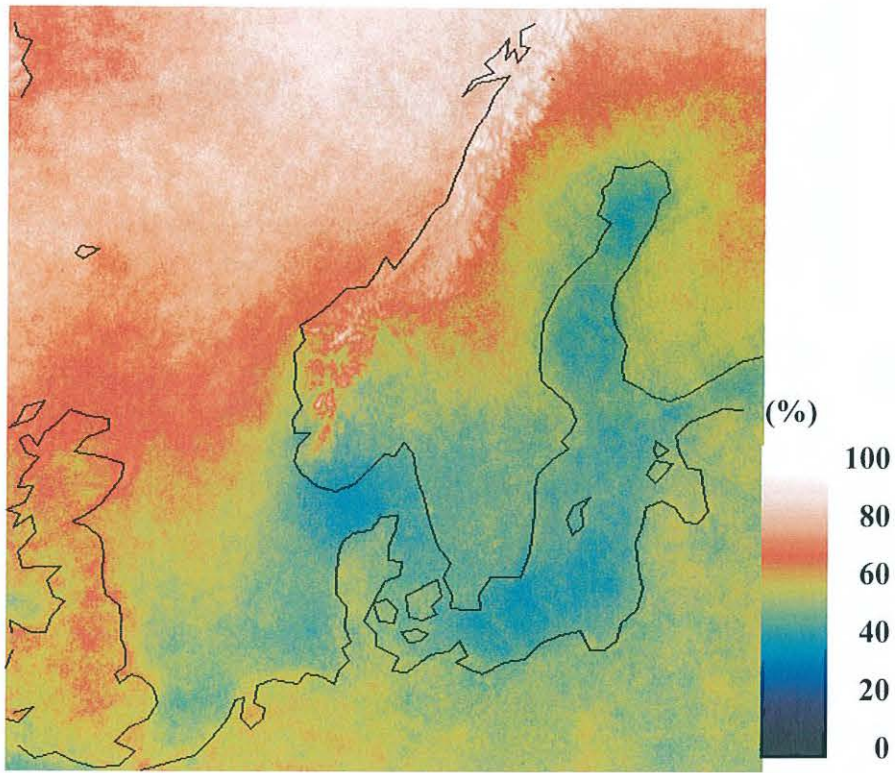


Figure 6.1 Monthly cloud frequencies in summer 1995 (June-August) for SCANDIA version 2 over the extended northern European area (area SCAN).

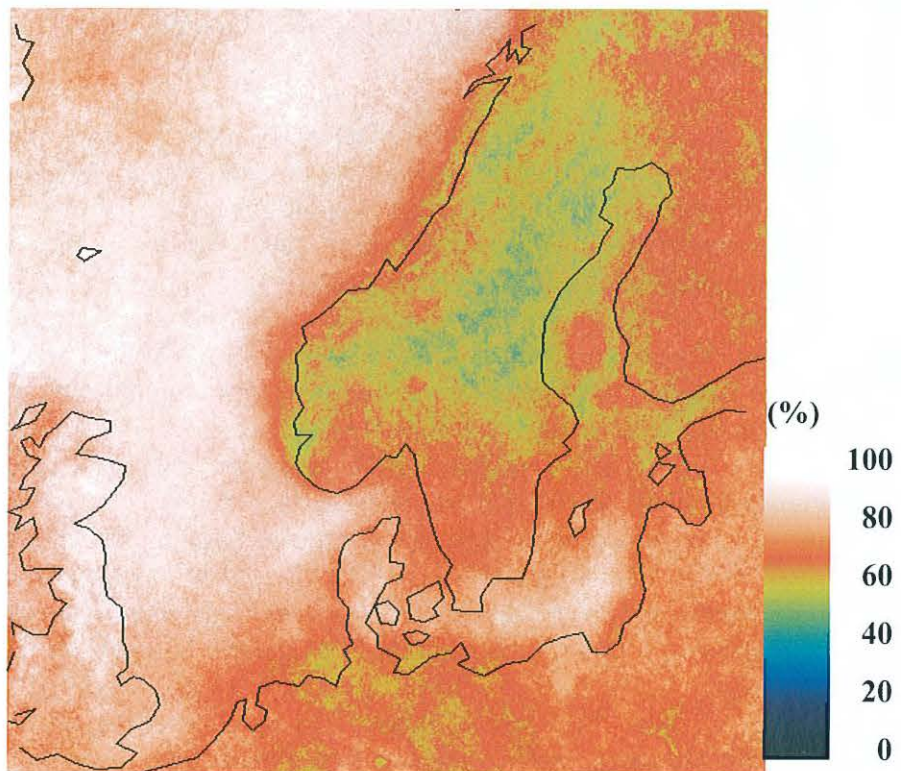


Figure 6.2 Monthly cloud frequencies in winter 1996 (December 1995 – February 1996) for SCANDIA version 2 over the extended northern European area (area SCAN).

The description of results for this modified and apparently improved version of SCANDIA is here limited to investigations of the wintertime cloud detection problem over the Scandinavian land area. Although interesting results also outside of Scandinavia could be noticed, it has to be remembered that the results compiled here are based on the same selection of satellite scenes and satellite passages as for SCANDIA version 1 (shown in Figure 4.1). Consequently, results in the western part of the shown SCAN area are based on data from AVHRR scenes rather close to or actually at the AVHRR swath edge (or alternatively, data is occasionally missing here simply due to lack of coverage). This means that we should expect to see enhanced cloud analysis problems here due to large viewing angles, missing data or in several cases also serious sun glint conditions with strongly anisotropic behaviour of both cloud and surface objects. The available project resources have not allowed the compilation of an adequately covered SCAN area utilising several consecutive NOAA passages over the area even if having access to the complete cloud classification data set in reality.

Finally, despite the shown positive impact here, an important aspect to mention is that the introduction of ancillary data in the form of NWP model forecasts can not always be assumed to be positive for the performance of cloud classification models. Also negative effects can be anticipate due to defects of the used NWP model (as discussed by Feijt and de Valk, 1998). Consequently, any future use of NWP model output in satellite cloud climate applications must be accompanied by a careful treatment of NWP data in order to avoid very complex error characteristics in the derived cloud climate data sets.

7 VALIDATION RESULTS

7.1 Comparisons with SYNOP observations

7.1.1 *Validation of cloud climatologies from SCANDIA Version 1*

The achieved SCANDIA cloud climatology results have been compared to corresponding cloud analyses based on surface observations (SYNOP observations) over Sweden. To make such comparisons meaningful, the spatial resolution of the satellite analyses were reduced to 36 km by an averaging procedure described previously in section 3. This would hopefully reduce errors due to differences in the compared quantities (surface-observed sky cover versus satellite-observed earth cover - discussed by Rossow and Garder, 1993b). The used averages are assumed to correspond better to the quantity mean cloud cover than the derived high-resolution cloud frequencies at pixel resolution. A coarser resolution than the proposed one here could be motivated since high-level cloud types are typically observed from ground at considerably larger distances in reality. However, the 36 km resolution has been chosen here to retain some of the characteristic small scale cloudiness features. Additionally, the closest area should be the most important for the surface observer and distant clouds would only give small contributions to the total cloud amount. Thus, a best fit between the satellite observed and the SYNOP observed area is believed to lie somewhere in the range 30-40 km (e.g., as indicated by Wollenweber, 2000).

Corresponding SYNOP analyses of mean cloud cover over Sweden have here been constructed using four daily observations at 00, 06, 12 and 18 UTC. If comparing with the corresponding satellite observation times (approximated in Table 3.1 and visualised in Figure 4.1), it is clear that only small deviations from the SYNOP observation times is at hand except for the 00 UTC observation. This comparison is limited to studies of exclusively the total cloud cover parameter which is believed to be the most appropriate parameter to be compared with satellite observations. The information on various cloud types in synoptical observations cannot easily be utilised in comparisons with satellite measurements. The reason is that the satellite observations are strongly biased towards the amounts of the topmost cloud layers (no information on underlying clouds is normally available) while the opposite is true for SYNOP observations.

A selection of in total 28 SYNOP stations has been used and their respective geographical locations are indicated in Figure 7.1. Unfortunately, major reductions in the synoptic network have occurred in Sweden during the period. Many of the selected stations were closed in 1996 and only 15 of the stations cover the entire ten-year period. Consequently, the validation data set presented here is biased towards the first half of the observation period when more observations were available.

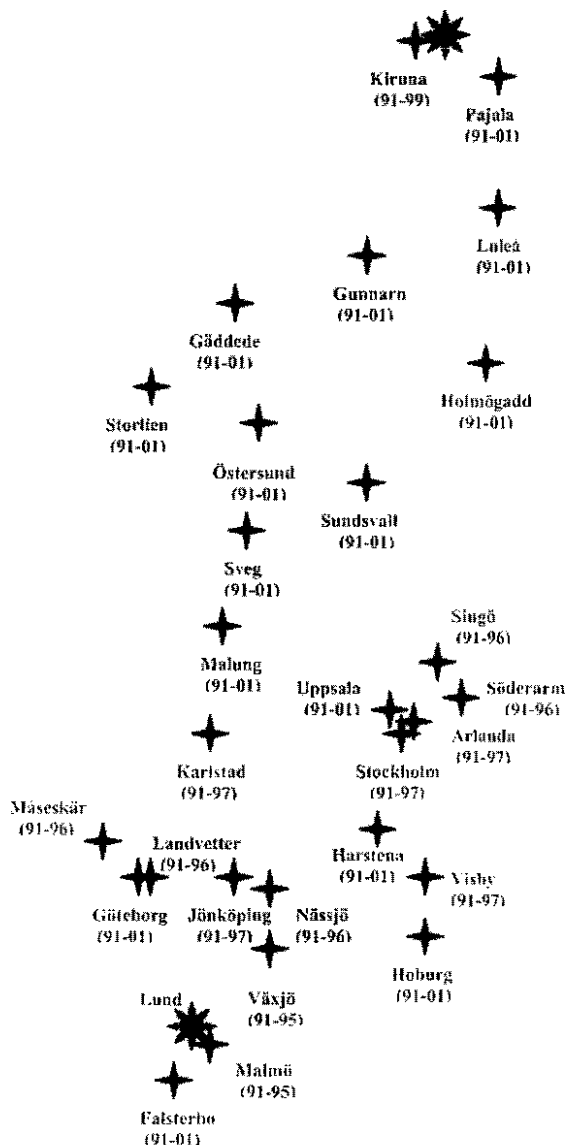


Figure 7.1 Positions for the used synoptical (SYNOP) stations in Sweden. In brackets are shown the available period of observations from each station in the period from 1991 to 2001. Notice also that the two stations Lund and Kiruna show the positions for two stations performing solar radiation measurements (to be discussed in the next section) and not synoptical weather observations.

Figure 7.2 shows a year-by-year summary of validation results for the entire period and the entire validation data set (including 12 470 satellite scenes compared with more than 250 000 SYNOP observations). Notice that the mean difference (bias error) deviates marginally from the apparent difference between the satellite and SYNOP mean in the second half of the period. This is explained by the fact that the satellite mean is computed over all 28 SYNOP

station positions for the entire period while the SYNOP mean does not include observations from all 28 stations in the second half of the period (as explained earlier). We can conclude that the annual mean of cloud cover does not vary much throughout the period (confined to the interval 60-70 %) over the Swedish area. Both data sets show this appearance, thus no major bias in the satellite data set can be seen (except from a possible negative bias of a few percent). In addition, both data sets show the same general behaviour of cloudiness over the Swedish area: The period starts with relatively high cloud amounts (1991-1993) which is followed by some years with lower cloud amounts (1994-1997) and it is finally ended with a new period of high cloud amounts (1998-2000). Despite this quite satisfying agreement between the two observation types, it is clear that the individual case-to-case variation is considerable as indicated by the quite high RMS error (exceeding 30 %). These results correspond rather well to results in previous validation experiments (Karlsson, 1993 and Karlsson, 1995) although the RMS error seems to be slightly higher here. The reason for this is probably the acceptance of a larger time difference between observation times for the two observations. Results from a separate test excluding comparisons if the time difference exceeded one hour supported this conclusion. In this case, RMS values dropped generally to between 26-30 % whereas bias errors remained practically the same. Comparing with Figure 4.1, it is clear that the observation time difference between SYNOP and satellite was especially large during some years (e.g., 1993-1994 and 1999-2001) for particularly the night and afternoon passages. Since these were compared with the 00 UTC and 12 UTC SYNOP observations, respectively, RMS errors could definitely be higher for these periods. This effect may explain the slight increase in RMS errors during the last years in the period.

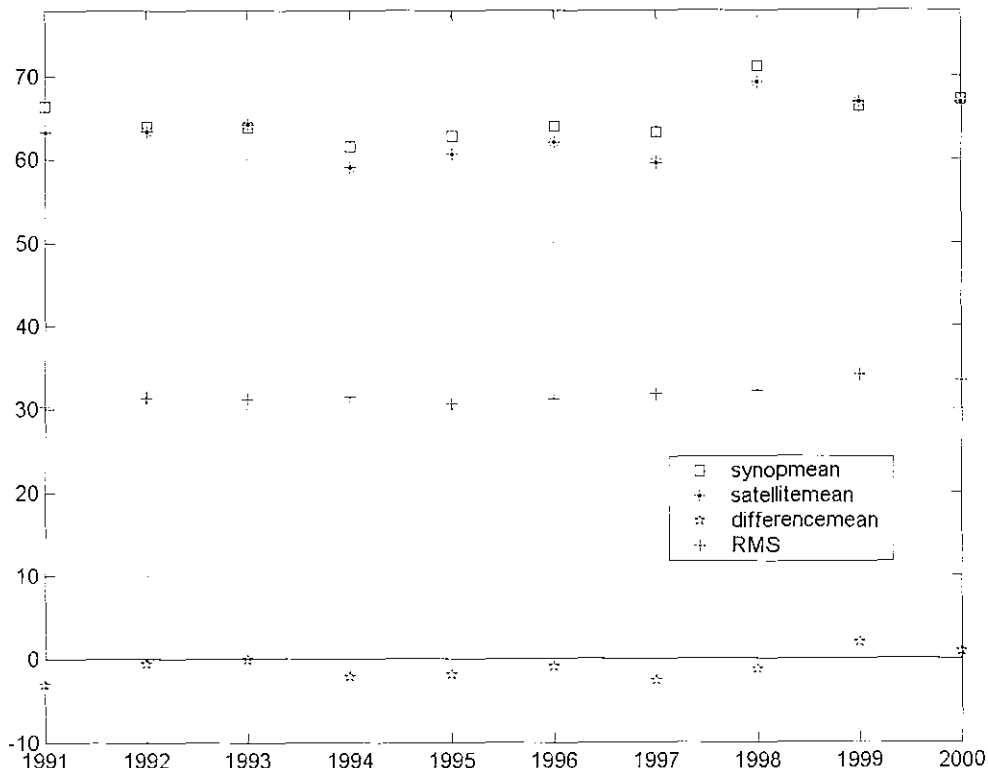


Figure 7.2 Yearly averages of total cloud cover (%) for SYNOP and satellite, the bias error (difference mean = satellite minus SYNOP) and RMS difference based on individual observations for the entire period.

It is clear from Figure 4.1 that the use of the 00 UTC SYNOP observation is quite inappropriate since the time difference from the satellite observation is in fact always larger than two hours. Furthermore, from experience we know that manual cloud observations near mid-night are very difficult to carry out. Therefore, we could expect to see additional differences emanating from uncertainties in the SYNOP observation here. Figure 7.3 shows the situation where we only study night observations to be compared with the corresponding situation based on all the daytime observations (morning, afternoon and evening) in Figure 7.4. An interesting pattern in the achieved results now appears. During dark conditions, RMS errors increase considerably (for some years exceeding 40 %) as could be expected. In addition, a generally positive bias appears reaching 6 % for some years. We could suspect that since the large time difference between observations would only (or at least predominately) affect the RMS error, a true cloud analysis problem could exist here where the satellite observation systematically overestimates the cloud amount during night. Such an effect is well known to occur in very cold situations when cold ground surfaces often were misclassified as mid- or high-level clouds by SCANDIA. However, Karlsson (1996) also reported that the surface observer often seemed to underestimate cloud cover at night in cases with overcast Cirrus or Cirrostratus cloudiness. It is not possible here to quantify the respective contributions here for the two effects.

For the daytime conditions in Figure 7.4 we notice that RMS differences are generally below 30 % but here, a negative bias is found. Thus, even if the internal difference between individual observations decrease, the satellite seems to systematically underestimate cloud amounts during daytime.

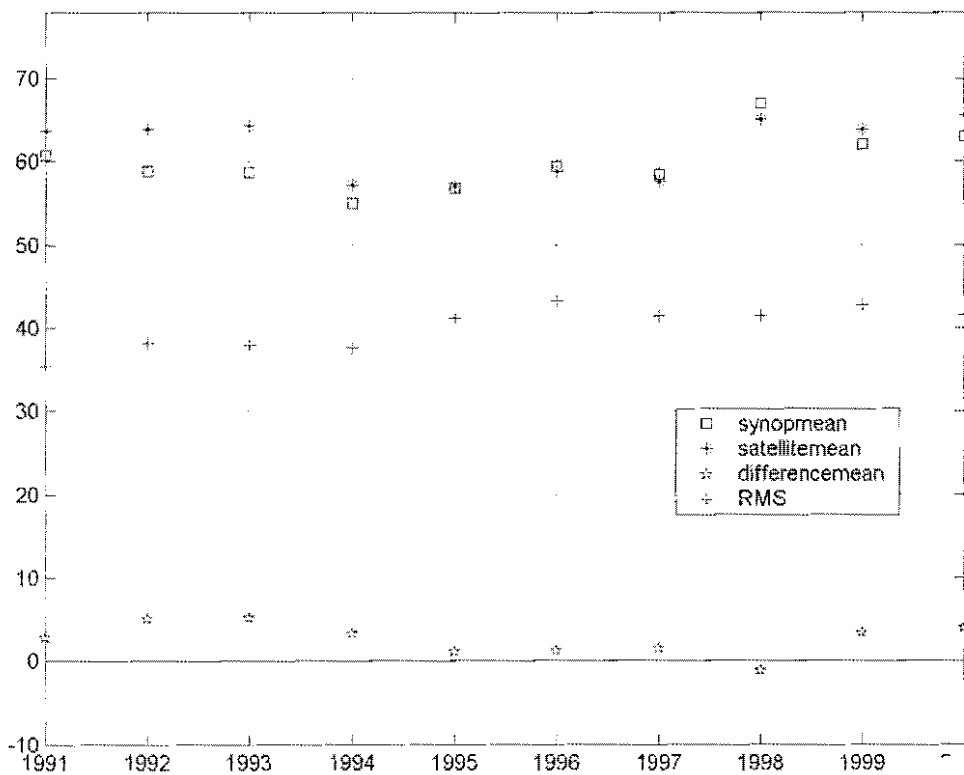


Figure 7.3 Same as in Figure 7.2 but exclusively for the night observations.

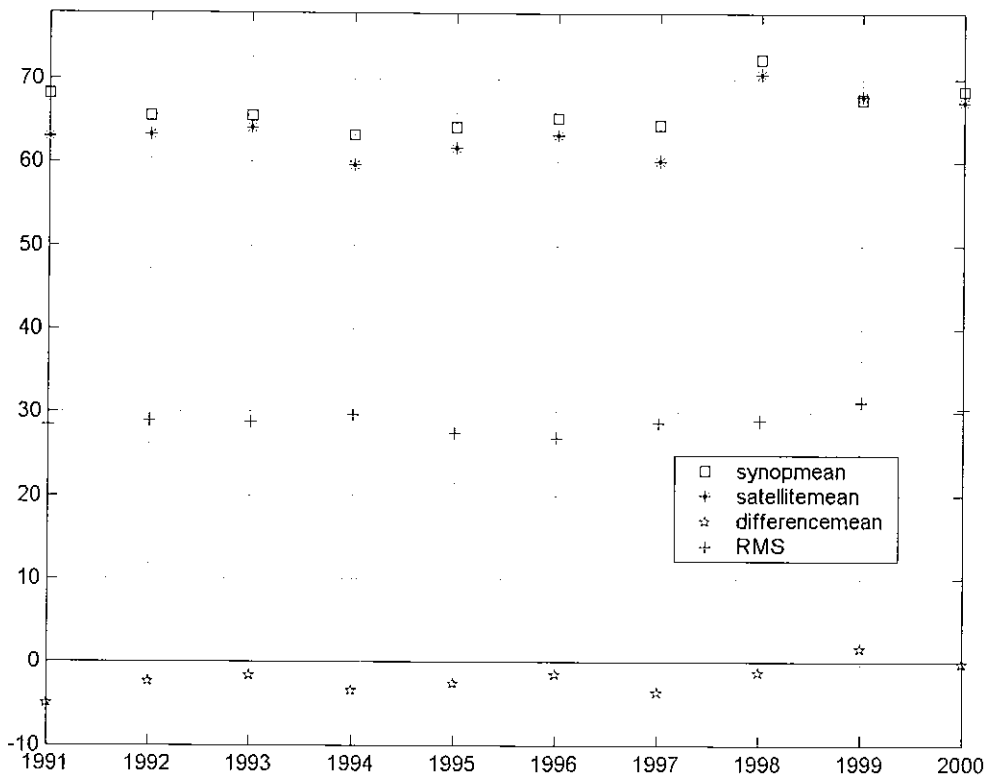


Figure 7.4 Same as in Figure 7.2 but for all observations excluding the night observations.

To bring more details for describing the relation between SYNOP and satellite observations, Figure 7.5 shows monthly averages of validation results throughout the period, thus allowing an evaluation of the seasonal variation. Notice here in particular the sinusoidal appearance of the bias error experiencing a positive maximum in the winter season and a negative maximum in the summer season. We can also here see the effect of the loss of a large part of available SYNOP observations after 1996 giving a less pronounced and clear sinusoidal pattern. If making the same subdivision of the validation material as above (i.e., separation of night cases and daytime cases), it was found that for the night cases almost all bias error values were positive (for some months as high as 15 %). The sinusoidal pattern was still visible but much less pronounced. For the daytime cases, the sinusoidal pattern of the bias error was again pronounced but all values were shifted towards negative values. Summertime negative biases as low as -12 % (i.e, one octa if translated to SYNOP observed cloudiness units) were found for some months but in general the bias error for the winter season was still positive and between 5-10 %. This could be interpreted as a consequence of the fact that most of the morning and evening observations during the winter season were actually made during dark conditions with error characteristics more resembling the night case.

A very interesting feature in Figure 7.5 is that the summertime negative peak of the bias error is generally accompanied by high values of the correlation coefficient and by a minimum of the RMS error. This could indicate that the found negative bias might rather be caused by an overestimation of cloud amounts in the SYNOP observation than by a systematic underestimation by the satellite observation. It is well known that the surface observer encounters problems in describing the proper cloud amount in case of convective cloud cover

with scattered cloud elements with a rather high vertical extension. The effect of these vertically extended clouds will be to shield away cloud-free portions between individual clouds when viewed at off-zenith angles. Thus, the observer will tend to overestimate the true total horizontal cloud cover. Another fact that supports this explanation of the found bias error in summer is that the multispectral method for discrimination of clouds in satellite imagery normally has its greatest capability in summer (as often shown by various class discrimination indices). The reason is that the optimal illumination conditions and the favourable temperature lapse rates in the atmosphere (free of near-surface temperature inversions) provides the maximum amount of useful information in the available spectral channels of the AVHRR instrument. This is further supported by many years of experience from visual inspection of cloud classification images showing no particular problems during summer. Consequently, it is here assumed that the negative bias in summer is an artefact caused by an overestimation of total cloud cover in SYNOP observations.

On the other hand, the situation in winter cannot possibly be explained to a greater extent by the previously mentioned problems encountered by the SYNOP observer at dark conditions. We can see that the high positive bias is generally accompanied by a decrease in the correlation coefficient and an increase in the RMS error. Thus, it is obvious that we have not only a problem with overestimation of cloud amounts during winter. In addition, there is also evidently a frequent occurrence of underestimation of cloud cover explaining the dip in correlation and the increase of RMS errors. For some winter months (e.g., December 1997 and January 1998) we have even cases when cloud amounts are, on the average, seriously underestimated which is a bit contradictory to the mean conditions found for other winter months. Some evidence of an underestimation of low-level clouds at twilight conditions have previously been reported (Karlsson, 1996) due to the loss of the typical day- or night cloud signature in image feature 4. Also night-time cases with superposed semi-transparent Cirrus clouds over Stratus clouds give the same result and might result in a failure in cloud detection due to the unfortunate mixing of the cloud signatures in feature 4. This results in a cancellation of the brightness temperature difference required for cloud detection. A closer look at the conditions during these months, including a visual inspection of cloud classifications, revealed that these months were warmer than normal and very cloudy. Thus, it is possible that the nighttime and twilight problems of correctly estimating low-level cloudiness may have dominated during these months compared to previously mentioned and often dominating factors giving rise to overestimation of cloud amounts.

To get an idea of the importance for the cloud analysis quality on whether it is performed in a warm or cold winter season we can study conditions for two individually selected SYNOP stations: Falsterbo and Pajala (see Figure 7.1).

Falsterbo is a coastal station at the southernmost tip of Sweden. Consequently, the wintertime ice free conditions (prevailing here for all years in the studied period) and the relatively warm sea surface temperatures in the surrounding Baltic Sea brings relatively mild winter seasons. As a contrast, Pajala in the inland part of northern Sweden experiences generally very cold winter temperatures. Even during relatively warm winter seasons (e.g. in 1995 as is indicated by Table 5.1), some periods with very cold winter weather generally occurs here. Monthly results for the two stations based on all four daily observations are shown in Figure 7.6 and 7.7.

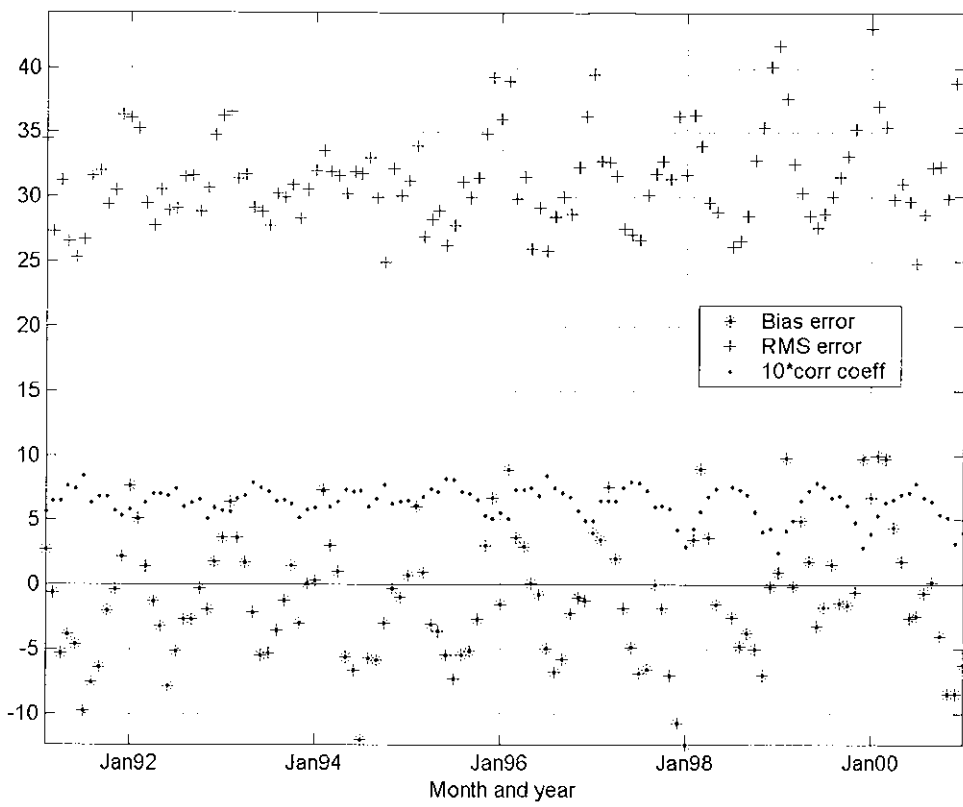


Figure 7.5 Monthly averages of bias errors, RMS errors and correlation coefficient for the entire validation data set.

Wintertime positive bias errors for Falsterbo are seen to be at maximum approximately 10 % while at Pajala several cases with bias errors exceeding 20 % can be seen. Similarly, wintertime RMS errors are generally below 35 % at Falsterbo while at Pajala RMS errors exceeding 55 % can be found for some individual months. For the correlation coefficient, fairly reasonable values (approximately 0.5-0.6) can be found for winter months at Falsterbo while at Pajala values drop to almost zero or even becoming slightly negative for some months. A further illustration of these differences is shown in Figure 7.8 where conditions for an individual month are shown for the two stations.

The revealed differences between Falsterbo and Pajala hold also when comparing the majority of the SYNOP stations in the southern part of the area with the majority of stations in the northern part of the area. It also shows very clearly that the stations producing the largest number of cases with very large deviations (cloud amount differences exceeding 50 %) come predominantly from the northern part of the area (see example from 1996 in Figure 7.9). As regards the corresponding bias errors it was also found that stations in the northern part (although with some exceptions) more often had a positive bias error compared to stations in the southern half of the area (see Figure 7.10).

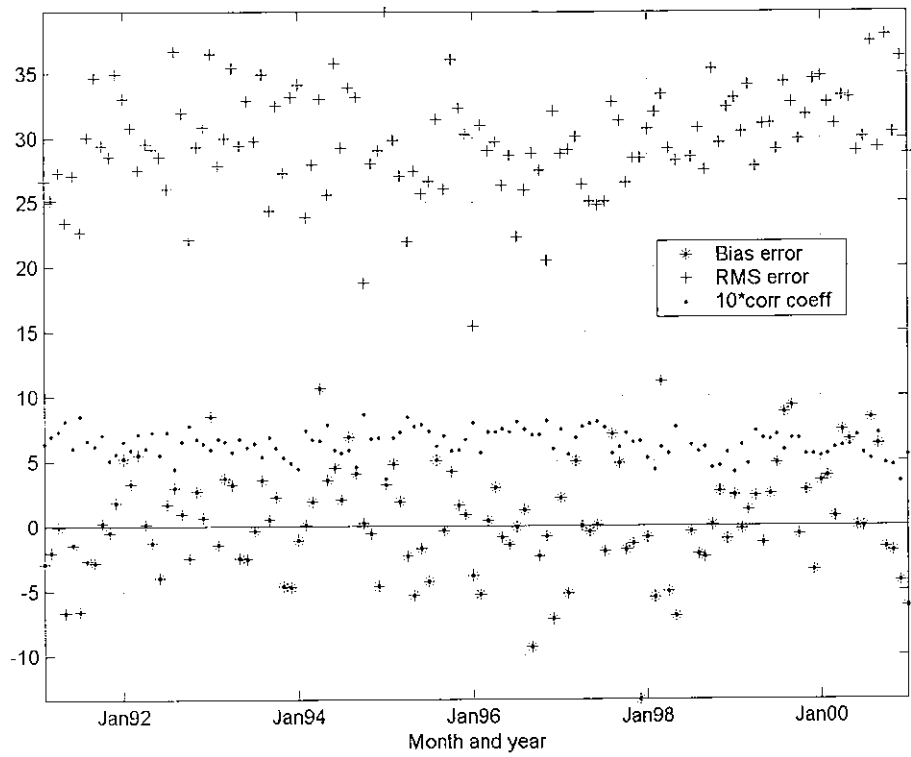


Figure 7.6 Monthly bias errors, RMS errors and correlation coefficients for the SYNOP station of **Falsterbo** over the entire ten year period.

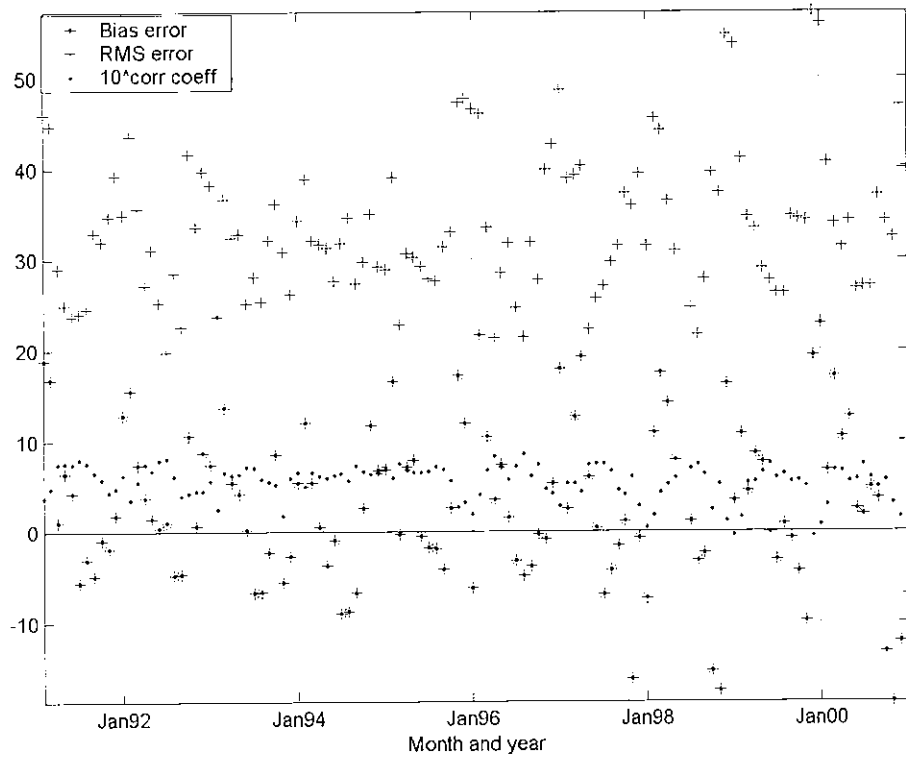


Figure 7.7 Monthly bias errors, RMS errors and correlation coefficients for the SYNOP station of **Pajala** over the entire ten year period (notice change of ordinata)..

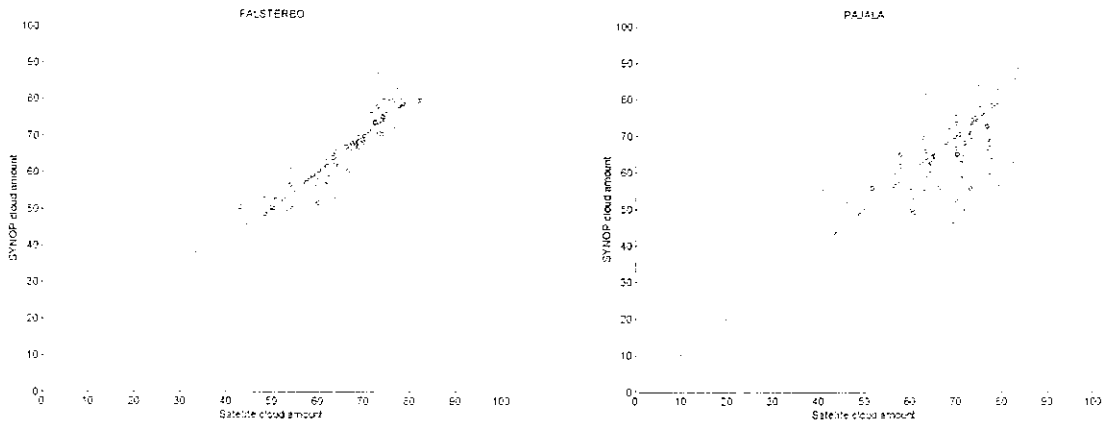


Figure 7.8 Scatterplots of SYNOP-observed and satellite-observed monthly cloud cover (composed by utilising four observations per day) between February 1991 and January 2001 for Falsterbo (left) and Pajala (right).

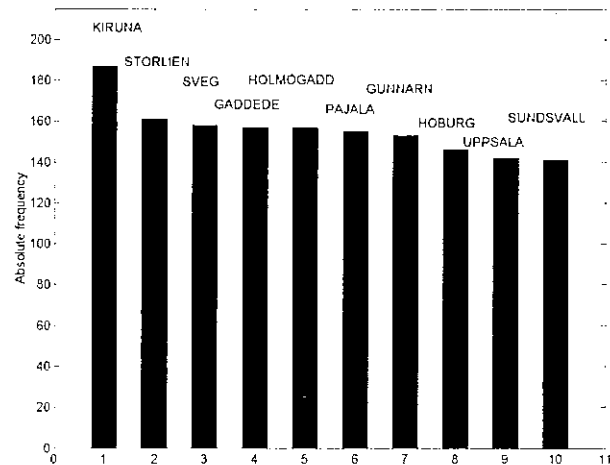


Figure 7.9 Diagram for 1996 showing the ten SYNOP stations with the highest frequencies of cases with cloud amount observation differences exceeding 50 % during 1996.

To see if these results also could be systemised according to a categorisation based on the NAO index as previously discussed in section 5.1.3, the monthly validation results in Figure 7.5 were sorted according to the categories in Table 5.1. Results are summarised in Table 7.1. Results here show somewhat surprisingly that bias errors are generally positive and quite high for the categories with high NAO indices while at the lower NAO index categories bias errors stay close to zero. However, it is also seen a very large variation among individual months for the latter groups. For example, in January 1997 the bias error is -12.3 while for March 2000 (in the same category Low NAO index) the bias error is 9.7. Consequently, this indicates that the overestimation of cloud cover in winter may not predominately come from the false interpretation of very cold ground surfaces. Instead, other factors (like the enhanced anisotropic reflection from land surfaces at very low sun elevations) seem to be more important. Furthermore, it is also possible that the well-known variation of the noise levels in AVHRR channel 3 may have contributed here in giving this quite unexpected result.

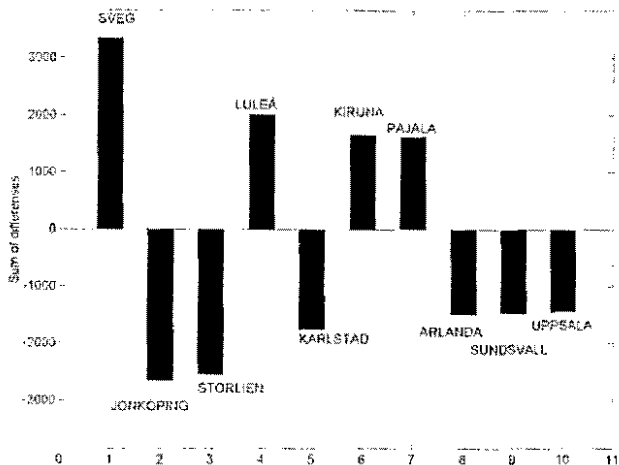


Figure 7.10 Diagram for 1996 showing the ten SYNOP stations with the highest summed differences for the same data set as in Figure 7.9.

Table 7.1 Monthly validation results for the bias error according to the previously defined NAO groups in Table 5.1.

NAO-index	Bias error
category	(%)
Very High NAO	5.2
High NAO	3.4
Low NAO	0.9
Very Low NAO	0.4

Thus, we may finally conclude that the quality of SCANDIA climatologies in the winter season is significantly degraded compared to results for other seasons. In these cases, extremely cold and cloud free land surfaces are often mis-classified as clouds and this effect is also further enhanced by the increasing problems with AVHRR channel 3 noise causing spurious stripes with erroneous clouds in cloud classifications. In addition, even if not always being exposed to cold winter seasons, problems due to an enhanced anisotropic reflection by land areas at very large solar zenith angles and the underestimation of low-level cloudiness when the sun is very close to or under the horizon give winter-time results high RMS errors and a rather low correlation when compared to observed cloud amounts. However, for other seasons the quality of SCANDIA climatologies appears to be good. In fact, results for the summer season were subjectively judged as being excellent despite the negative bias being seen when compared to SYNOP observations. The found deviations here are concluded to be more or less entirely caused by an underestimation of cloud amounts by the surface observer.

7.1.2 Validation of cloud climatologies from SCANDIA Version 2

Validation results for SCANDIA version 1 was compared to the limited data set with results from SCANDIA version 2 covering the period July 1994 to January 1997. Results month by month (corresponding to results shown previously in Figure 7.5) for the entire SYNOP validation data set in this period are displayed below in Figure 7.11. The most striking feature here is that the wintertime positive bias for SCANDIA version 1 has been dramatically reduced and for some months even turned into a negative bias. Consequently, the example of the improvement shown previously in Figure 6.2 is also seen in the SYNOP validation data set covering also other winter periods. Summertime results have also improved marginally. Unfortunately, the achieved very small improvements of the correlation coefficients and RMS deviations (not shown here) in winter indicates that mostly other sources of error (listed in the previous section) than the rather spectacular and easily identified cold land surface problem are indeed responsible for the large scatter in the results. A typical illustration of this problem is the change of the bias error in January 1996 in Figure 7.11 from -2 % to -10 % for SCANDIA version 2. This month was relatively warm and windy (as opposed to the previous December and the following February months) meaning that a high frequency of Stratus, Stratocumulus and also Cirrus clouds often prevailed. Consequently, the problem of correctly identifying these clouds in twilight and at night conditions seems to have dominated for this month. This became even more evident after removing the relatively small number of overestimated cloud amounts in cold situations by SCANDIA version 2.

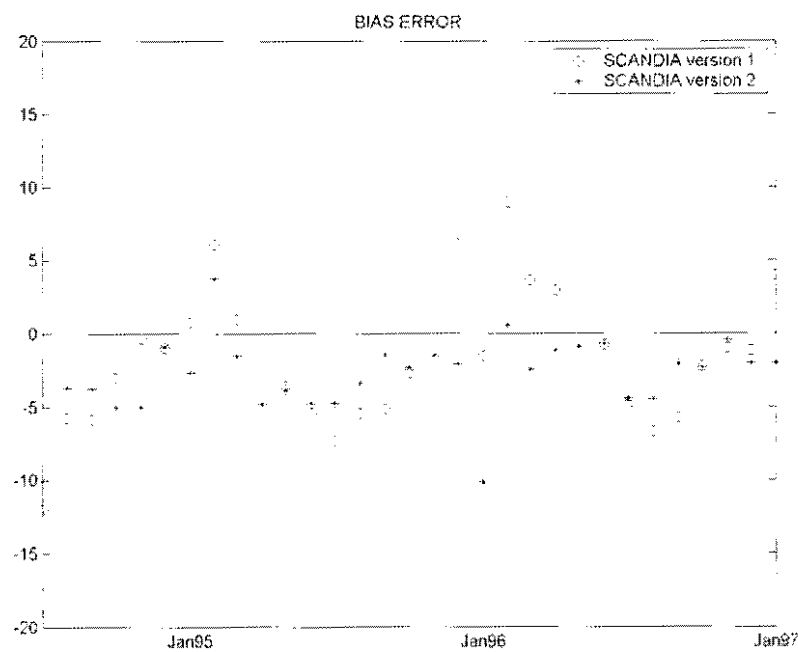


Figure 7.11 Monthly averages of bias errors for SCANDIA versions 1 and 2 based on the entire SYNOP validation data set in the period July 1994 to January 1997.

7.2 Comparisons with solar radiation measurements

A potential use of satellite-derived cloud climate information is as input information to simulations or calculations of radiation conditions at the surface by use of radiative transfer models (RTM). Several such applications have already been reported (e.g., Pinker and Laszlo, 1992), most often based on cloud information retrieved from geostationary satellite data with a high temporal resolution. Consequently, it would be interesting here to see if the achieved cloud climatologies bear any realistic resemblance to solar radiation measurements performed during the same time period.

A network consisting of 12 stations for high quality solar radiation measurements exists in Sweden. This network and the set of measurements carried out at each station were described in detail by Persson (2000). The best way of directly comparing the cloud climatology information with the solar radiation data set is believed to be to compare cloud amounts with the relative sunshine duration at each solar radiation station. In this way, we avoid the complicating factor that the incoming solar radiation amounts are by definition high at high sun elevations and low at low sun elevations while the cloud amount parameter does not have any direct relation to the sun elevation. Sunshine duration is here calculated from measurements of direct solar radiation and it is defined as the time when the direct solar radiation (measured with a pyrheliometer) exceeds 120 Wm^{-2} . This method has been recommended by the Commission for Instruments and Methods of Observations (CIMO). To get the relative sunshine duration, i.e., the percentage of the daily theoretical maximum sunshine duration, the measurement is compared to the theoretical maximum of sunshine duration according to astronomical calculations.

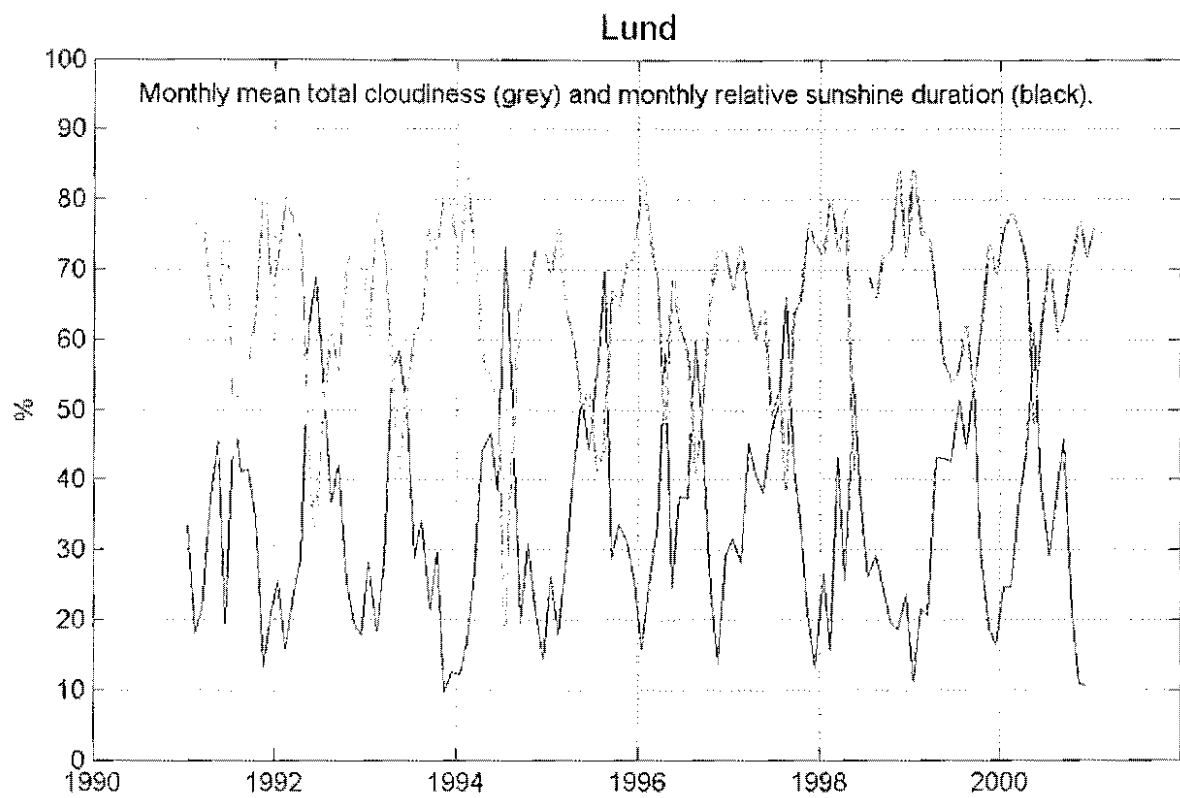
Results from two selected solar radiation stations (with positions indicated in Figure 7.1) will be shown here. One is situated in southern Sweden (Lund) and another in northern Sweden (Kiruna). Measurements in Lund represent the situation where winters are in general rather warm and snow-free which was shown to give the best correspondence between satellite- and SYNOP-observed cloudiness in the previous two sections. As a contrast, measurements in Kiruna represent the situation with a frequent occurrence of cold and snowy winter conditions which were shown to give serious problems for the satellite retrieval of cloudiness. Results for the two stations are shown in Figure 7.12 and Figure 7.13, respectively. Notice that a perfect match between relative sunshine duration and total cloud cover would yield an inversely proportional relation (i.e., 100 % total cloud cover means 0 % sunshine duration and vice versa).

Results for Lund show a very clear inversely proportional relation between the two compared parameters. The curve for cloud amount appears to be almost an exact mirroring of the sunshine duration curve in the axis defined by the cloud amount level of 50 %. From the scatter diagram we can also see that the differences between the total data set and the data set exclusively for the summer half of the year are small. Thus, we cannot see any noticeable effect of the previously found summertime overestimation of cloudiness when comparing with surface observations. In contrast, for high cloud amounts (i.e., exceeding 60 %) there is a slight tendency for too low cloud amounts in comparison to sunshine duration values. However, since the viewing perspective problem presumably would affect also direct solar radiation measurements we could here suspect that this might influence and limit the sunshine duration measurements. This is even more evident when observing that the deviations are found especially during the winter half of the year when the sun is predominately viewed at high solar zenith angles.

For Kiruna in Figure 7.13, results are not as good which indeed was anticipated. The disagreement between the two observation types is especially large during the winter seasons where the surface-observed apparent cloud amounts (as deduced from sunshine duration measurements) seem to be significantly larger than the satellite-observed cloud amounts. However, if studying exclusively the summer half of the year results are almost comparable to the results for Lund albeit with a larger scatter and a somewhat decreased correlation.

Wintertime results for Kiruna appear again somewhat surprising if compared with the generally positive bias for the satellite-retrieved cloudiness that was found when comparing to SYNOP observations in northern Sweden. A probable explanation is that the used quantity relative sunshine duration is not fully applicable for comparison with the satellite data set in winter and especially not in northern Sweden. Here, the maximum sunshine duration is very short in the winter half of the year and, in fact, zero in Kiruna at mid-winter! This means that the comparison with the satellite data set is not meaningful since most of the satellite observations are made during completely dark conditions. Furthermore, consider also that we have predominantly high solar zenith angles in the winter half of the year in northern Sweden. Consequently, the apparent cloud amounts will tend to be overestimated in relative sunshine measurements in the same way as being done for SYNOP observations when viewing clouds at off-zenith angles.

In conclusion, there seems to be a very good agreement between the retrieved cloud amounts and the parameter relative sunshine duration, at least for the summer half of the year and for places in the southern part of the area. It is also somewhat surprising to see such a good correspondence of the results when considering the very coarse time resolution of the NOAA AVHRR measurements compared to the high temporal resolution of the direct solar radiation measurements (in fact based on measurements every second). This indicates that despite the rather small time scale for the evolution of individual cloud elements (e.g., small cumulus clouds), the time scale or the persistence of the larger scale cloud fields seems to be much longer. Finally, when interpreting results here it should also be remembered that results for the winter half of the year may be contaminated or obscured to some extent by the fact that most of the cloudiness observations are made during completely dark conditions, thus not during the time when the relative sunshine duration is measured.



Lund

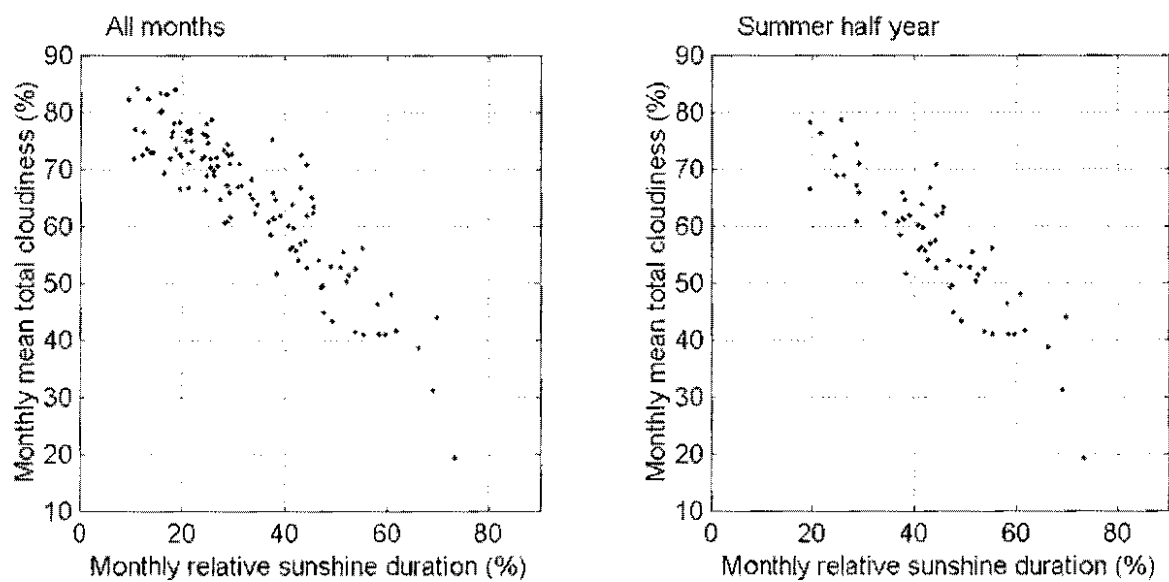


Figure 7.12 *Top:* Monthly relative sunshine duration for Lund plotted against monthly satellite-retrieved cloud amounts for the period February 1991 to January 2001. *Bottom left:* Same quantities as for top figure but plotted as a scatter diagram. *Bottom right:* Same scatter diagram but now including only months from the summer half of the year (April-September).

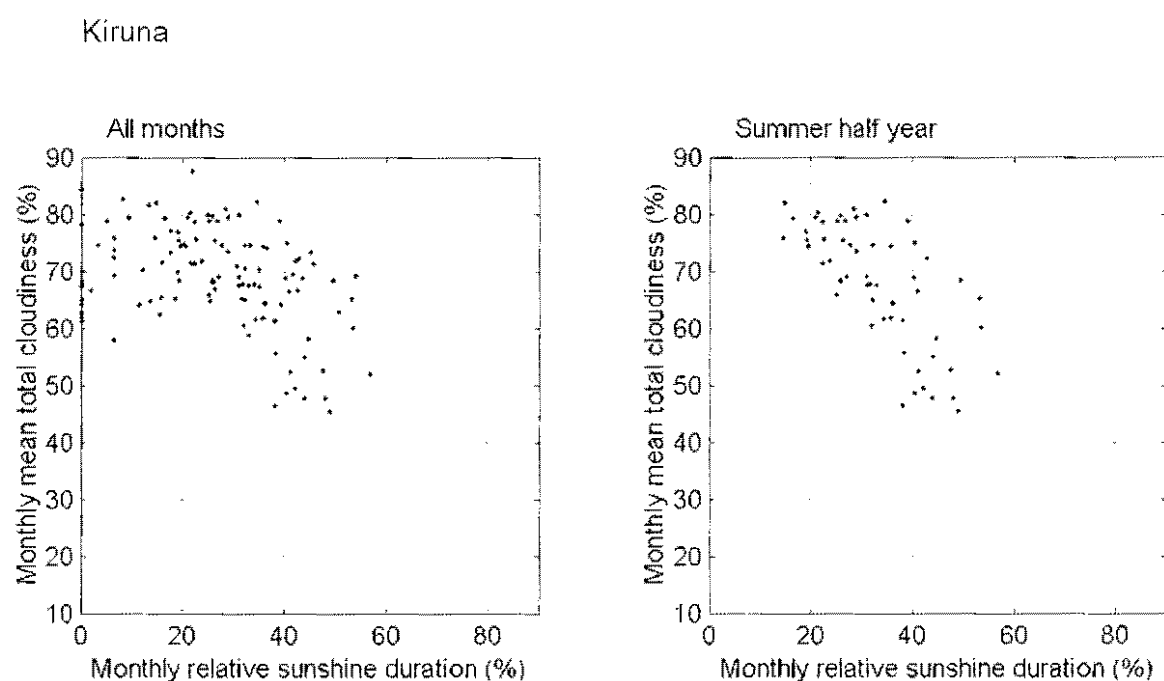
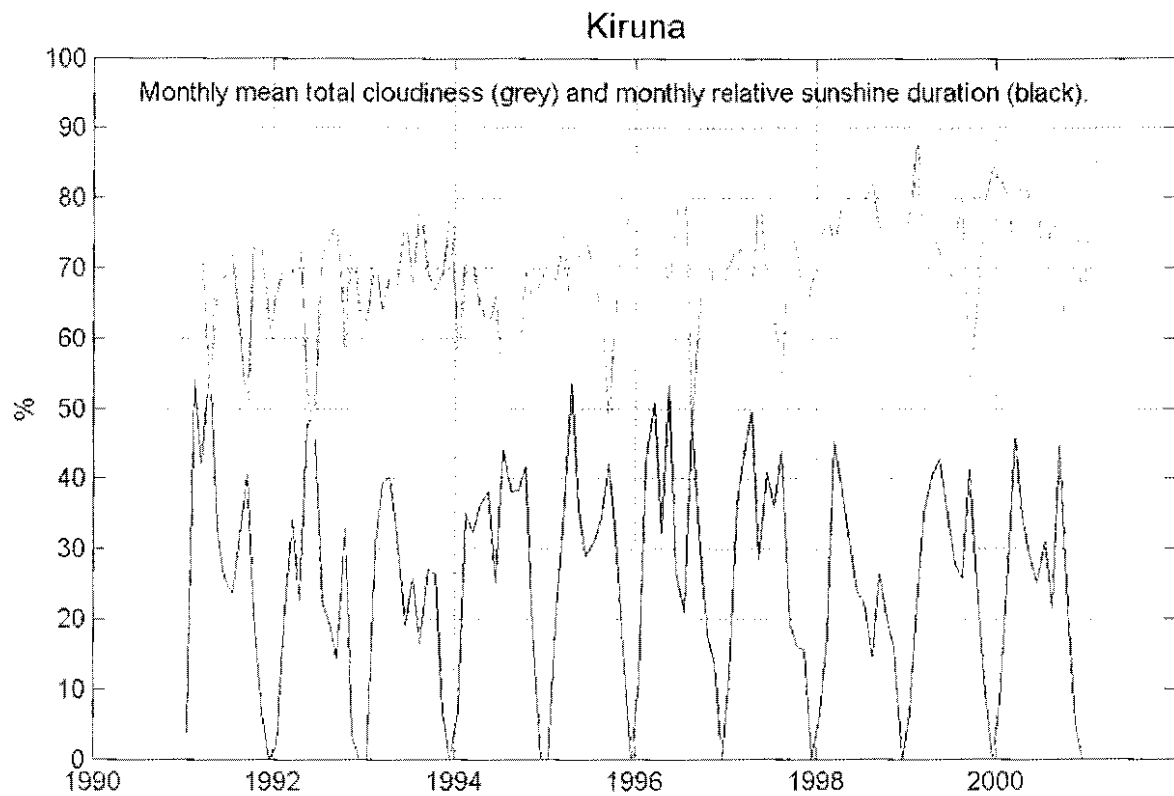


Figure 7.13 *Top:* Monthly relative sunshine duration for Kiruna plotted against monthly satellite-retrieved cloud amounts for the period February 1991 to January 2001. *Bottom left:* Same quantities as for top figure but plotted as a scatter diagram. *Bottom right:* Same scatter diagram but now including only months from the summer half of the year (April-September).

7.3 Comparisons with ISCCP, CRU and climate simulation datasets

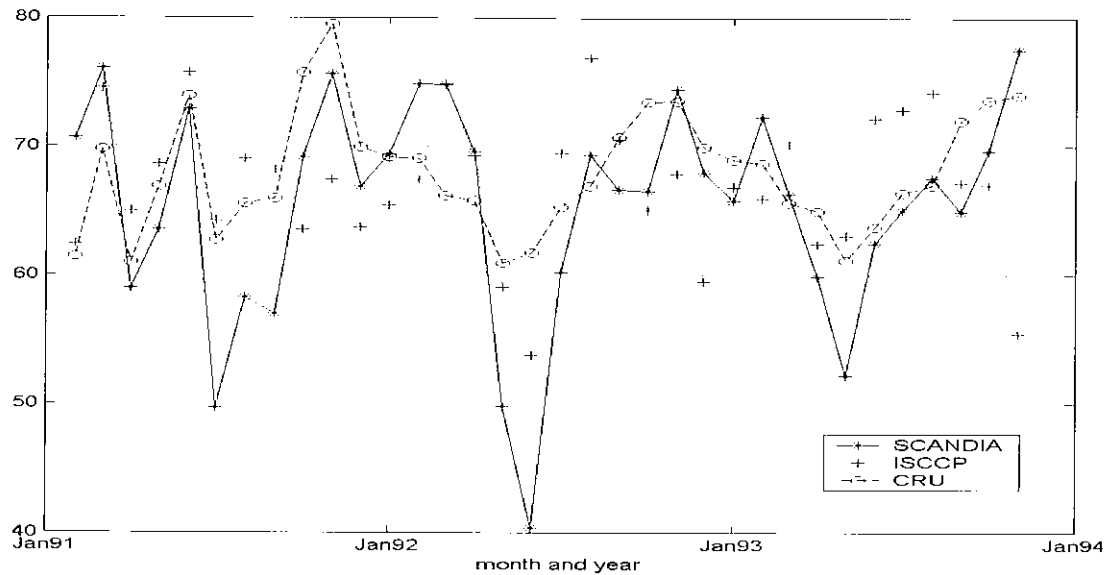
A limited comparison of SCANDIA cloud climatologies with two other internationally available cloud climate data sets has also been performed. The two data sets are the SYNOP-based gridded data set denoted CRU which is compiled by the Climate Research Unit at University of East Anglia, UK (see New et al., 2000) and the satellite-derived cloud climate data set from ISCCP (Rossow and Garder, 1993 and Rossow and Schiffer, 1999). Since ISCPP data is not yet available for the entire period 1991-2000, the period 1991-1993 has been studied here. In addition, also a comparison with results from climate model simulations has been included over oceanic surfaces (without CRU coverage). Results for SCANDIA land points are shown in Figure 7.14 (upper panel) for SCANDIA version 1, the two other observation data sets and the simulation data set over the oceanic portion of the area for this particular period. For the SCANDIA land points in Figure 7.14 (upper panel), SCANDIA and ISCCP results are shown exclusively for the land portion of the area covered by SCANDIA to make the comparison with the CRU dataset (not available over ocean areas) meaningful. Results for all pixels belonging to the SCANDIA-used land mask were extracted. The corresponding CRU data set was available in a 0.4° grid (approximately corresponding to 44-km grid resolution) and the 2.5° ISCCP data set was interpolated to the same grid resolution by a bi-linear interpolation technique. The ISCCP results here are from the recently updated ISCCP data set, denoted the ISCCP D2 series (the updated method described by Rossow and Schiffer, 1999).

We notice that the CRU and SCANDIA data sets agree reasonably well over the SCANDIA land point area in the first part of the period. CRU gives here slightly higher cloud amounts than SCANDIA during the summer half of the year while the opposite is at least partly true in the winter half of the year. This is consistent and agrees rather well with the results previously presented in section 7.1. However, discrepancies between the SCANDIA and CRU data sets increase for the second half of the studied period. This is explained by a an increasing lack of available surface observations in the CRU data set. It means that the CRU estimate more and more resembles an overall statistical average of a cloud climatology and not a truly representative climatology based on real observations (as described by New et al., 2000).

The ISCCP results for the SCANDIA land points in Figure 7.14 lies fairly close to the CRU and SCANDIA data sets. Thus, the revised results in the ISCCP D2 series appear to give more realistic values than the previous C2 series where cloud amounts at these latitudes often were found to be significantly underestimated. However, a smaller annual amplitude and variation of ISCCP cloud amounts compared with the other two data sets (especially SCANDIA) can be noticed. This difference between CRU and ISCCP was even more pronounced if studying areas in central Europe (not shown here) where the amount of available SYNOP observations was large. Here, the summertime cloud amounts were also clearly overestimated by ISCCP which further weakened the annual amplitude in ISCCP cloudiness. Karlsson (1997) has also reported this feature in a previous study.

For the results over the oceanic part of the area in Figure 7.14, the differences between SCANDIA and ISCCP have increased further. Here, SCANDIA-derived cloud amounts are generally significantly lower than ISCCP cloud amounts. The differences are most pronounced for summer months were differences of almost 20 % could be seen for some individual months (July 1991 and June 1992). Even if some of this difference may be explained to some extent by the different spatial resolution of the two compared data sets, it is

SCANDIA Land Points



SCANDIA Sea Points

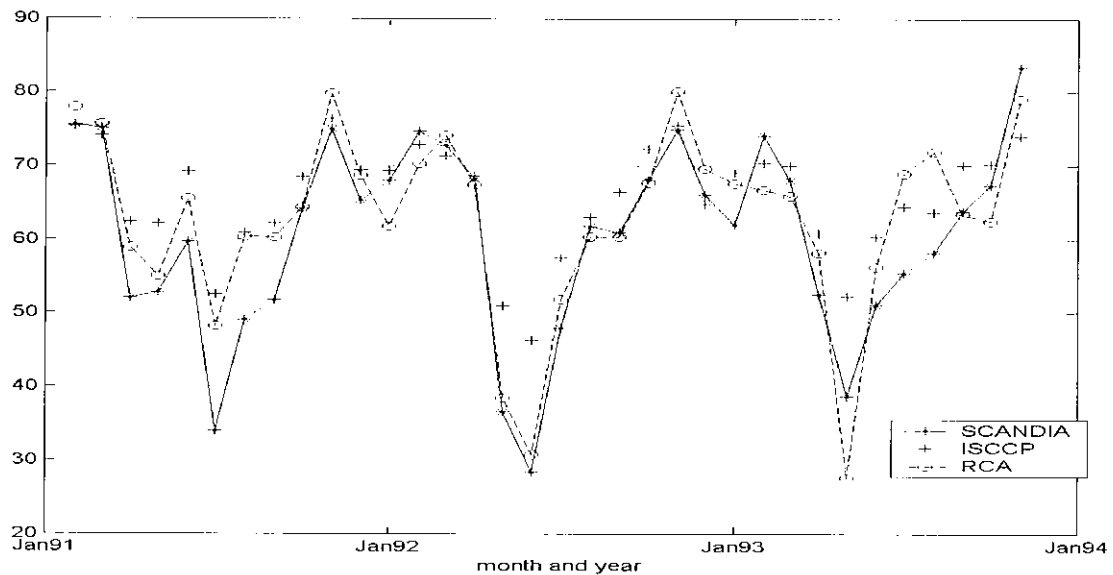


Figure 7.14 Upper panel: Plot of monthly mean of cloud cover (%) over SCANDIA land points for SCANDIA (solid), the ISCCP D2 dataset (dotted) and the CRU data set (dashed) for the period February 1991 until November 1993. **Lower panel:** Plot of monthly mean of cloud cover (%) over SCANDIA ocean points for SCANDIA (solid), the ISCCP D2 dataset (dotted) and the RCA data set (dashed) for the same period.

here suggested that the ISCCP D2 series cloud amounts are overestimated over the northern European region. Furthermore, the seasonal and annual amplitude variations appear to be too small. The latter conclusion is valid for both land and ocean areas.

It is interesting to compare the SCANDIA results for the oceanic part of the area in Figure 7.14 (lower panel) with simulated cloud amounts from the RCA model used by the SMHI Rossby center (Rummukainen et al., 2001 and Jones and Willén, 2001). The agreement is here surprisingly good, especially for the simulation of the cloudiness evolution in 1992.

8 THE IMPORTANCE OF INHERENT CALIBRATION ERRORS IN THE NOAA AVHRR DATASET

8.1 Background and status of the AVHRR calibration problem for visible channels

Essential for all climate and climate change studies is that when studying the evolution of one particular quantity measured by several instruments, one must take into account the possibility that detected trends and changes may be caused by defects of individual instruments and by differences between instruments. This problem is particularly important for measurements made from a space-based platform (as discussed by e.g. Cracknell, 2001) where methods for normalising the measurements must be found in order to produce reliable results. At the same time, this problem has been shown to be quite difficult to handle since a large number of influencing environmental factors may be at least partly unknown.

As concerns radiance measurements from operational meteorological satellite sensors, most problems are found for radiometers in the visible spectral region. Here, no on-board calibration is possible in contrast to measurements in the infrared region where internal blackbodies can serve to provide reference calibration targets. Instead, visible sensors are calibrated on ground prior to being launched in the final space orbit and it is assumed that this would provide a sufficiently firm estimation of instrument characteristics for the later use in space. However, the invalidity of this assumption has been known for more than 15 years now and several papers on this subject have been published (e.g. Che and Price, 1992, Rao and Chen, 1996 and Rao and Chen, 1999). Most of them are based on comparisons with various reference objects on ground (e.g., homogeneous desert areas).

The problem has two aspects where the first is manifested as an inter-satellite difference of calibrated visible radiances and the other concerns the temporal degradation of each individual sensor (i.e., reduction of instrument sensitivity). The temporal degradation problem is illustrated in Figure 8.1. An exact value of the sensor degradation rate is difficult to

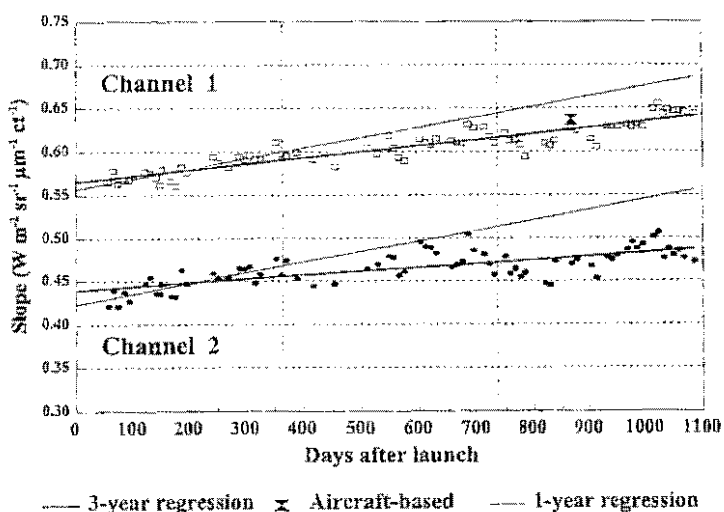


Figure 8.1 Evolution of the NOAA-14 AVHRR calibration slope values for the two visible channels as a function of time after satellite launch as determined from post-launch activities utilising desert reference targets and aircraft measurements. (from Rao and Chen, 1999)

estimate and it varies also between the instruments on different satellites. However, degradation rates exceeding 5 % per year appear to be quite common.

Various attempts to normalise visible radiance measurements have been made. The most ambitious and extensive effort is perhaps the methodology developed for the ISCCP project (Brest and Rossow, 1992 and Brest and Roiter, 1997). ISCCP utilises sensors from both polar orbiting and geostationary satellites and, in addition, data from the latter are provided by several space agencies. As concerns pure NOAA AVHRR data sets, a specific action has been taken by NOAA to serve the user community with updated calibration coefficients for the satellites with afternoon passages (i.e., for satellites with passage times close to noon with the optimal solar illumination). For the NOAA-14 satellite, monthly updated AVHRR calibration coefficients for the two visible channels are now available in delayed mode. The basic methodology for recalculation of the calibration coefficients was introduced in 1996 (see Rao and Chen, 1996) but a revision of the methodology was made in 1998 (see Rao and Chen, 1999).

8.2 Impact on the SCANDIA cloud climatology

Since the described SCANDIA cloud climatology in this report is based on cloud classification results produced in near real-time covering a period starting as early as in 1991, the previously described method for normalisation of AVHRR visible radiances has not been applicable. In addition, even if having used the updated calibration coefficients for the afternoon passages, the corresponding information for the morning passages would not be available which should have introduced additional inconsistencies in the compiled data set. However, despite this fact, the opportunity to make an update of the NOAA-14 calibration coefficients was nevertheless taken at SMHI in July 1998 based on the revised coefficients available for January 1998. The effect of this attempt to update the calibration information is discussed further below.

As a complete reprocessing of the cloud classification data set was not possible, the only way to take the calibration problems fully into account was to use the available validation data set and try to identify trends that could be correlated to what we know about the behaviour of degrading AVHRR sensors and the inter-satellite AVHRR instrument differences.

Results for the NOAA-11, NOAA-12 and NOAA-14 satellites have been separated and studied individually. Data from the two remaining satellites (NOAA-10 and NOAA-15) were excluded here since they were only available for quite short periods within the studied ten-year period. An overall summary of the validation results for all data from the three individual satellites is shown in Table 8.1. Corresponding time series of monthly results are given in Figures 8.2-8.4 illustrating also the respective time periods with data available for the different satellites.

The satellite with the longest time series here is NOAA-12 which has produced data during almost the entire ten year period (1992-2001). Knowing about the degradation problem from the AVHRR sensor on previous satellites, we should definitely see the largest impact on this very long time series as compared to results from the time series of the other two satellites. Since the sensitivity of the AVHRR sensor decreases for the visible channels, it should mean

Table 8.1 Overall summary of validation results for the three satellites NOAA-11, NOAA-12 and NOAA-14.

Quantity	NOAA-11	NOAA-12	NOAA-14
SATELLITE MEAN (%)	62.9	62.0	65.1
SYNOP MEAN (%)	63.2	64.6	64.5
MEAN DIFFERENCE (%)	-0.3	-2.6	1.4
RMS ERROR (%)	32.6	29.3	33.9
CORRELATION COEFFICIENT	0.69	0.78	0.62

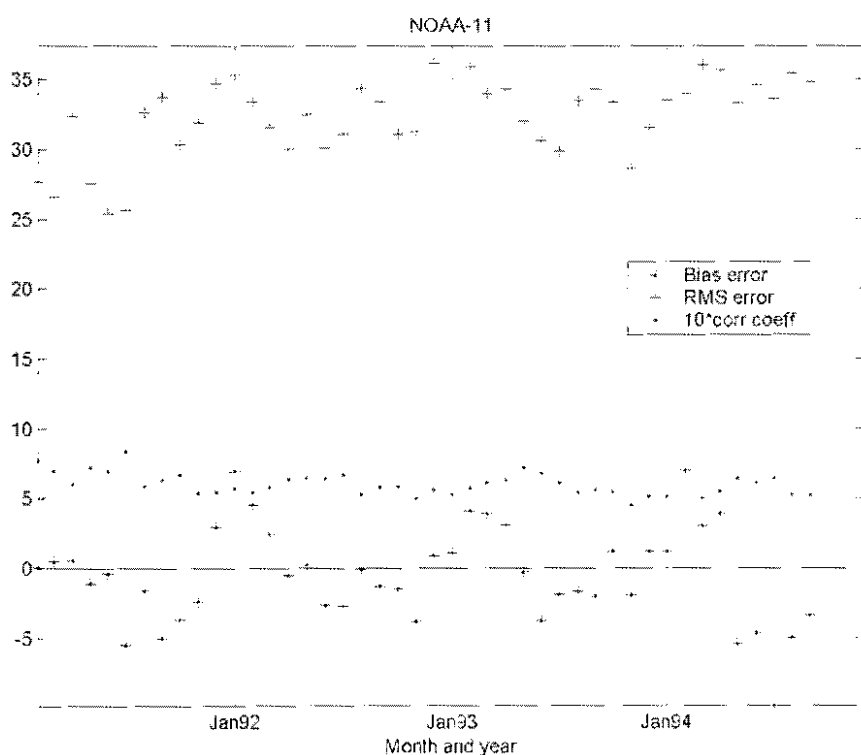


Figure 8.2 Monthly averages of RMS errors, bias error and correlation coefficient for the complete validation data set with NOAA-11 data.

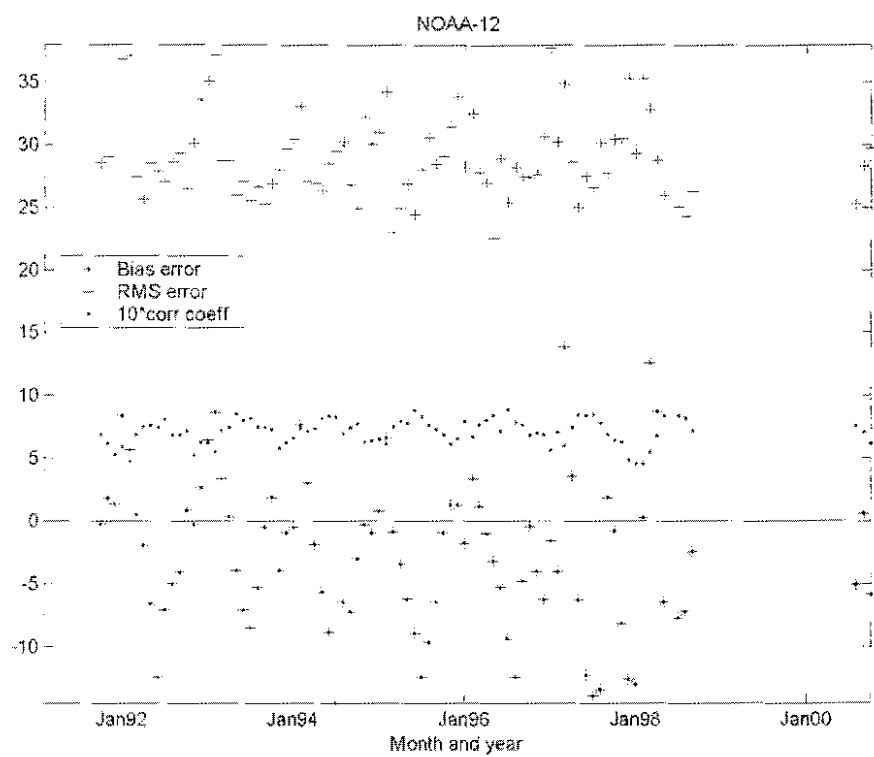


Figure 8.3 Monthly averages of RMS errors, bias error and correlation coefficient for the complete validation data set with NOAA-12 data.

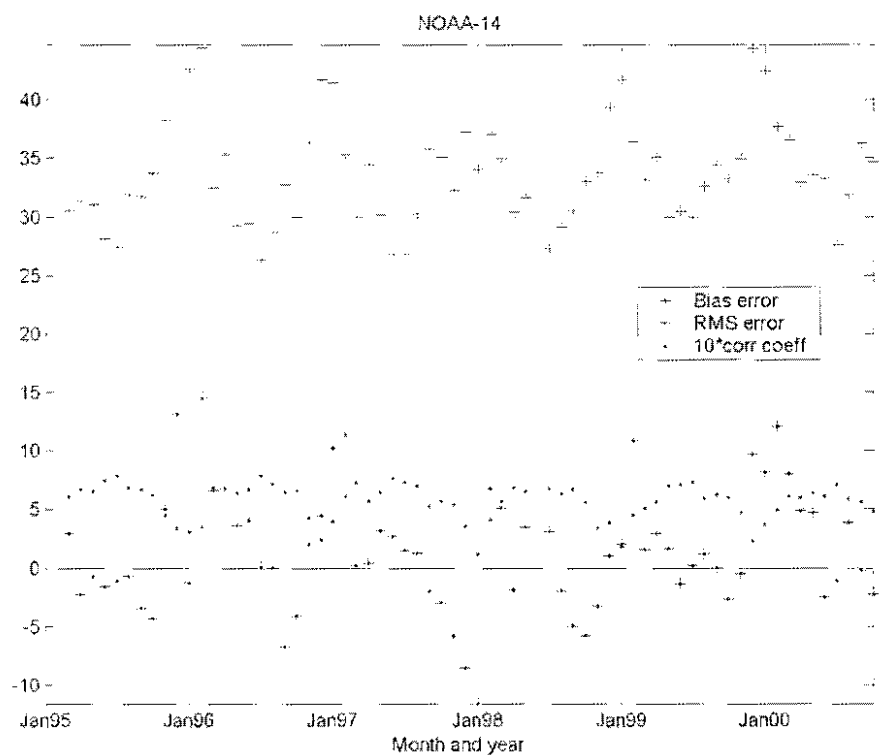


Figure 8.4 Monthly averages of RMS errors, bias error and correlation coefficient for the complete validation data set with NOAA-14 data.

that less and less clouds would be detected by the ageing sensor for a cloud classification scheme utilising static thresholds in the visible channels (like SCANDIA). This expectation is also verified in Figure 8.3 where the bias error tends to become dominantly negative the further we move away from the launch date. However, this tendency is to some extent obscured by an increased scatter in the results after 1996, probably due to the drastic reduction of available SYNOP observations in the validation data set. In the overall summary in Table 8.1 we can also see that there is a bias of -2.6% in cloudiness for the entire period with NOAA-12 data. Thus, we may conclude that the negative bias found between the years 1994 to 1998 in Figure 7.2 could at least partly be explained by the degradation of the visible AVHRR channels of NOAA-12.

For the other two satellites, no signs of a similar negative trend in the achieved cloud amounts could be noticed in Figures 8.2 and 8.4. For NOAA-14, the overall performance in Table 8.1 shows even a slight overestimation of cloud amounts. This may partly be explained by the occurrence of more difficult cloud analysis conditions during the winter seasons from 1996 and onwards resulting in an enhanced positive bias compared to the winters in the first half of the 1990s. It is also possible that the action to update the calibration coefficients almost in the middle of the period with NOAA-14 data (in summer 1998) helped to adjust values back to a reasonable level.

If mutually comparing results from the three satellites it is generally not possible to detect any remarkable differences. What could be noticed is that the correlation coefficient seems to be slightly lower for NOAA-14 at the same time as experiencing slightly higher RMS errors. This could be an effect of that SCANDIA was initially tuned and developed having access to data from NOAA-10 (with very similar passage times as NOAA-12) and NOAA-11. Consequently, the difference may be due to slightly differing passage times but it could also be a real calibration difference between the NOAA-14 AVHRR sensor and the AVHRR sensor on other used satellites.

9 DISCUSSION

9.1 Summary of achievements regarding SCANDIA cloud climatologies

This report has demonstrated the capability of the SCANDIA method, based on multi-spectral processing of radiance measurements from the AVHRR instrument as supplied by several NOAA satellites, for the compilation of cloud climatologies with a high horizontal resolution over the Scandinavian region. Results are made available as both individual monthly cloud climatologies and as period averages for individual months. A further time separation into four daily observations has also permitted a limited study of the diurnal variation of cloudiness over the area.

The annual average cloud amounts over the area were found to vary slowly in the range between 60-70 % throughout the period. Cloud amounts were at a minimum in the middle of the period while the highest mean cloud amounts occurred during the last three years.

Studies of the distribution of total cloud amounts in the region revealed remarkable differences between land and sea areas. The Baltic Sea was shown to suppress cloudiness in the summer half of the year and this generally affected neighbouring land areas, including the major parts of southern Scandinavia and the Baltic states. These differences were particularly obvious in the results from afternoon satellite passages. Interesting deviations from this pattern was seen in the Scandinavian mountain range and over the Norwegian Sea. The annual course of cloudiness appeared here to be inverted in comparison to the areas in or adjacent to the Baltic Sea. Highest cloud amounts were found in the summer season, although the amplitude of the annual cycle of cloud amounts was found to be considerably smaller than over the Baltic Sea. This summertime peak in cloudiness over the mountain range is suggested to be caused mainly by convective cloudiness forming at mountain peaks by slope-valley wind circulation systems (illustrated in Figure 9.1).

A particularly interesting feature was a secondary minimum in cloudiness appearing during spring and early summer close to the Norwegian coast over the Norwegian Sea. This minimum is believed to be caused by several coinciding and collaborating factors. The following factors are suggested (without giving priorities):

- the occurrence of a minimum in sea surface temperatures in spring (assumed to be caused by large contributions of cold fresh water from the melting snow in adjacent mountain areas)
- the ‘normal’ sea-breeze subsidence which is created along and outside the coast line
- the enhanced subsidence due to the formation of slope-valley wind circulation systems over the Scandinavian mountain range (partly also explaining the summertime cloud maximum over the mountains – see Figure 9.1)
- the contributions from lee subsidence during occasions with a cyclonic circulation pattern in southern Scandinavia yielding an easterly flow across the mountain range

A further separation of the cloud data set into the various contributions from different cloud types or cloud groups was also made. However, it was apparent that the quality of this separation was strongly reduced during the winter half of the year (discussed further in next

section) which means that firm conclusions on the mean cloud type distribution can only be made for the summer half of the year. Here, it was shown that the summertime maximum of cloud amounts over the Norwegian Sea consisted predominately of low-level water clouds (Cumulus, Stratocumulus and Stratus). Over land areas, high-level ice clouds tended to dominate except over the mountains where water clouds and ice clouds were almost equal in frequency. The high frequency of ice clouds over land areas in the region was interpreted as a relatively high occurrence of lee-wave Cirrus clouds eastward of the Scandinavian mountain range and a frequent occurrence of Cumulonimbus clouds (especially for afternoon passages). The high Cirrus cloud amounts may, however, be slightly overestimated due to spurious misclassification of small sub-pixel Cumulus cloud elements as very thin Cirrus clouds.

An attempt to also estimate the average precipitation climate in the area through the interpreted information on precipitating cloud types showed limited skill and did not match details in previously recorded and well-documented climatology patterns of precipitation over the area. However, some useful contribution to the knowledge of the climatic pattern of convective precipitation over the area is proposed. A climatology of the most reflecting and coldest clouds revealed interesting patterns showing a dependency on e.g. sea-breeze fronts and the general distribution of land and sea surfaces. The most striking feature here is naturally the very low frequency of these cloud groups over major parts of the Baltic Sea having frequencies less than a fifth of the corresponding frequencies over adjacent land areas. As a contrast, relatively high frequencies were found in January and February in the eastern part of the Baltic Proper, presumably caused by outbreaks of cold air in connection with a northerly wind flow over the Baltic Sea.

9.2 The quality of SCANDIA cloud climatologies

A comparison of the SCANDIA cloud climatologies with a similar data set based on SYNOP observations for the same period (however, here restricted to the parameter total cloud amount) revealed interesting seasonal patterns in the error structure. Cloud amounts were generally overestimated in winter with a bias error ranging from 5-10 % in the mean over all studied SYNOP stations. In contrast, an underestimation of the same order was noticed for the summer months. The wintertime problems were found to be trustworthy but the summertime deviations were believed to be artificially caused by problems for the surface observer to correctly estimate the cloud amounts in case of convective cloud cover. These clouds occur frequently during summer and their quite large vertical extension makes a correct cloud amount estimation difficult because of viewing perspective problems. Experience from the use of SCANDIA cloud classifications in operational forecasting applications supported this conclusion since cloud classifications were generally judged to have the highest quality in the summer season.

It was concluded that the error complexity is very large in the winter season and not easily corrected by single or isolated actions. Several problems related to the prevailing dark and occasionally cold conditions in the winter half of the year contribute to give a quite low skill, at least during periods. It seems also likely that a true non-separability of clouds and cloud-free surfaces do exist in some winter situations. Future activities will show if the access to additional spectral bands on new or modified sensors and an improved use of ancillary information may be able to solve or at least reduce these quite serious cloud analysis problems.

The separation of cloudy pixels into different cloud types during winter conditions appeared especially problematic. A remarkable and artificial positive bias in the interpreted distribution of ice and water clouds (ice clouds overestimated) is suspected in the data set. Especially over ocean surfaces, unrealistically large ice cloud frequencies (in some cases exceeding 70 %) were found. Corresponding high ice cloud frequencies over adjacent land areas could not be seen. This illustrates very clearly the defects of cloud classification schemes using static thresholds in the split-window channel difference formed by brightness temperature differences between AVHRR channels 4 and 5. For an efficient use of this feature in cloud detection during dark conditions and especially for the separation of water and ice clouds, it appears to be essential to have not only a temperature difference between the surface and the cloud itself but also a typical water or ice cloud signature in AVHRR channel 3 (i.e., a brightness temperature difference between AVHRR channels 3 and 4). Over ocean areas this latter signature appears often to be lacking, probably caused by previously observed typical cloud microphysical features (i.e., large droplets at cloud top level). In addition, sub-pixel water cloud elements over oceans are also often mis-interpreted by SCANDIA as thin Cirrus clouds in winter (similar to the situation over land areas in summer).

Over land areas, the largest problems in winter were the following:

- Overestimation of cloud amounts due to anisotropically enhanced reflection of cloud-free land surfaces when the sun is very close to the horizon
- Mis-interpretation of very cold and cloud free ground surfaces as mid- and high-level ice clouds
- Underestimation of low-level water cloud amounts at night and in twilight due to the loss of a typical water cloud signature in AVHRR channel 3.

Any cloud detection method is assumed to face the most serious conditions just after sunrise when ground temperatures are at a minimum and when there is no typical cloud signature (i.e., different from the cloud-free signature) in the AVHRR brightness temperature difference between channels 3 and 4. During these conditions, serious underestimation as well as serious overestimation of cloudiness may occur which gives rise to remarkably high RMS errors and low correlation coefficients when compared with surface observations.

A separate comparison of SCANDIA results with measurements from the Swedish network of solar radiation stations showed very promising results. During summertime conditions, the existence of an almost perfect inversely proportional relation between SCANDIA cloud amount and recorded relative sunshine duration was found. Wintertime results were degraded but this was most probably caused by an inappropriate comparison during this time of year (i.e., sunshine duration is not correlated well with the daily mean of cloudiness in winter).

The SCANDIA climatologies were also compared to results from the most up to date version of the ISCCP cloud datasets (the ISCCP D2 series) for the first three years of the studied period. SCANDIA was shown to give a significantly larger seasonal variability of cloudiness than ISCCP during this period. Even if it is true that the latter data set admittedly could be affected by factors related to a used coarse resolution, the SCANDIA results were also supported by corresponding SYNOP-based data sets. Also preliminary comparisons with modelled cloud amounts from climate simulation models favoured strongly the SCANDIA results.

A special study focusing on the possible influences on the results from degrading sensitivities of the visible channels of the AVHRR instruments and on inter-satellite calibration differences showed a significant impact on results based on data from the NOAA-12 satellite. This satellite was used during almost the entire ten-year period. Here, it was found from comparisons with SYNOP information that cloud amounts were on the average slightly underestimated in contrast to the results from other satellites. A temporal trend with increasing negative bias errors could also be seen for this satellite in accordance with the expected degraded sensitivity of the AVHRR visible channels. However, since SCANDIA is a supervised classification scheme developed using a training data set including information from both old and new AVHRR sensors from three NOAA-satellites in the period 1986-1990, the overall impact of these problems on the results are considered to be quite small except for the NOAA-12 satellite. The monitored very large variability of cloudiness over the studied area by SCANDIA is believed to be rather well captured and only marginally affected by sensor drift and inter-satellite calibration problems. However, for real long term monitoring of the cloud climate these problems must, of course, be carefully taken into account and compensated for.

Finally, it is worth mentioning that the work with compilation of the cloud climatology in itself revealed features that were not easily deduced from the above mentioned validation data sets. For example, the observed imbalance between ice cloud occurrence over land and sea surfaces in winter would probably not have been discovered through ‘normal’ validation activities. Consequently, the actual compilation of climatologies of various satellite-derived parameters is therefore proposed as one additional and important component of validation activities in the evaluation of satellite-based algorithms.

9.3 Future plans: The successor to SCANDIA and engagements in international climate monitoring programmes

9.3.1 Future use of SCANDIA cloud climatologies

As mentioned in the previous section, the SCANDIA results have previously been used for validation of forecasted cloud amounts from NWP models (Karlsson, 1996b) or modelled cloudiness from climate simulation models (Jones and Willén, 2001). This work will continue and it is also intensified in the near future. A co-operation with scientists at the SMHI Rossby centre for regional climate studies (an essential part of SWECLIM – the Swedish Regional Climate Modelling programme) has been initiated. Specifically, the SCANDIA results in the summer half of the year regarding the diurnal cycle of cloudiness and the distribution of water and ice clouds will be utilised for more detailed cloud parameterisation studies (some of them outlined by Jones and Willén, 2001).

The entire or selected parts of the SCANDIA cloud climate data set could be made available to external users on demand. An interface to the data set based on the hierarchical data file format (HDF5) has been developed. Studies related to surveys of solar energy conditions, environmental issues (e.g., the importance of accumulated solar energy input to ocean waters in connection to algal bloom events) and tourism activities (sun duration statistics) could potentially benefit from the results of the SCANDIA cloud climatologies.

It is uncertain if the SCANDIA ten-year series of data will be extended much further into the future. The reason is the appearance of the new 1.6 micron channel on the NOAA-16 satellite and its successors. No upgrading of the SCANDIA schemes to include data from this new

spectral band has yet been made and it is likely that a more dramatic change of the used cloud schemes at SMHI will occur before an upgrading of SCANDIA can take place (see next section).

9.3.2 *The successor to SCANDIA*

A first step towards the implementation of a drastically restructured and improved SCANDIA cloud classification algorithm was taken during the ten-year period in connection with the introduction of the previously described SCANDIA version 2 model. Results here showed that the problem with the handling of very cold winter situations was significantly reduced, yielding almost a removal of the previous positive bias error for SCANDIA version 1 during winter conditions. However, RMS errors were still high and, furthermore, correlation coefficients were not drastically improving which called for more fundamental improvements of the scheme.

In 1997, SMHI became engaged in the EUMETSAT SAFNWC (Satellite Application Facility on support to Nowcasting and Very-short range forecasting) project. Here, the main task of SMHI is to develop algorithms and software to extract four cloud and precipitation parameter products based on polar orbiting satellite data aimed for use in Nowcasting and Very-short Range Forecasting applications. A detailed design work has been completed involving a major development effort during five years (1997-2002). The most fundamental change here compared to the SCANDIA model is the systematic use of RTM models to simulate in advance of satellite passages the anticipated cloud-free radiances for the definition of dynamic thresholds. Prototypes for the four cloud products were ready in the year 2000 (see Dybbroe et al., 1998, Dybbroe et al., 2000 and Dybbroe, 2001) and after that implementation activities remain for the last two years in the project (2001-2002). The software for generation of these cloud products is planned for release for use by NMS's of the EUMETSAT member states in 2003. A future report in this report series will give a detailed description of the four involved products developed by SMHI. However, operational introduction of the new cloud schemes at SMHI is foreseen before 2003 and this also means that the production of SCANDIA cloud climatologies will most probably be replaced at the same time.

An example of a compiled cloud climatology based on the new SAFNWC cloud mask method is given below in Figure 9.2 showing the mean cloud conditions for the afternoon passages in September 2000. This data set was compiled for use in the EU Framework 5 research project CLIWANET (Cloud Liquid Water Network) and it is described by Dybbroe et al. (2001). CLIWANET is a contribution to the BALTEX project (see Karlsson, 2000 and related papers in the same journal), one of the sub-studies in the GEWEX programme. The results here can be compared to corresponding SCANDIA results in Appendix 2. However, it has to be remembered here that the latter is based on four observations per day.

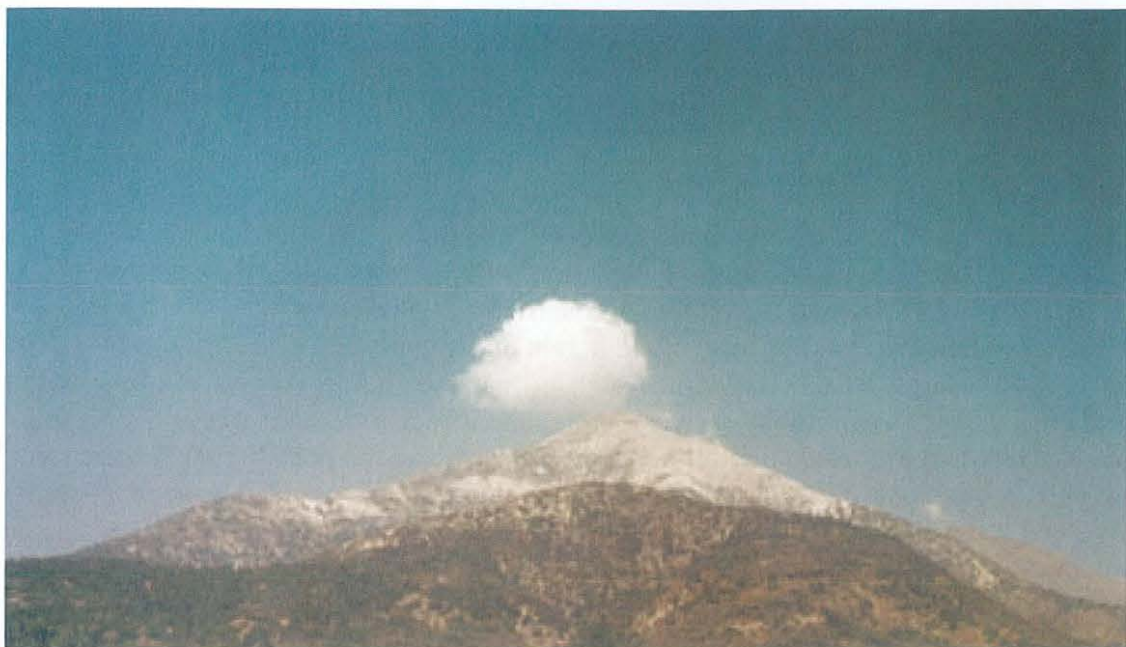


Figure 9.1 Illustration of how a convective cloud element forms over a mountain peak by slope-valley wind circulation systems. (courtesy of Bertil Lindén)

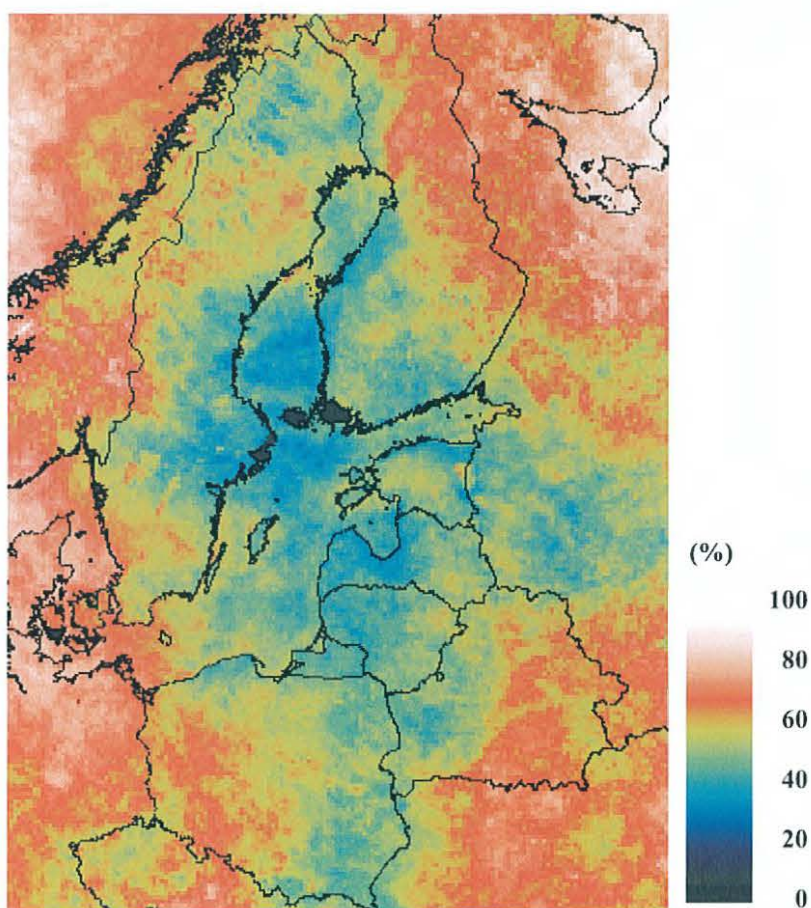


Figure 9.2 Mean cloud frequencies in 10 km resolution over the Baltic Sea drainage basin derived from the SAFNWC cloud mask scheme and applied on afternoon passages in September 2000. The data was prepared for the first intensive CLIWANET campaign, CNN1.

9.3.3 SMHI engagements in future international cloud climate monitoring activities

Since 1998, SMHI is engaged in yet another EUMETSAT SAF, namely the SAF on Climate Monitoring (CM-SAF, described by Woick et al., 2000). Here, the SMHI task is to contribute to the development of methods for operational monitoring of cloud climate parameters, especially concerning the utilisation of data from the future polar orbiting NOAA and EPS (EUMETSAT Polar Satellites) satellites. A consistent set of cloud parameters (including also detailed information on cloud phase, cloud height and cloud water content) will be produced together with a large set of other climate-related parameters (see Woick et al., 2000). The primary analysis area will initially cover Europe and adjacent oceanic areas but an extension of the analysis area to include the full METEOSAT disk and the polar area is foreseen to take place later. Operational production of climate parameters is foreseen to start in 2004 at the earliest and it is also planned to have a capacity for repeated reprocessing activities. The latter component has been shown to be an essential part of any climate monitoring activity (as deduced from e.g., the ISCCP experience).

10 ACKNOWLEDGEMENTS

This work has been sponsored by the Swedish National Space Board under contracts Dnr 59/95, Dnr 113/96 and Dnr 152/98.

The author wants to thank many colleagues at SMHI for their most valuable contributions to this work. First of all, Camilla Andersson must be acknowledged for her thorough and careful assistance with the work of performing the SYNOP validation of satellite-derived results. Camilla has also produced many of the MATLAB figures comparing results from SYNOP and satellite data in this report. In the same context, the author wants to thank Mikael Gollvik for his assistance in checking out the technical quality of the archived cloud classifications and Karl-Ivar Ivarsson and Nils-Åke Andersson for preparing the SYNOP observation database. Furthermore, Sten Orrhagen, Gunnar Pettersson and Christina Sverker is credited for their assistance in accessing and retrieving information from the SMHI tape archive.

The author is also very grateful to Colin Jones for preparing the CRU and ISCCP datasets and to Thomas Persson for assisting with solar radiation measurements. Finally, many thanks is given to Adam Dybbroe, Daniel Michelson, Tomas Landelius and Johan Jansson for all the Python and MATLAB programming support and to Erik Liljas, Hans Alexandersson, Halldo Vedin, Michael Heen, Sten Bergström and Weine Josefsson for their valuable comments and remarks on the manuscript.

11 REFERENCES

- Allam, R.J., Holpin, G., Jacksson, P. and Liberti, G.-L., 1993: GPCP AIP-2 Workshop Report, 23-26 August 1993, Shinfield Park, Reading, UK, Available from UK Meteorological Office.
- Arking, A., 1991: The radiative effects of clouds and their impact on climate, *Bull. Amer. Meteorol. Soc.*, **71**, 795-813.
- Atkinson, B.W., 1981: Meso-scale atmospheric circulations: Slope and Valley Wind Circulation (Chapter 6), Academic Press Inc., London, 495 pp.
- Bordes, P., Brunel, P. and Marsouin, A., 1992: Automatic adjustment of AVHRR navigation, *J. Atmosph. Ocean. Technol.*, **9**, 15-27.
- Brest, C.L. and Roiter, M.D., 1997: Update of radiance calibrations for ISCCP, *J. Atmos. Oceanic Technol.*, **14**, 1091-1109.
- Brest, C.L. and Rossow, W.B., 1992: Radiometric calibration and monitoring of NOAA AVHRR data for ISCCP, *Int. J. Remote Sens.*, **13**, 235-273.
- Brunel, P. and Marsouin, A., 2000: Operational AVHRR navigation results, *Int. J. Remote Sensing*, **21**, 951-972.
- Che, N. and Price, J.C., 1992: Survey of radiometric calibration results and methods for visible and near infrared channels of NOAA-7, -9, and -11 AVHRRs, *Remote Sens. Environ.*, **41**, 19-27.
- Coakley, J.A. and Brethertone, 1982: Cloud cover from high-resolution scanner data: Detecting and allowing for partially filled fields of view, *J. Geoph. Res.*, **87**, 4917-4932.
- Cracknell, A.P., 2001: Remote sensing and climate change – the role of earth observation, Springer Praxis Books, 400 pp, ISBN 1-85233-321-9
- Derrien, M., Farki, B., Harang, L., LeGléau, H., Noyalet, A., Pochic, D. and Sairouni, A., 1993: Automatic cloud detection applied to NOAA-11/AVHRR imagery, *Rem. Sens. of Env.*, **46**, 246-267.
- Dybbroe, A., Karlsson, K.-G., Moberg, M. and Thoss, A., 2000: Scientific Report for the SAFNWC Mid Term Review, SMHI, 166 pp.
- Dybbroe A., Thoss, A. and Karlsson, K.-G., 1998: The AVHRR & AMSU products of the Nowcasting SAF, *Proc.2000 EUMETSAT Meteorological Satellite Data Users' conference, Bologna, Italy, 29 May-2 June 2000*, EUMETSAT, EUM P 29, 729-736. See also <http://www.smhi.se/saf>.
- Dybbroe, A., Thoss, A. and Karlsson, K.-G., 2001: Mean cloudiness derived from satellite data over the Baltic Sea drainage basin during CLIWA-NET campaigns, To appear in *Proc of 3rd Study Conference on BALTEX, Mariehamn, Finland, 2-4 July, 2001*.
- EUMETSAT, 1998: Format Guide No 4; Climate Data Set (CDS), open MTP format, January 1998,
<http://www.eumetsat.de/en/area3/marf/marfonline/htdocs/documentation/cdsopenmtp.htm>
- Eyre, J.R., Brownscombe, J.L. and Allam, R.J., 1984: Detection of fog at night using Advanced Very High Resolution Radiometer (AVHRR) imagery, *Meteor. Mag.*, **113**, 266-271.
- Feijt, A. and de Valk, P., 1998: Quantifying the difference between NWP surface temperatures and cloud free satellite apparent brightness temperatures, *Contr. Atm. Phys.*, **71**, 455-460.
- Glasser, M.E. and Lulla, K.P., 2000: An evaluation of the global 1-km AVHRR land dataset, *Int. J. Remote Sens.*, **21**, 1987-2022.

- Godøy, Ø., 1998: Cloud classifications in cold winter situations in northern Europe, *SMHI Reports Meteorology*, No 94.
- Gutman, .G.G., 1989: On the relationship between monthly and mean maximum-value composite vegetation indices', *Int. J. Remote Sens.*, **10**, 1317-1325.
- Hultgren P., Dybbroe, A. and Karlsson, K.-G., 1999: SCANDIA – its accuracy in classifying low clouds, *SMHI Reports Meteorology*, No 91.
- Hunt, G. E., 1973: Radiative properties of terrestrial clouds at visible and infrared thermal window wavelengths, *Quart. J. R. Met. Soc.*, **99**, 346-369.
- Häggmark, L., Ivarsson, K.-I. and Olofsson, P.-O., 1997: MESAN – mesoscale analysis (in Swedish), *SMHI Reports Meteorology and Climatology*, No. 75, 77 pp.
- Häggmark, L., Ivarsson, K.-I., Gollvik, S. and Olofsson, P.-O., 1997: MESAN, an operational mesoscale analysis system, *Tellus*, **52A**, 2-20.
- Inoue, T., 1987: Cloud type classification with NOAA-7 split window measurements, *J. Geophys. Res.*, **92**, 3991-4000.
- Jones, P.D., Jónsson, T. and Wheeler, D., 1997: Extension to the North Atlantic Oscillation using early instrumental pressure observations from Gibraltar and South-West Iceland. *Int. J. Climatol.* **17**, 1433-1450.
- Jones, C. and Willén, U., 2001: The diurnal cycle of clouds and precipitation, To appear in *Proc of 3rd Study Conference on BALTEX, Mariehamn, Finland, 2-4 July, 2001*.
- Kästner, M. and Kriebel, K.T., 2001: Alpine cloud climatology using long-term NOAA-AVHRR satellite data, *Theor. Appl. Climatology*, **68**, 175-195.
- Karlsson, K.-G., 1993: Comparison of operational AVHRR-based cloud analyses with surface observations, *Proc. 6th European AVHRR Data Users' Meeting, Belgirate, Italy, 28 June – 3 July, 1993*, EUMETSAT, 223-230.
- Karlsson, K.-G., 1994: Satellite-estimated cloudiness from NOAA AVHRR data in the Nordic area during 1993, *SMHI Reports Meteorology and Climatology*, No. 66, 51 pp.
- Karlsson, K.-G., 1995: Estimation of cloudiness at high latitudes from multispectral satellite measurements, *Ambio*, **24**, 33-40.
- Karlsson, K.-G., 1996a: Cloud classifications with the SCANDIA model, *SMHI Reports Meteorology and Climatology*, No. 67, 36 pp.
- Karlsson, K.-G., 1996b: Validation of modelled cloudiness using satellite-estimated cloud climatologies, *Tellus*, **48A**, 767-785.
- Karlsson, K.-G., 1997: Cloud climate investigations in the Nordic region using NOAA AVHRR data, *Theor. Appl. Climatol.*, **57**, 181-195.
- Karlsson, K.-G., 2000: Satellite sensing techniques and applications for the purposes of BALTEX, *Meteorologische Zeitschrift*, **9**, 109-115.
- Karlsson, K.-G. and Liljas, E., 1990: The SMHI model for cloud and precipitation analysis from multispectral AVHRR data. *SMHI PROMIS Reports*, No. 10, 74 pp.
- Kidder, S.Q. and Vonder Haar, T.H., 1995: Satellite Meteorology - An introduction, Academic Press, page 270, Figure 8.3, ISBN-0-12-406430-2, in total 466 pp.
- Källén, E. (Editor), 1996: HIRLAM documentation manual, system 2.5.
- Lauritson, L., Nelson, G.J. and Porto, F.W., 1979: Data extraction and calibration of Tiros-N/NOAA radiometers, NOAA Technical Memorandum NESS 107.
- Matson, M., Stephens, G. and Robinson, J., 1987: Fire detection using data from the NOAA-N satellites, *Int.J. Rem. Sens.*, **8**, 961-970.
- Michelson, D.B., V.L. Foltescu, L. Häggmark, B. Lindgren, 2000: MESAN – Mesoscale analysis of precipitation. *Meteorf. Z.*, **9**, 85-96.
- Morel, C. and Sénési; S., 1998: A fully automated detection and tracking of Mesoscale Convective Systems based on the Meteosat infrared channel, *Proc. 9th Conference on*

- Satellite Meteorology and Oceanography, Paris, France, 25-29 May 1998*, AMS, EUMETSAT and Société Météorologique de France, 377-380.
- Morel, C., Sénési, S. and Orain, F., 1997: Automated detection and characterization of MCS using the Meteosat infrared channel, *Proc. 1997 Meteorological Satellite Data Users' Conf., Brussels, Belgium*, 213-220.
- New, M., Hulme, M. and Jones, P., 2000: Representing twentieth-century space-time climate variability. Part II: Development of 1901-96 monthly grids of terrestrial surface climate, *J. Climate*, **13**, 2217-2238.
- NOAA/NESDIS and CIRA: GOES 3.9 μm Channel Tutorial, NOAA/NESDIS, Cooperative Institute for Research in the Atmosphere (CIRA), Colorado State University, USA, <http://www.cira.colostate.edu/rainm/goes39/>
- Persson, T., 2000: Measurements of solar radiation in Sweden 1983-1998, *SMHI Reports Meteorology and Climatology*, No. 89, 74 pp.
- Pinker, R.T. and Laszlo, I., 1992: Modelling surface solar irradiance for satellite applications on a global scale, *J. Appl. Meteor.*, **31**, 194-211.
- Rao, C.R.N. and Chen, J., 1996: Post-launch calibration of the visible and near-infrared channels of the Advanced Very High Resolution Radiometer of the NOAA-14 spacecraft, *Int. J. Remote Sens.*, **17**, 2743-2747.
- Rao, C.R.N. and Chen, J., 1999: Revised post-launch calibration of the visible and near-infrared channels of the Advanced Very High Resolution Radiometer of the NOAA-14 spacecraft, *Int. J. Remote Sens.*, **20**, 3485-3492.
- Rosborough, G.W., Baldwin, D.G. and Emery, W.J., 1994: Precise AVHRR image navigation, *IEEE Transactions on Geoscience and Remote Sensing*, **32**, 644-657.
- Rossow, W. B. and Garder, L. C., 1993a: Cloud detection using satellite measurements of infrared and visible radiances for ISCCP. *J. Climate*, **6**, 2341-2369.
- Rossow, W.B. and Garder, L.C., 1993b: Validation of ISCCP cloud detections, *J. Climate*, **6**, 2370-2393.
- Rossow, W. B. and Schiffer, R. A., 1999: Advances in understanding clouds from ISCCP, *Bull. Amer. Meteor. Soc.*, **80**, 2261-2287.
- Rummukainen, M., Bergström, S., Källén, E., Moen, L., Rodhe, J. and Tjernström, M., 2000: SWECLIM – The first three years
- Rummukainen, M., Räisänen, J., Bringfelt, B., Ullerstig, A., Omstedt, H., Willén, U., Hansson, U. and Jones, C., 2001: A regional climate model for northern Europe: model description and results from the downscaling of two GCM control simulations. *Climate Dynamics*, **17**, 339-359.
- Saunders, R.W. and Kriebel, K.T., 1988: An improved method for detecting clear sky and cloudy radiances from AVHRR data, *Int. J. Rem. Sens.*, **9**, 123-150.
- Woick, H., Wollenweber, G., Karlsson, K.-G., Feijt, A., Gratzki, A., Hollman, R., Laine, V., Dewitte, S., Löwe, P. and Nitsche, H., 2000: The SAF on Climate Monitoring: Objectives and concept, *Proc. of 2000 EUMETSAT Meteorological Satellite Data Users' Conference, Bologna, Italy, 29 May–2 June 2000*, EUMETSAT, EUM P 29, 609-612.
- Wollenweber, G., Bissolli, P. and König, M., 2000: Comparative climate monitoring of METEOSAT-derived cloud cover and corresponding surface observations over Germany, *Proc. of 2000 EUMETSAT Meteorological Satellite Data Users' Conference, Bologna, Italy, 29 May–2 June 2000*, EUMETSAT, EUM P 29, 586-593.

APPENDIX 1. ACRONYM LIST

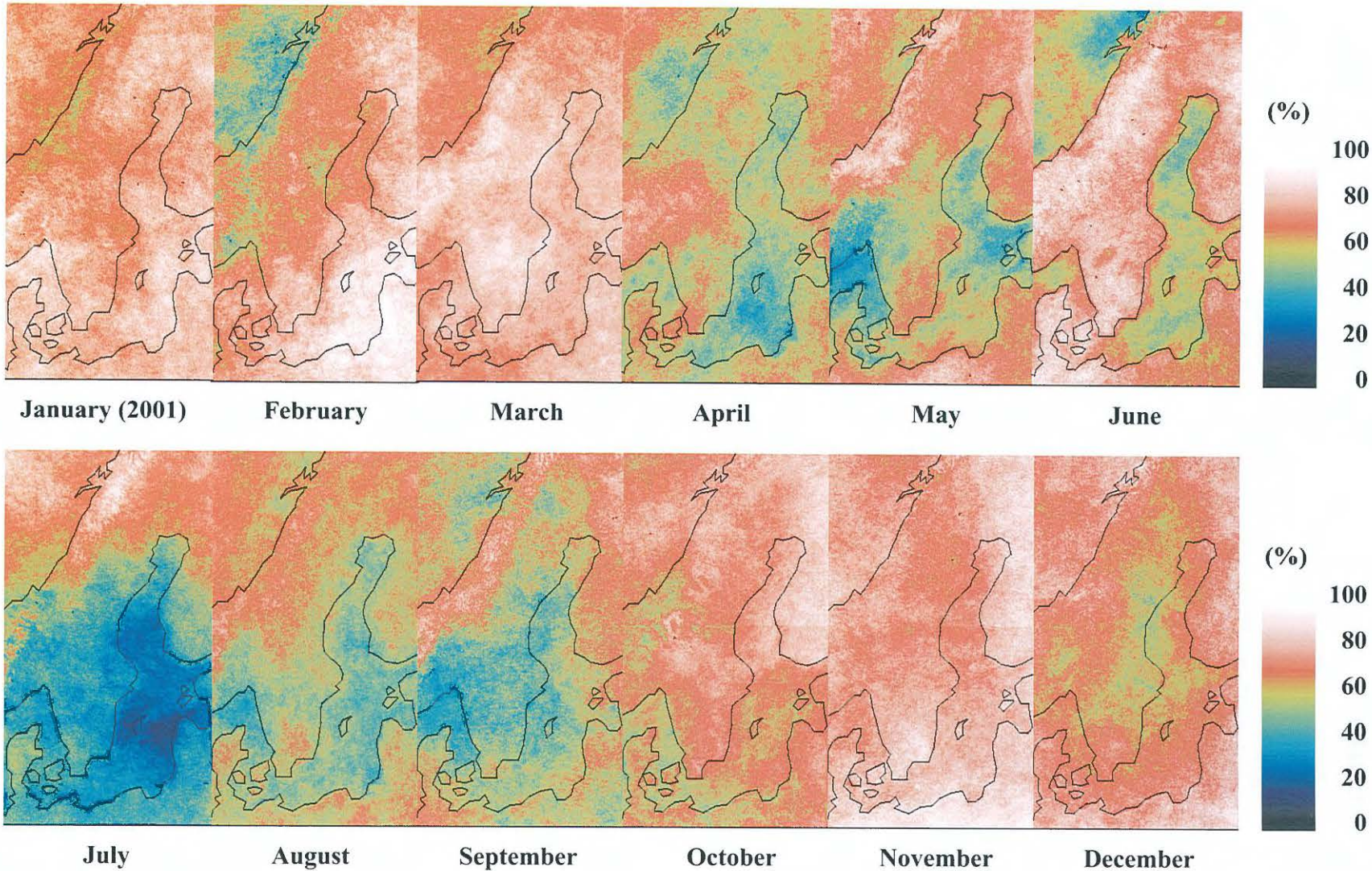
AVHRR	Advanced Very High Resolution Radiometer (NOAA satellite)
BALTEX	The BALTic sea Experiment (part of GEWEX)
CDS	EUMETSAT METEOSAT Cloud Climate Dataset
CET	Central European Time (UTC/GMT+1)
CIMO	Commission for Instruments and Methods of Observations
CM-SAF	EUMETSAT SAF on Climate Monitoring
CRU	Climate Research Unit (University of East Anglia)
EPS	EUMETSAT Polar System (METOP satellites)
EUMETSAT	EUropean organisation for the exploitation of METeorological SATellites
GEWEX	Global Energy and Water Cycle Experiment (part of WCRP)
HDF	Hierarchical Data Format
HIRLAM	High Resolution Limited Area Model – NWP model developed by the meteorological institutes in the Nordic countries plus Ireland, the Netherlands and Spain.
HRPT	High Resolution Picture Transmission (NOAA satellites)
IR	Infrared
ISCCP	International Satellite Cloud Climatology Project
LUX	Luminance Utilisee en eXploitation (CMS/Lannion cloud classification scheme)
METEOSAT	Geostationary METEOrological SATellite (EUMETSAT)
METOP	METeorological Operational polar orbiting satellite (EUMETSAT)
MSG	METEOSAT Second Generation
NAO	North Atlantic Oscillation
NDVI	Normalised Difference Vegetation Index
NMS	National Meteorological Service
NOAA	National Oceanographic and Atmospheric Administration (USA)
NWP	Numerical Weather Prediction
RTM	Radiative Transfer Model
SAFNWC	EUMETSAT SAF on support to Nowcasting and Very short-range forecasting
SCANDIA	SMHI Cloud Analysis model using Digital AVHRR data
SMHI	Swedish Meteorological and Hydrological Institute
SST	Sea Surface Temperatures
SWECLIM	Swedish Regional Climate Modelling Programme
SYNOP	SYNOptical weather observations at surface stations
UTC	Universal Time Coordinated (same as Greenwich Mean Time)
VIS	Visible
WCRP	World Climate Research Programme (WMO)
WMO	World Meteorological Organisation (United Nations)

APPENDIX 2. MONTHLY CLOUD CLIMATOLOGIES 1991-2001

In the following pages, a display of monthly cloud frequencies for each individual month in the period February 1991 to January 2001 is presented. Please notice that for practical reasons results for January 2001 is displayed together with results for February-December 1991.

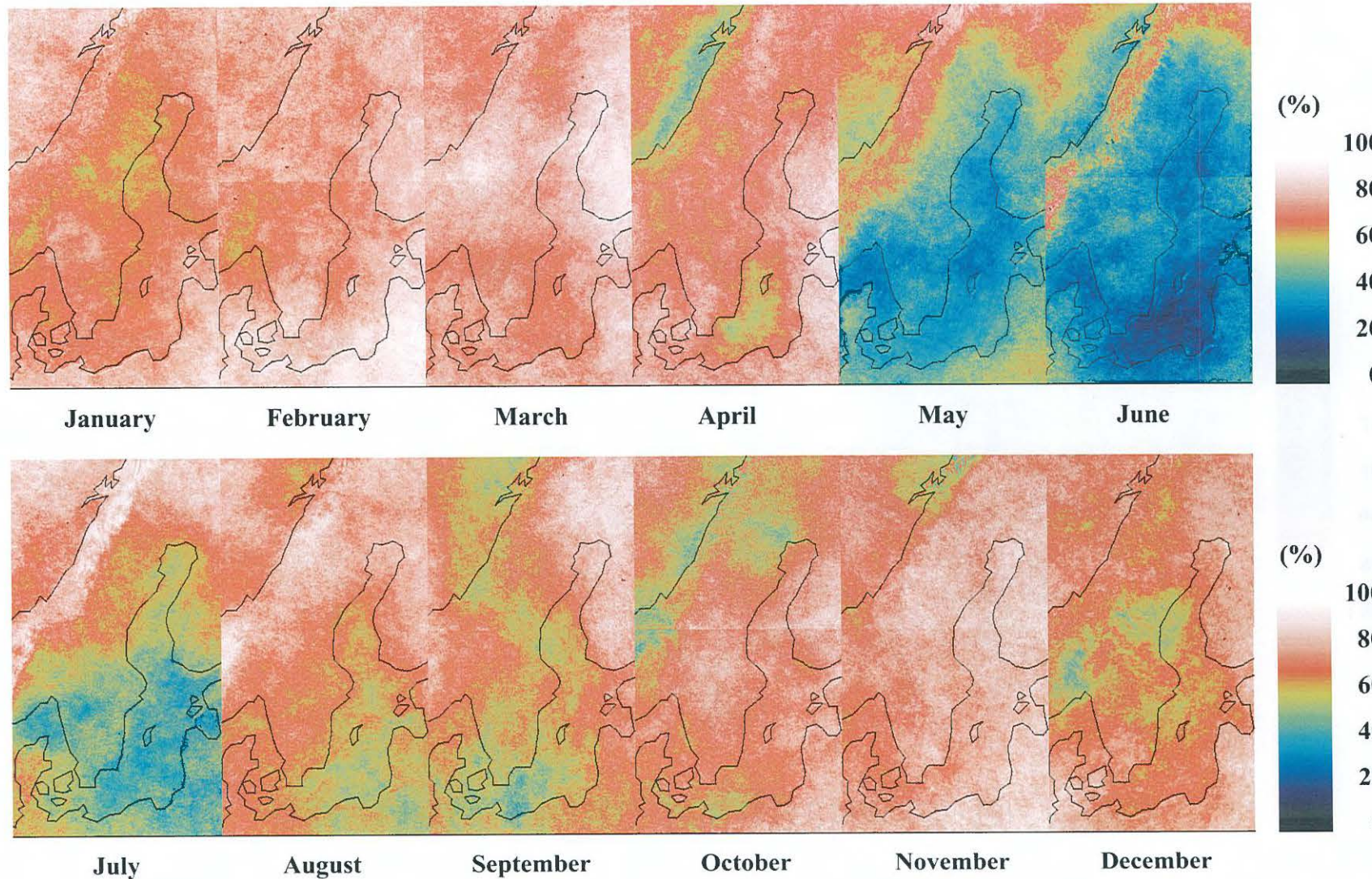
Monthly cloud frequencies in 1991

98



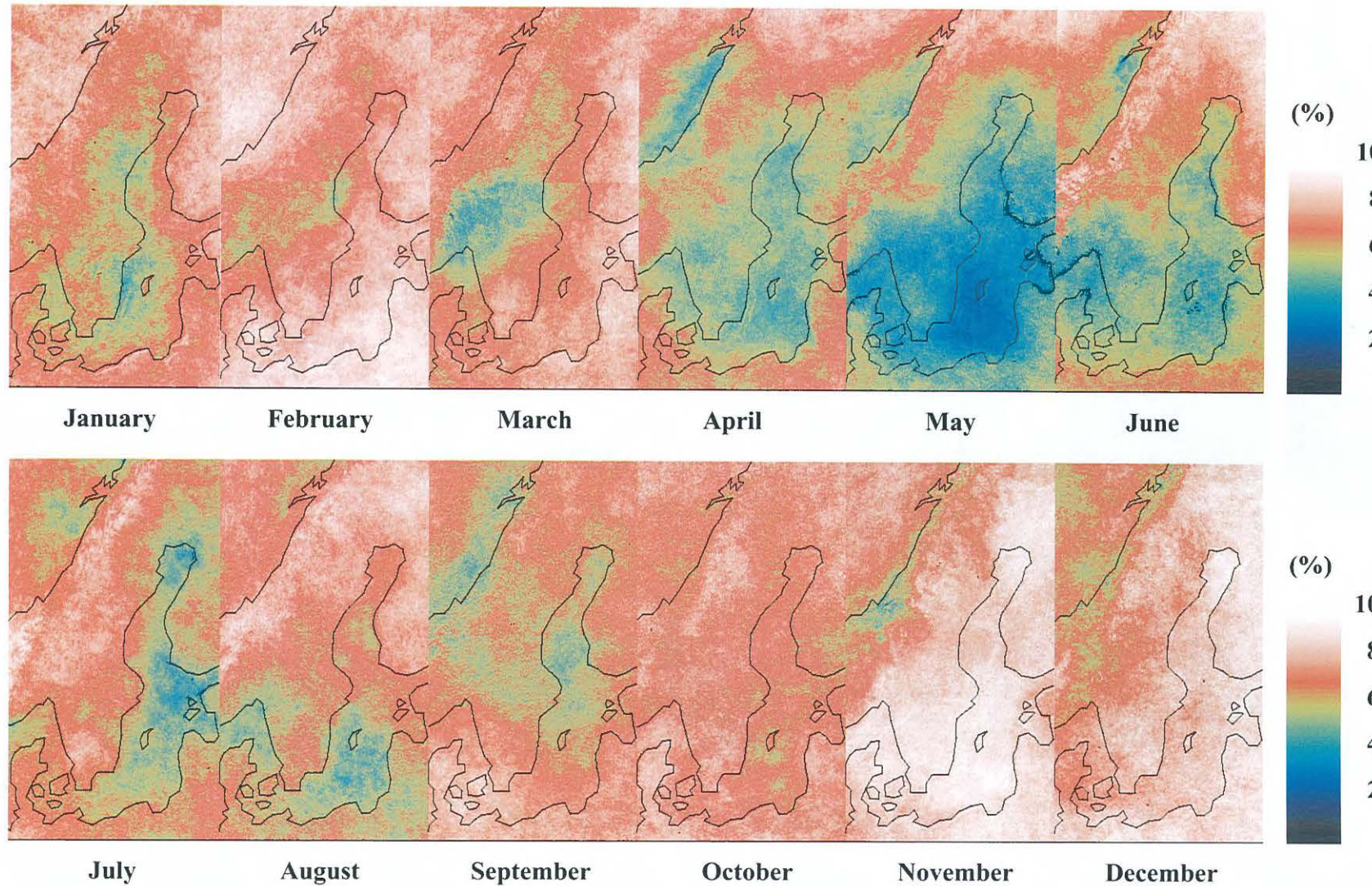
Monthly cloud frequencies in 1992

87



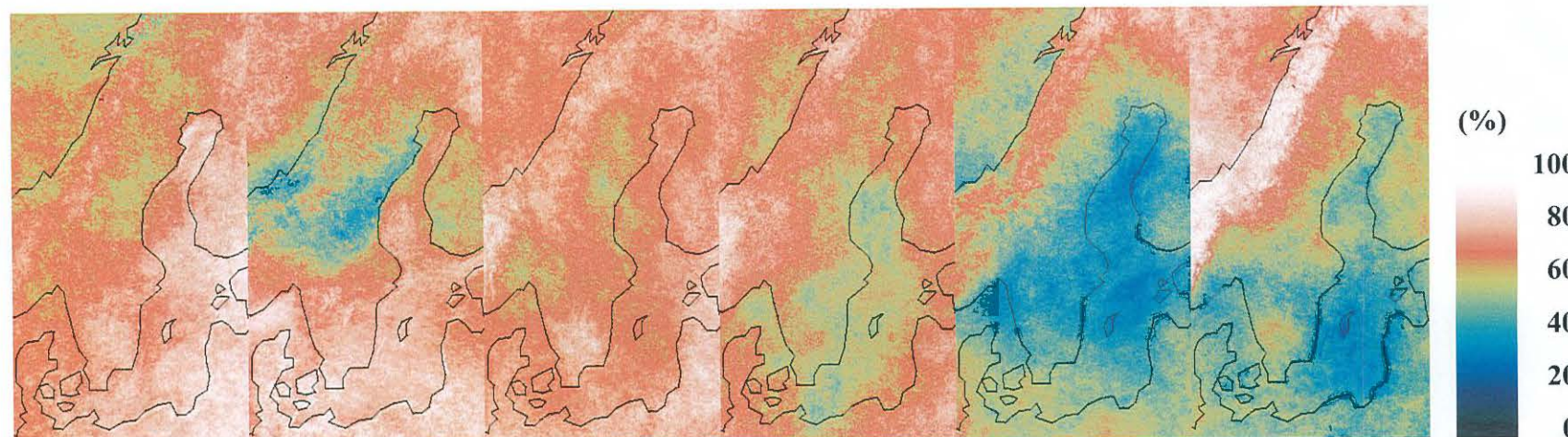
Monthly cloud frequencies in 1993

88



Monthly cloud frequencies in 1994

68



January

February

March

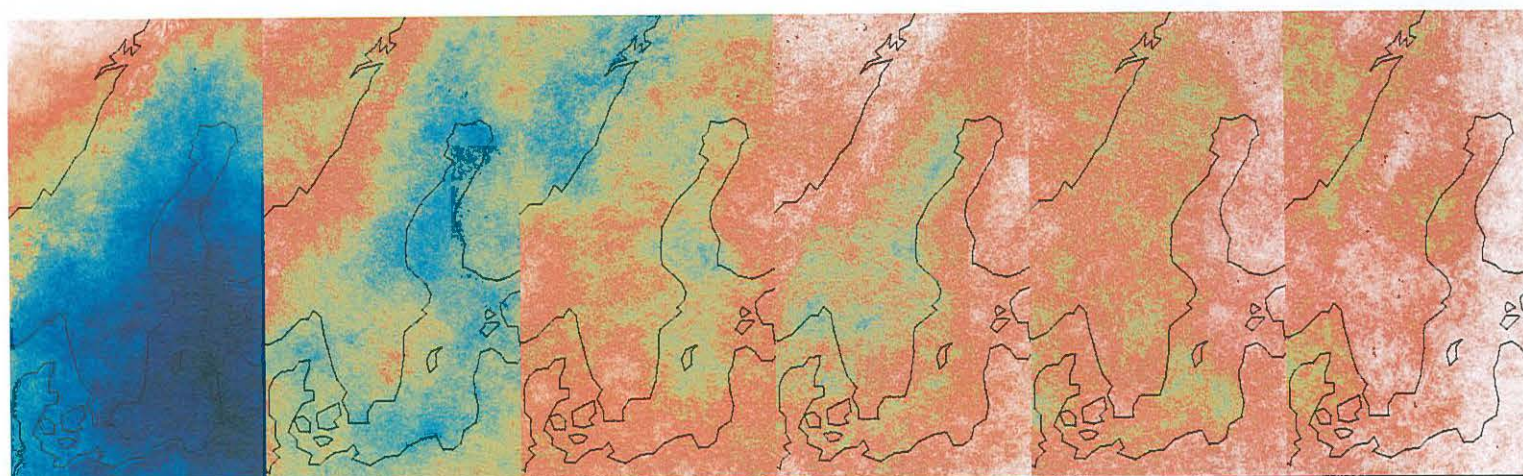
April

May

June

(%)

100
80
60
40
20
0



July

August

September

October

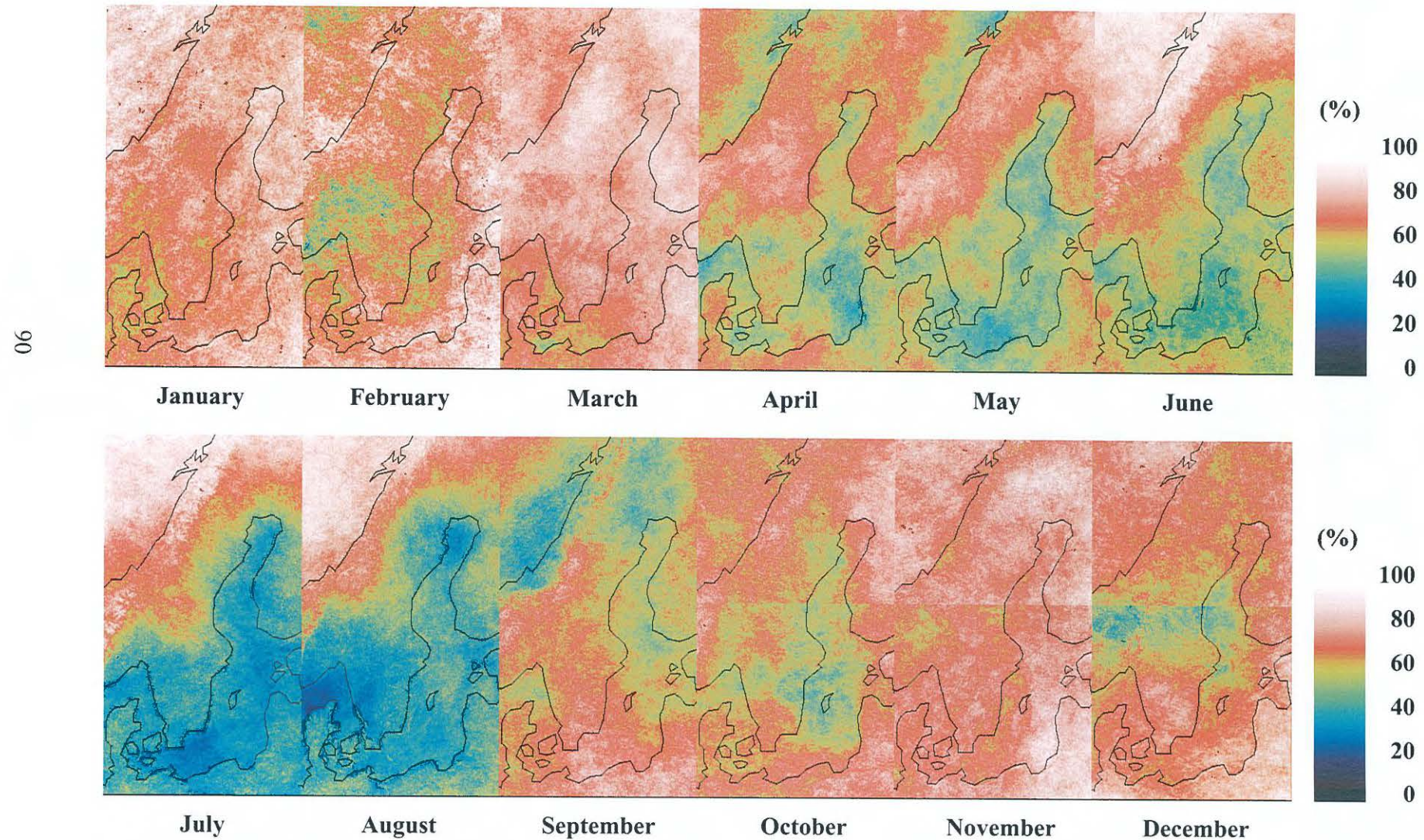
November

December

(%)

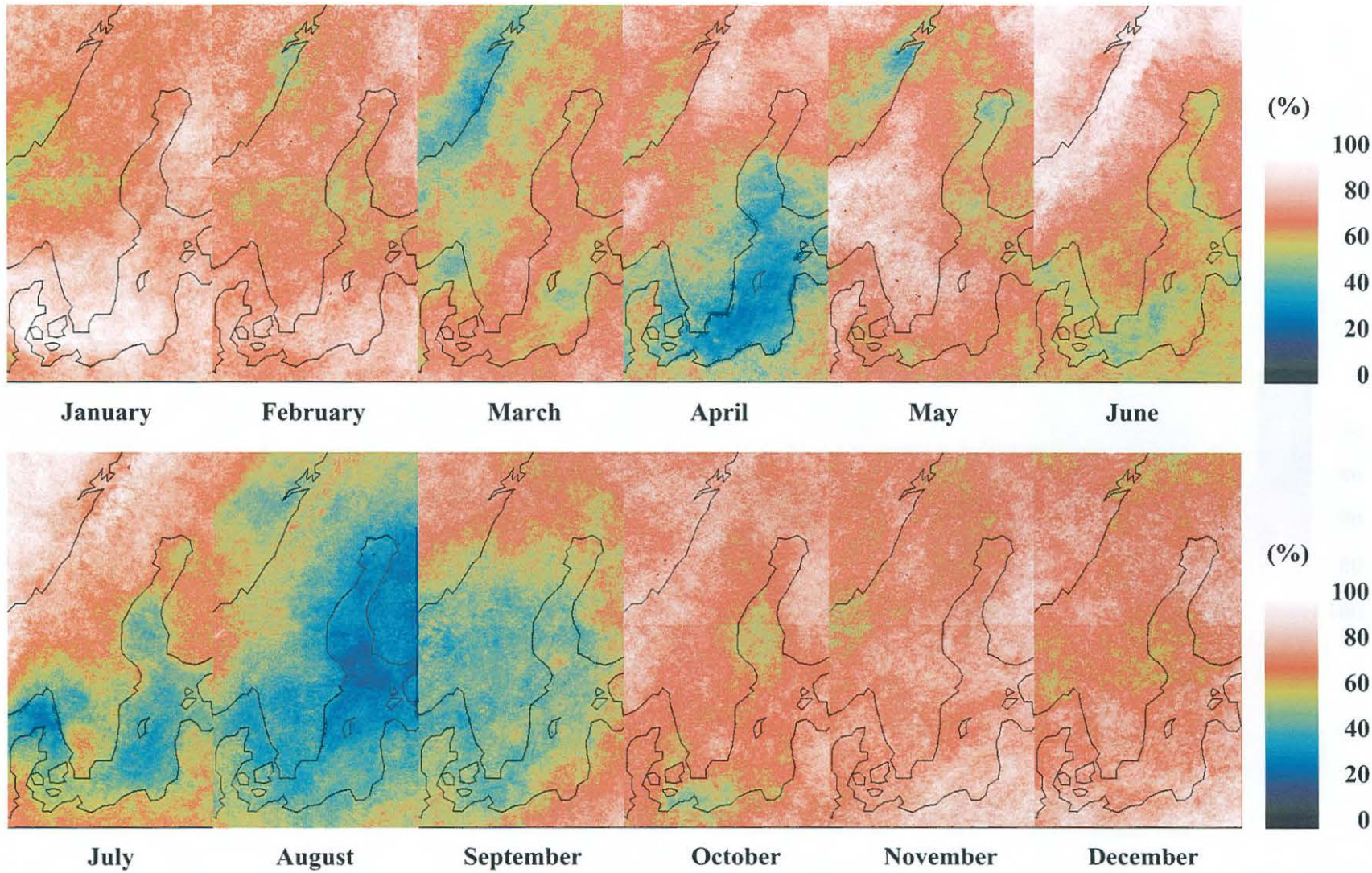
100
80
60
40
20
0

Monthly cloud frequencies in 1995



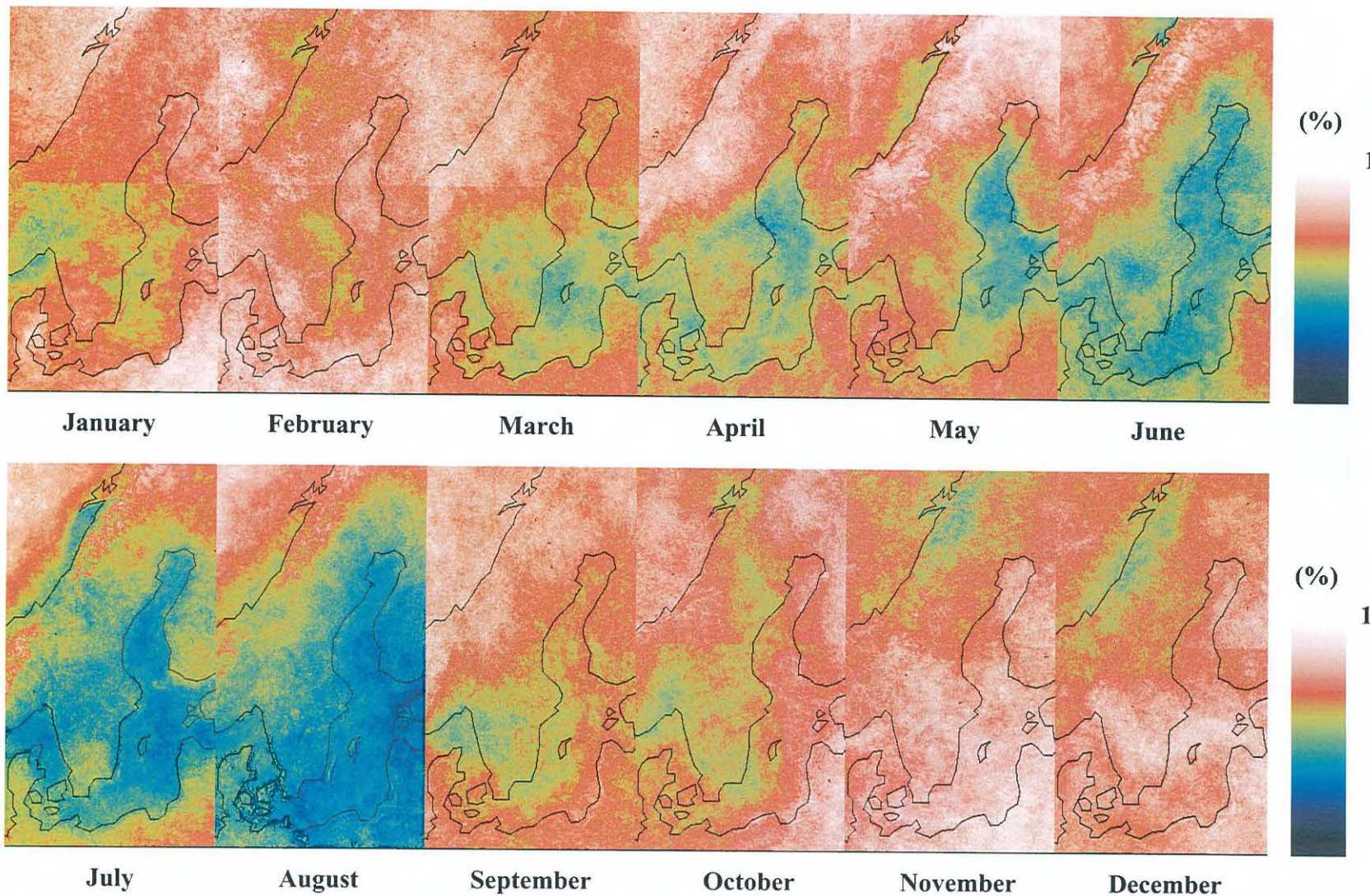
Monthly cloud frequencies in 1996

16



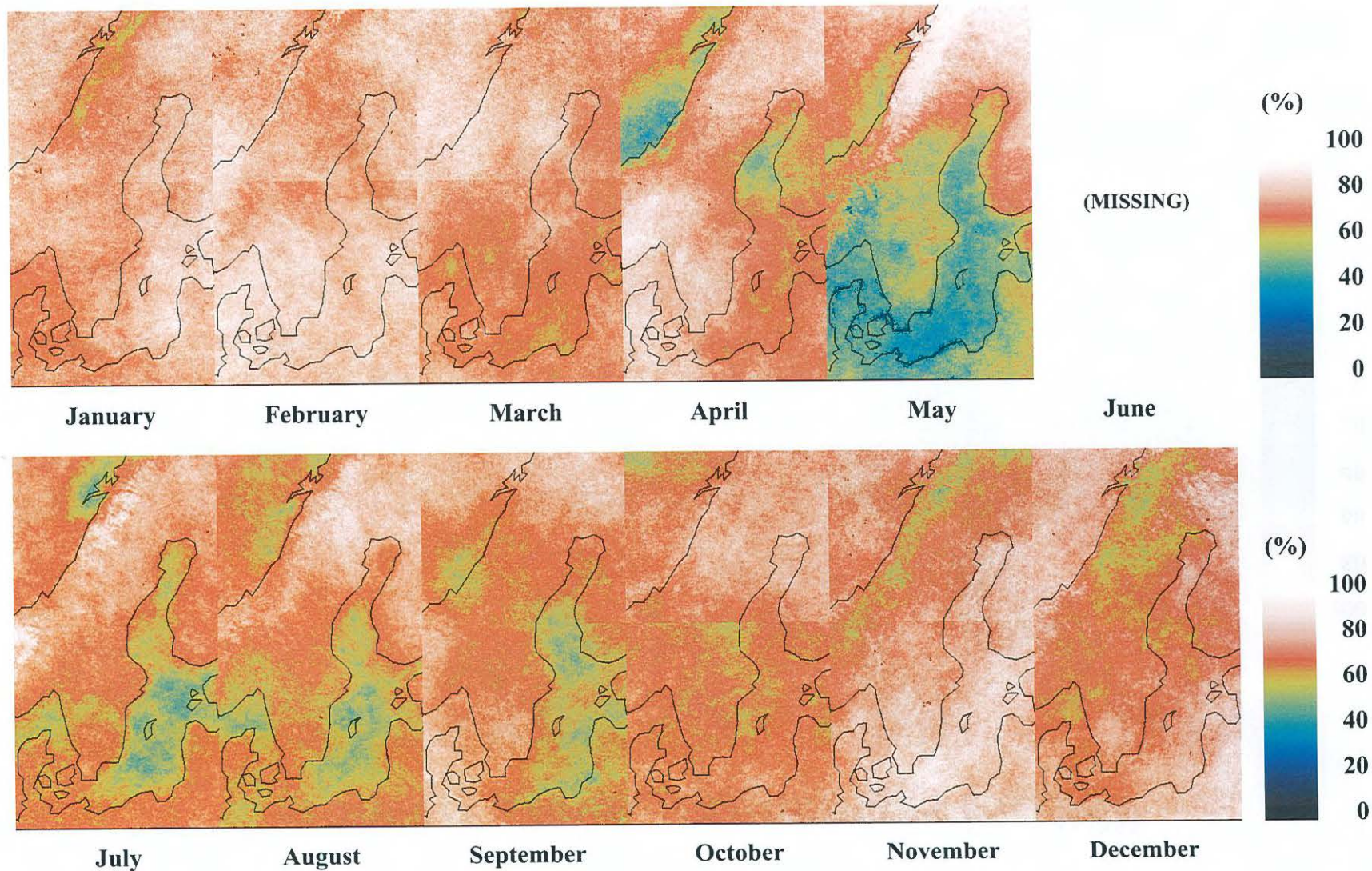
Monthly cloud frequencies in 1997

92

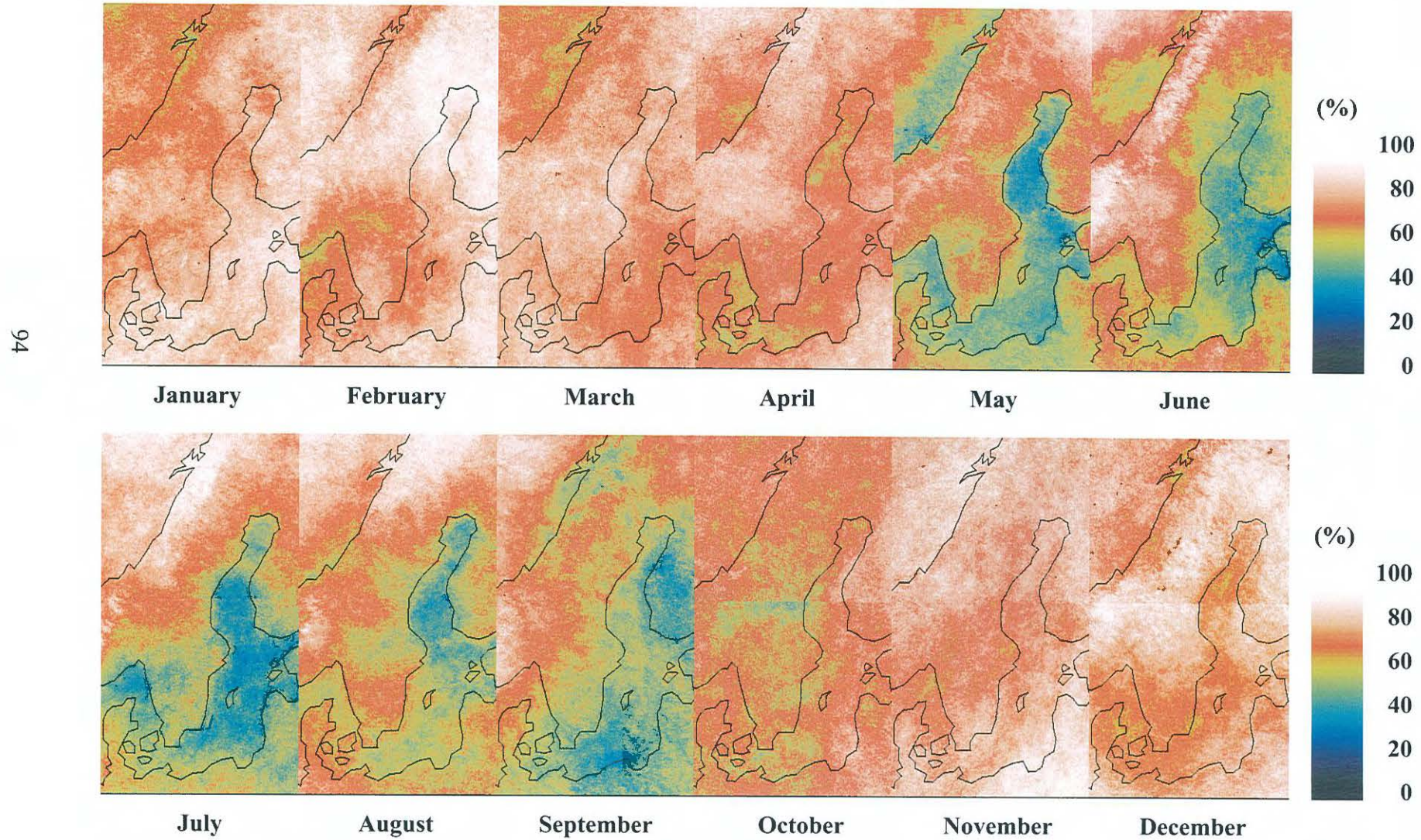


Monthly cloud frequencies in 1998

93

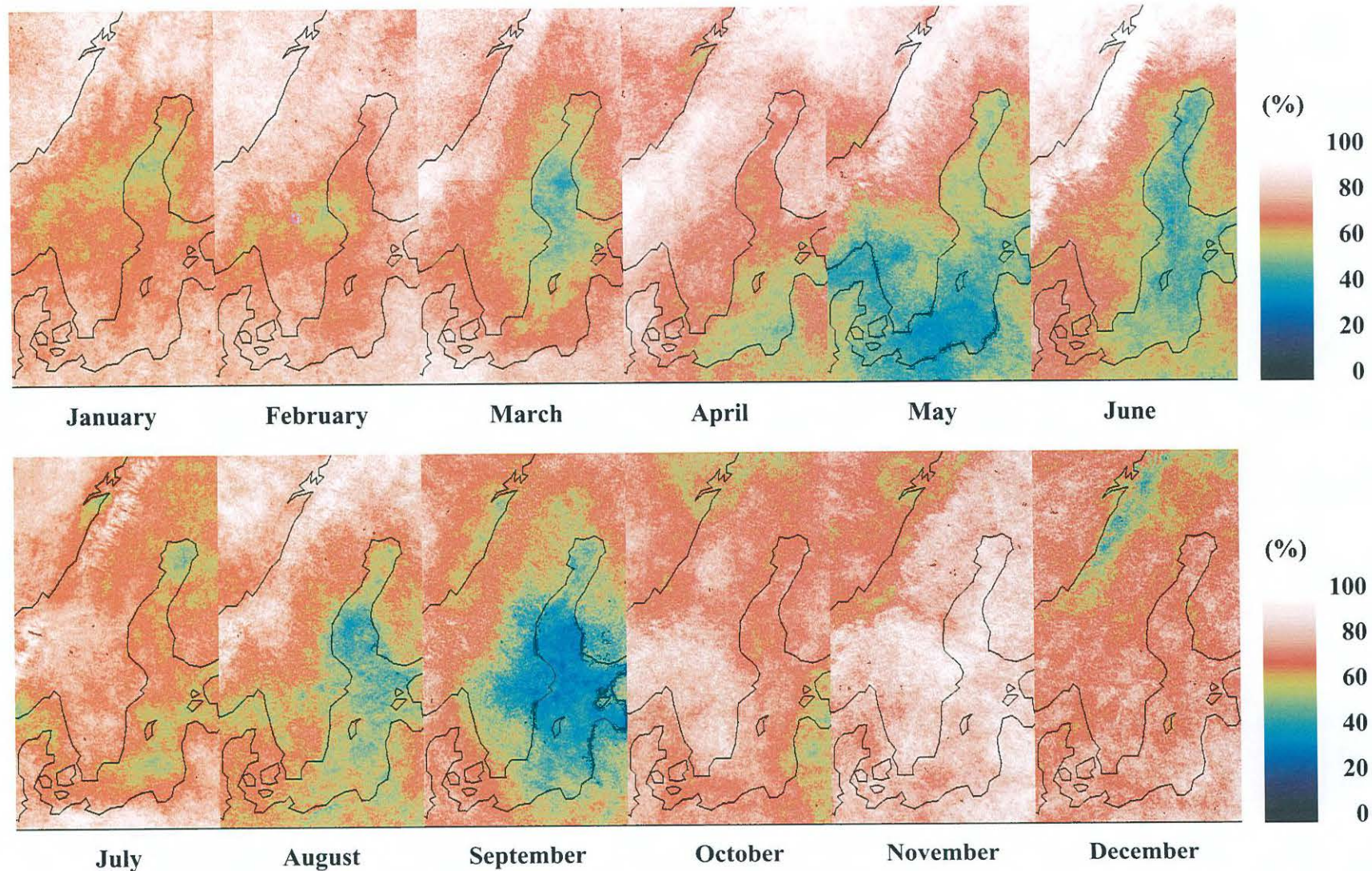


Monthly cloud frequencies in 1999



Monthly cloud frequencies in 2000

95



SMHIs publications

SMHI publishes six report series. Three of these, the R-series, are intended for international readers and are in most cases written in English. For the others the Swedish language is used.

Names of the Series

Published since

RMK (Report Meteorology and Climatology)	1974
RH (Report Hydrology)	1990
RO (Report Oceanography)	1986
METEOROLOGI	1985
HYDROLOGI	1985
OCEANOGRAFI	1985

Earlier issues published in serie RMK

- 1 Thompson, T., Udin, I., and Omstedt, A. (1974)
Sea surface temperatures in waters surrounding Sweden.
- 2 Bodin, S. (1974)
Development on an unsteady atmospheric boundary layer model.
- 3 Moen, L. (1975)
A multi-level quasi-geostrophic model for short range weather predictions.
- 4 Holmström, I. (1976)
Optimization of atmospheric models.
- 5 Collins, W.G. (1976)
A parameterization model for calculation of vertical fluxes of momentum due to terrain induced gravity waves.
- 6 Nyberg, A. (1976)
On transport of sulphur over the North Atlantic.
- 7 Lundqvist, J.-E., and Udin, I. (1977)
Ice accretion on ships with special emphasis on Baltic conditions.
- 8 Eriksson, B. (1977)
Den dagliga och årliga variationen av temperatur, fuktighet och vindhastighet vid några orter i Sverige.
- 9 Holmström, I., and Stokes, J. (1978)
Statistical forecasting of sea level changes in the Baltic.
- 10 Omstedt, A., and Sahlberg, J. (1978)
Some results from a joint Swedish-Finnish sea ice experiment, March, 1977.
- 11 Haag, T. (1978)
Byggnadsindustrins väderberoende, semi-narieuppsats i företagsekonomi, B-nivå.
- 12 Eriksson, B. (1978)
Vegetationsperioden i Sverige beräknad från temperaturobservationer.
- 13 Bodin, S. (1979)
En numerisk prognosmodell för det atmosfäriska gränsskiktet, grundad på den turbulenta energiekvationen.
- 14 Eriksson, B. (1979)
Temperaturfluktuationer under senaste 100 åren.

- 15 Udin, I., och Mattisson, I. (1979)
Havsis- och snöinformation ur datorbearbetade satellitdata - en modellstudie.
- 16 Eriksson, B. (1979)
Statistisk analys av nederbörsdata. Del I.
Arealnederbörd.
- 17 Eriksson, B. (1980)
Statistisk analys av nederbörsdata. Del II.
Frekvensanalys av månadsnederbörd.
- 18 Eriksson, B. (1980)
Årsmedelvärden (1931-60) av nederbörd, avdunstning och avrinning.
- 19 Omstedt, A. (1980)
A sensitivity analysis of steady, free floating ice.
- 20 Persson, C., och Omstedt, G. (1980)
En modell för beräkning av luftföroreningars spridning och deposition på mesoskala.
- 21 Jansson, D. (1980)
Studier av temperaturinversioner och vertikal vindskjutning vid Sundsvall-Härnösands flygplats.
- 22 Sahlberg, J., and Törnevik, H. (1980)
A study of large scale cooling in the Bay of Bothnia.
- 23 Ericson, K., and Hårsman, P.-O. (1980)
Boundary layer measurements at Klockrike. Oct. 1977.
- 24 Bringfelt, B. (1980)
A comparison of forest evapotranspiration determined by some independent methods.
- 25 Bodin, S., and Fredriksson, U. (1980)
Uncertainty in wind forecasting for wind power networks.
- 26 Eriksson, B. (1980)
Graddagsstatistik för Sverige.
- 27 Eriksson, B. (1981)
Statistisk analys av nederbörsdata. Del III.
200-åriga nederbördsserier.
- 28 Eriksson, B. (1981)
Den "potentiella" evapotranspirationen i Sverige.
- 29 Pershagen, H. (1981)
Maximisnödjup i Sverige (perioden 1905-70).
- 30 Lönnqvist, O. (1981)
Nederbörsstatistik med praktiska tillämpningar.
(Precipitation statistics with practical applications.)
- 31 Melgarejo, J.W. (1981)
Similarity theory and resistance laws for the atmospheric boundary layer.
- 32 Liljas, E. (1981)
Analys av moln och nederbörd genom automatisk klassning av AVHRR-data.
- 33 Ericson, K. (1982)
Atmospheric boundary layer field experiment in Sweden 1980, GOTEX II, part I.
- 34 Schoeffler, P. (1982)
Dissipation, dispersion and stability of numerical schemes for advection and diffusion.
- 35 Undén, P. (1982)
The Swedish Limited Area Model. Part A. Formulation.
- 36 Bringfelt, B. (1982)
A forest evapotranspiration model using synoptic data.
- 37 Omstedt, G. (1982)
Spridning av luftförorening från skorsten i konvektiva gränsskikt.
- 38 Törnevik, H. (1982)
An aerobiological model for operational forecasts of pollen concentration in the air.
- 39 Eriksson, B. (1982)
Data rörande Sveriges temperaturklimat.
- 40 Omstedt, G. (1984)
An operational air pollution model using routine meteorological data.
- 41 Persson, C., and Funkquist, L. (1984)
Local scale plume model for nitrogen oxides. Model description.

- 42 Gollvik, S. (1984)
Estimation of orographic precipitation by dynamical interpretation of synoptic model data.
- 43 Lönnqvist, O. (1984)
Congression - A fast regression technique with a great number of functions of all predictors.
- 44 Laurin, S. (1984)
Population exposure to SO and NO_x from different sources in Stockholm.
- 45 Svensson, J. (1985)
Remote sensing of atmospheric temperature profiles by TIROS Operational Vertical Sounder.
- 46 Eriksson, B. (1986)
Nederbörs- och humiditetsklimat i Sverige under vegetationsperioden.
- 47 Taesler, R. (1986)
Köldperioden av olika längd och förekomst.
- 48 Wu Zengmao (1986)
Numerical study of lake-land breeze over Lake Vättern, Sweden.
- 49 Wu Zengmao (1986)
Numerical analysis of initialization procedure in a two-dimensional lake breeze model.
- 50 Persson, C. (1986)
Local scale plume model for nitrogen oxides. Verification.
- 51 Melgarejo, J.W. (1986)
An analytical model of the boundary layer above sloping terrain with an application to observations in Antarctica.
- 52 Bringfelt, B. (1986)
Test of a forest evapotranspiration model.
- 53 Josefsson, W. (1986)
Solar ultraviolet radiation in Sweden.
- 54 Dahlström, B. (1986)
Determination of areal precipitation for the Baltic Sea.
- 55 Persson, C. (SMHI), Rodhe, H. (MISU), De Geer, L.-E. (FOA) (1986)
The Chernobyl accident - A meteorological analysis of how radionuclides reached Sweden.
- 56 Persson, C., Robertson, L. (SMHI), Grennfelt, P., Kindbom, K., Lövblad, G., och Svanberg, P.-A. (IVL) (1987)
Luftföroreningsepisoden över södra Sverige 2 - 4 februari 1987.
- 57 Omstedt, G. (1988)
An operational air pollution model.
- 58 Alexandersson, H., Eriksson, B. (1989)
Climate fluctuations in Sweden 1860 - 1987.
- 59 Eriksson, B. (1989)
Snödjupsförhållanden i Sverige - Säsongerna 1950/51 - 1979/80.
- 60 Omstedt, G., Szegö, J. (1990)
Människors exponering för luftföroreningar.
- 61 Mueller, L., Robertson, L., Andersson, E., Gustafsson, N. (1990)
Meso-γ scale objective analysis of near surface temperature, humidity and wind, and its application in air pollution modelling.
- 62 Andersson, T., Mattisson, I. (1991)
A field test of thermometer screens.
- 63 Alexandersson, H., Gollvik, S., Meuller, L. (1991)
An energy balance model for prediction of surface temperatures.
- 64 Alexandersson, H., Dahlström, B. (1992)
Future climate in the Nordic region - survey and synthesis for the next century.
- 65 Persson, C., Langner, J., Robertson, L. (1994)
Regional spridningsmodell för Göteborgs och Bohus, Hallands och Älvsborgs län. (A mesoscale air pollution dispersion model for the Swedish west-coast region. In Swedish with captions also in English.)
- 66 Karlsson, K.-G. (1994)
Satellite-estimated cloudiness from NOAA AVHRR data in the Nordic area during 1993.

- 67 Karlsson, K.-G. (1996)
Cloud classifications with the SCANDIA model.
- 68 Persson, C., Ullerstig, A. (1996)
Model calculations of dispersion of lindane over Europe. Pilot study with comparisons to measurements around the Baltic Sea and the Kattegat.
- 69 Langner, J., Persson, C., Robertson, L., and Ullerstig, A. (1996)
Air pollution Assessment Study Using the MATCH Modelling System. Application to sulfur and nitrogen compounds over Sweden 1994.
- 70 Robertson, L., Langner, J., Engardt, M. (1996)
MATCH - Meso-scale Atmospheric Transport and Chemistry modelling system.
- 71 Josefsson, W. (1996)
Five years of solar UV-radiation monitoring in Sweden.
- 72 Persson, C., Ullerstig, A., Robertson, L., Kindbom, K., Sjöberg, K. (1996)
The Swedish Precipitation Chemistry Network. Studies in network design using the MATCH modelling system and statistical methods.
- 73 Robertson, L. (1996)
Modelling of anthropogenic sulfur deposition to the African and South American continents.
- 74 Josefsson, W. (1996)
Solar UV-radiation monitoring 1996.
- 75 Häggmark, L., Ivarsson, K.-I. (SMHI). Olofsson, P.-O. (Militära väderjänsten). (1997)
MESAN - Mesoskalig analys.
- 76 Bringfelt, B., Backström, H., Kindell, S., Omstedt, G., Persson, C., Ullerstig, A. (1997)
Calculations of PM-10 concentrations in Swedish cities- Modelling of inhalable particles
- 77 Gollvik, S. (1997)
The Teleflood project, estimation of precipitation over drainage basins.
- 78 Persson, C., Ullerstig, A. (1997)
Regional luftmiljöanalys för Västmanlands län baserad på MATCH modell-beräkningar och mätdata - Analys av 1994 års data
- 79 Josefsson, W., Karlsson, J.-E. (1997)
Measurements of total ozone 1994-1996.
- 80 Rummukainen, M. (1997)
Methods for statistical downscaling of GCM simulations.
- 81 Persson, T. (1997)
Solar irradiance modelling using satellite retrieved cloudiness - A pilot study
- 82 Langner, J., Bergström, R. (SMHI) and Pleijel, K. (IVL) (1998)
European scale modelling of sulfur, oxidized nitrogen and photochemical oxidants. Model development and evaluation for the 1994 growing season.
- 83 Rummukainen, M., Räisänen, J., Ullerstig, A., Bringfelt, B., Hansson, U., Graham, P., Willén, U. (1998)
RCA - Rossby Centre regional Atmospheric climate model: model description and results from the first multi-year simulation.
- 84 Räisänen, J., Döscher, R. (1998)
Simulation of present-day climate in Northern Europé in the HadCM2 OAGCM.
- 85 Räisänen, J., Rummukainen, M., Ullerstig, A., Bringfelt, B., Ulf Hansson, U., Willén, U. (1999)
The First Rossby Centre Regional Climate Scenario - Dynamical Downscaling of CO₂-induced Climate Change in the HadCM2 GCM.
- 86 Rummukainen, Markku. (1999)
On the Climate Change debate
- 87 Räisänen, Jouni (2000)
CO₂-induced climate change in northern Europé: comparison of 12 CMIP2 experiments.
- 88 Engardt, Magnuz (2000)
Sulphur simulations for East Asia using the MATCH model with meteorological data from ECMWF.

- 89 Persson, Thomas (2000)
Measurements of Solar Radiation in Sweden
1983-1998
- 90 Daniel B. Michelson, Tage Andersson
Swedish Meteorological and Hydrological
Institute (2000)
Jarmo Koistinen, Finnish Meteorological
Institute
Christopher G. Collier, Telford Institute of
Environmental Systems, University of
Salford
Johann Riedl, German Weather Service
Jan Szturc, Institute of Meteorology and
Water Management
Uta Gjertsen, The Norwegian Meteorological
Institute
Aage Nielsen, Danish Meteorological
Institute
Søren Overgaard, Danish Meteorological
Institute
BALTEX Radar Data Centre Products and
their Methodologies
- 91 Josefsson, Weine (2000)
Measurements of total ozone 1997 – 1999
- 92 Andersson, Tage (2000)
Boundary clear air echos in southern Sweden
- 93 Andersson, Tage (2000)
Using the Sun to check some weather radar
parameters
- 94 Rummukainen, M., S. Bergström, E. Källén,
L. Moen, J. Rodhe, M. Tjernström (2000)
SWECLIM – The First Three Years
- 95 Meier, H. E Markus (2001)
The first Rossby Centre regional climate
scenario for the Baltic Sea using a 3D
coupled ice-ocean model
- 96 Landelius, Tomas, Weine Josefsson, Thomas
Persson (2001)
A system for modelling solar radiation
parameters with mesoscale spatial resolution



Swedish Meteorological and Hydrological Institute
SE 601 76 Norrköping, Sweden.
Tel +46 11-495 80 00. Fax +46 11-495 80 01